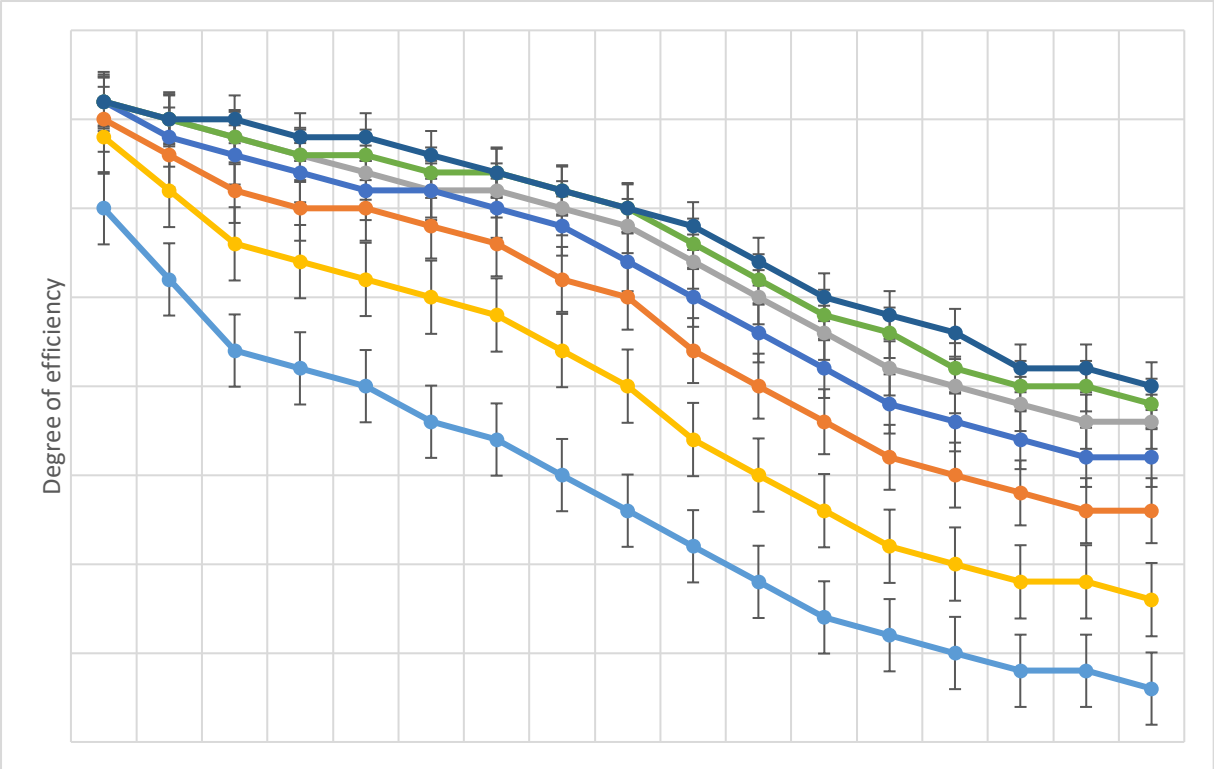

Thermal Performance Analysis of High Temperature Borehole Thermal Energy Storage Design from an Insulation Perspective

Joel Ljunggren
Tobias Magnusson

Division of Engineering Geology
Faculty of Engineering
Lund University

MSc Thesis, 30 ECTS

ISRN LUTVDG/(TVTG--5161)/1-136(2019)

Thermal Performance Analysis of High Temperature Borehole Thermal Energy Storage Design from an Insulation Perspective

Joel Ljunggren

Tobias Magnusson

LUND
UNIVERSITY

Master Thesis, Division of Engineering Geology, Faculty of Engineering, Lund University, Lund, 2019

Thermal Performance Analysis of High Temperature Borehole Thermal Energy Storage Design from an Insulation Perspective

Authors
Joel Ljunggren
Civil engineering
Lund University – Faculty of Engineering

Tobias Magnusson
Civil Engineering
Lund University – Faculty of Engineering

Supervisor
Jan-Erik Rosberg, Senior lecturer, Division of Engineering Geology, Faculty of Engineering, Lund University

Assistant supervisor
Olof Andersson, Senior Consultant, Geostrata – Geothermal Energy Systems

Examiner
Gerhard Barmen. Senior Lecturer, Division of Engineering Geology, Faculty of Engineering, Lund University

ISRN LUTVDG/(TVTG--5161)/1-136(2019)

Keywords
HT-BTES, High Temperature Borehole Thermal Energy Storage, Seasonal heat storage, Insulation Perspective

Teknisk Geologi
Lunds tekniska högskola
Lunds universitet
Box 118
221 00 Lund

www.tg.lth.se

Division of Engineering Geology
Faculty of Engineering
Lund University
P.O. Box 118
SE-221 00 Lund
Sweden

www.lunduniversity.lu.se/lucat/group/v1000204

Acknowledgements

There are many people to be thanked for the completion of this thesis, and we would like to reach out and sincerely thank everyone who helped us throughout the entire project.

We would like to thank Claes Regander, Sara Östberg, Sara Eriksson and Patricia Monzó at Sweco for letting us use their license for *TRNSYS* and helping us throughout the project.

Furthermore we would like to thank our supervisors Olof Andersson and Jan-Erik Rosberg for helping us and keeping the work on schedule.

We would also like to thank Ebrahim Parhamifar and Pajtim Sulejmani for giving us access to the sieving machine used during the material testing.

Lastly we want to thank Öresundskraft, Sweco and the institution of Engineering Geology, Faculty of Engineering, at Lund University for letting us perform our Master Thesis within this field.

Tobias Magnusson
Joel Ljunggren

Abstract

Thermal energy Storage is a growing concept within the sector of energy production. The concept is based on storage of excess thermal energy, for usage during high demand, as a mean of reducing the need for new production. By implementing thermal storage economic and environmental gains can be made as production can be kept more constant over time and less energy is wasted, furthermore the storage system can be used for cooling of thermal processes.

This Master Thesis focuses on analysing the thermal performance of *High Temperature Borehole Thermal Energy Storages* from a design and insulation perspective. The aim of which was to highlight the parameters critical for finding an optimized design with regards to thermal performance and economic profitability-potential. The analysis was based on the implementation of *TRNSYS* for modelling and simulations for a reference *HT-BTES*, from which a general perspective was lifted. The reference project comes in the form of a feasibility study for a planned *HT-BTES* at *Filborna* in *Sweden*. The reference storage is to be made in sedimentary bedrock beneath an existing gypsum deposit, and make up the outset for analysis. The thermal performance, with regards to design and insulation, was analysed by performing a sensitivity study highlighting the relation between thermal performance and design and insulation parameters. Complementing this sensitivity study was an economic analysis. Secondarily environmental effects were evaluated. Limiting the analysis is the lack of modelling possibility for groundwater and highly conductive zones which may cause additional unpredicted thermal losses. Lastly the effects if implementing a heat pump into the system were analysed.

The results from the sensitivity study showed clear indications of greater and minor dependencies between thermal performance and design/insulation parameters. Parameters such as “storage volume” showed tendencies for reduced thermal performance with increasing parameter value, whilst parameters such as “borehole depth” showed improved thermal performance with increasing parameter value.

When considering the insulation aspect of *HT-BTES* the results were found quite intuitive. Increased insulation thickness, and decreased thermal conductivity of insulation, reduces top losses. It is from this evaluation of dependency between thermal conductivity of insulation and thermal performance that the insulation material perspective could be implemented. The material perspective accounts for effects on thermal properties from temperature and moisture content, highlighting the importance of moisture protection. When implementing an economic perspective into the thermal performance analysis regarding insulation design, the economic value was found in the extracted energy. This value needed to exceed the value the thermal energy had when it was stored, and cover for all cost aspects included in the system design.

The main conclusion drawn from the project was that in order to derive modelling results close to reality, extensive work is needed for determining all parameters of the thermal storage model. The sensitivity study showed that uncertainties in parameters may yield significant impact on the final results.

Key words: High Temperature Borehole Thermal Energy Storage, HT-BTES, Thermal Energy Storage, TRNSYS

List of figures

List of tables

Abbreviations

ATES – Aquifer Thermal Energy Storage
BHE – Borehole Heat Exchanger
BTES – Borehole Thermal Energy Storage
CFC – Chlorofluorocarbons
COP – Coefficient Of Performance
DST – Duct Storage
EPS – Expanded polystyrene
GWP – Global Warming Potential
HT-BTES – High Temperature Borehole Thermal Energy Storage
ODP – Ozone Depleting Potential
PTES – Pit thermal energy storage
TFA – Trifluoroacetic acid
TES – Thermal Energy Storage
TRNSYS – Transient System Simulation
TTES – Tank Thermal Energy Storage
XPS – Extruded polystyrene

Nomenclature

α	- Heat transfer coefficient [J/(s m K)]
α_v	- Heat transfer coefficient considering volume [J/(s m^3 K)]
α_p	- Heat transfer coefficient considering pipe length [J/(s m K)]
β	- Damping coefficient [-]
λ	- Thermal conductivity [J(s m K)]
ρ	- Density of carrier fluid [kg/m^3]
B	- Borehole spacing [m]
C_f	- Volumetric heat capacity of carrier fluid [J/(m^3 K)]
L_p	- Total pipe length [m]
r_1	- Radius of influence [m]
r_b	- Borehole radius [m]
R_b	- Thermal resistance per unit length of pipe [(s m K)/J]
R_{sf}	- Resistance between carrier fluid and storage medium [(K s m)/J]
t	- Time [s]
T_a	- Temperature of surrounding ground [°C]
T_b	- Average temperature of borehole wall [°C]
T_f	- Temperature of carrier fluid [°C]
T_{fin}	- Inlet temperature [°C]
T_{fout}	- Outlet temperature [°C]
T_g	- Temperature of undisturbed ground [°C]
T_m	- Average local temperature [°C]
V	- Storage volume [m^3]
q	- Heat transfer [J/(s m^2) or J/(s m)]
q_f	- Flowrate of carrier fluid [m^3/s]
Q_f	- Total flowrate of carrier fluid [m^3/s]
q_t	- Heat extraction [W/m]

Table of content

1. Introduction

A noticeable trend in today's society is the global increase in energy demand (International Energy Agency 2018 A). With the trend comes challenges for future sustainability within the energy sector, as it happens in the same era as a transition to more sustainable energy alternatives (International Energy Agency 2018 B). The reasons behind this increase in energy demand are both societal, and technological, such as economic and industrial growth (OECD 2012). Hence a link can be identified between sustainability and energy demand from social, environmental, and economic perspectives. Therefore one must look at all factors from energy production to energy utilization, in order to achieve sustainability.

As brought up by *OECD* (2012) there is significant potential for sustainability development via the implementation of new methods, techniques, and technology within the energy sector. One field of interest brought forward as in need of technological advancement, by the *International Energy Agency* (N.D.), is the field of thermal energy, and more specifically thermal energy storage. The aspect entails both energy utilization and energy production, hence relates to all sustainability parameters coupled with these two stages of the energy sector.

Focusing on the aspect of thermal energy utilization, it is brought up by the *International Energy Agency* (N.D. that thermal energy storage is one of many factors needed in driving the transition from CO_2 heavy means of energy production to more sustainable alternatives. As a mean of meeting the global demand, whilst limiting the usage of resources, finite or renewable, and maintaining a more consistent energy production over time. Enabling further parallels to be drawn from the sustainability perspective, as the technology benefits economic, environmental, and sociological sustainability. Furthermore the method shows potential for reduced energy production costs and allows for greater utilization of produced energy.

Conceptually the method of thermal energy storage can be identified as a field within which experience is limited, because of which room for development and optimization is prominent. The concept of thermal energy storage entails storage of excess heat for later utilization during high demand, as a mean of reducing production demands. Design wise there are very different concepts of thermal energy storage, ranging from pit and borehole storage to processes using chemical processes (Olesen & Krasimiroy 2011).

This Master Thesis will focus on the concept of *High Temperature Borehole Thermal Energy Storage* (*HT-BTES*), from an insulation perspective. The insulation perspective mainly entails the insulation design regarding geometry and material alternatives. Secondarily, perspective is to entail economic, as well as environmental, aspects related to the insulation design.

This Master Thesis is performed as part of a feasibility study for a planned *HT-BTES* at the *Filborna* cogeneration plant in *Helsingborg*, *Sweden*. The cogeneration plant primarily produces electricity, from which the generating process yields thermal energy used for district heating. During summer the demand for district heating is low, and thermal energy is in surplus, hence a thermal energy storage solution becomes justifiable. This motivation is based on both the need for cooling of the thermal process during the summer, as well as utilization of the excess energy during high demand. The storage volume is to be located in sedimentary bedrock,

with a topmost part made up of a gypsum layer, from an existing gypsum deposit. The analysis included in the feasibility study is to grasp a multitude of parameters, mainly including: Thermal performance of storage design alternatives, economic, and environmental aspects of these alternatives, as well as a comparative study of an alternative system design.

The analysis of the insulation perspective, making up the central basis of the Master Thesis, was based on the utilization of the *TRNSYS* software for modelling and simulations. The analysis was performed from the basis of the design of the reference project at *Filborna*. From the reference project a sensitivity study of parameter dependency of thermal performance was performed. These results were thereafter theoretically verified in order to lift a general perspective.

1.1 Aim of Master Thesis

As the Master Thesis is part of a feasibility study, it is of an investigatory nature. Hence the concept, as well as the conceptual entailments, are still under development, as knowledge within the field is limited. As the outline entails a feasibility study, this Master Thesis strives towards providing an addition to the knowledge base upon which future thermal storage designs can be based. This is done by integrating an insulation perspective to the design aspect of borehole thermal energy storage.

The central aim of this Master Thesis is to analyse the thermal performance of *Borehole Thermal Energy Storage* originating from a sensitivity study of design and insulation parameters. Where the insulation perspective is to take a central role. Complementing the thermal performance analysis is an economic analysis aiming to show the economic value dependent on insulation design. Analysis is to be based on the reference design for the planned *HT-BTES* at *Filborna,* from which a generalised perspective will be implemented.

A secondary aim, which is integrated into the central aim regarding thermal performance, is analysing the material alternatives for insulation of high temperature thermal storages. In the reference project, this material aspect entails analysis of the suitability of slag gravel to be used for insulation of the thermal storage. The reason is that the cogeneration plant at *Filborna* does not have any major areas of utilization for the material at the time.

Thirdly a comparative study of the original design for the reference project is to be analysed, highlighting the pros and cons of integrating a heat pump into the system for thermal storage.

The thermal performance analysis is to be performed as a sensitivity study aiming towards providing an understanding for parameter dependency.

1.1.1 Limitations and simplifications

This Master Thesis is to focus on a reference project, from which a general perspective is to be lifted. Focus will hence mainly be on the key geometric, system, and insulation parameters central to the reference project, while other parameters are given less focus.

2 Background

The background of this Master Thesis includes the history of the concept of thermal energy storage, description of the concept itself, description of the reference project, as well as existing projects within the field.

2.1 The history of thermal energy storage

Thermal Energy Storage (TES) has been more or less present throughout history, dating back to seasonal storage of ice into summer hundreds of years ago. The modern interest for large-scale seasonal storage of thermal energy can be backtracked to the oil crisis during the early 1970s. The method initially aimed towards seasonal storage of solar energy, but great potential in the storage of thermal energy from industrial processes were identified (Nordell 2000).

Conceptually *TES* is based on the principle of storing surplus thermal energy for utilization as demand increases. The aim is to limit the use of resources, finite or renewable, at the same time as production fluctuations are limited due to production being able to be kept more constant using the thermal reserve to cover for peaks demand (Heier 2013). The concept of *TES* relates to the desire for sustainability as brought up by the *International Energy Agency* (N.D.).

Principally the design of a thermal storage system is based around a source of thermal energy, such as solar collectors, thermal energy generating industrial processes, or other thermal energy generating processes, which via an intermediate medium connects to a thermal storage unit. The thermal energy is then stored within a storage medium until it is desired, at which point the thermal process is reversed and energy is extracted from the storage. The layout of the system can vary a lot dependent on thermal sources e.g. and the concept is applicable on different scales, ranging from local applications for industries to district heating used in communities. The methods used for storing are hence very different and range from water pit storages (State of Green N.D.), storage in bedrock and aquifer storage, to more technologically advanced methods, such as molten salt technology (Sandia National Laboratories 2006), which is based on chemical reactions (Cuypers et al. 2016).

The main complication for *TES*, as brought forward by *Nordell* (2000), lies in the difficulty of assigning economic value to environmental advantages of the concept. The technology itself needs to be made economically beneficial in comparison to the new production of thermal energy. In other words, the value of the injected heat needs to be less than the value of the extracted heat, from which the value margin is to cover additional cost aspects. These additional cost aspects include thermal losses, investment costs, and operational costs (Nordell 2000). The concept hence strives towards providing environmental sustainability, at the same time as it needs to be economically beneficial.

This Master Thesis will focus on the concept of *High Temperature Borehole Thermal Energy Storage* (*HT-BTES*) in relations to a planned storage at *Filborna* in *Helsingborg*, *Sweden*, mainly from an insulation perspective. As brought forward by *Sundberg* (1991), the insulation perspective of a thermal storage is highly dependent on the thermal properties of the ground in which it is to be placed, which shows the direction in which the analysis is to strive. The focus will be on material parameters, as well as storage design aspects.

2.2 The concept of HT-BTES

The method of *BTES* uses the ground for storage of thermal energy via boreholes (also called ducts) acting as heat exchangers (Nordell 2000), see *Figure 2.1*. One advantage with the use of *BTES* brought forward by *Nordell* (2000), is the possibility of using this for both heating and cooling. In the reference project at *Filborna*, this advantage relates to the implementation of an *HT-BTES*, which wants to utilize the storage for cooling during excess heat, and heating during increased thermal energy demand.

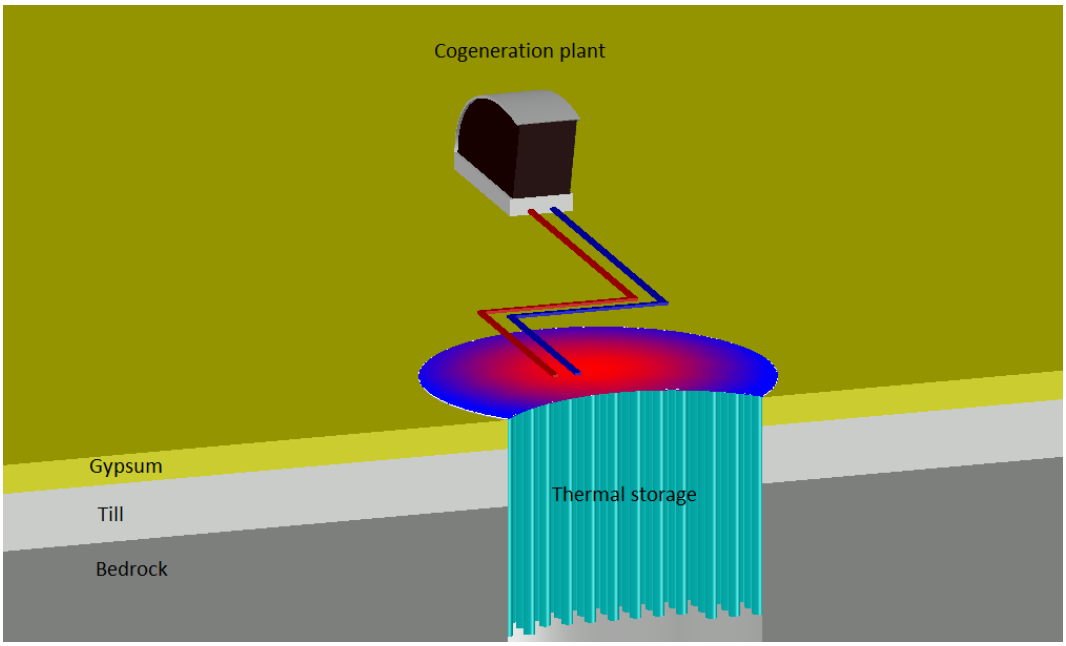

Figure 2.1 – Conceptual cross-section of a Borehole Thermal Energy Storage.

As the name suggests, a *HT-BTES* deviates from conventional *BTES* by having higher storage temperatures. The higher temperatures not only causes greater challenges for the system design itself, but also imposes greater risk for increased thermal losses, as the driving force behind these are temperature differences. A *HT-BTES* becomes implementable when high charging, and storage, temperatures are present, something which can be the case from industrial processes, as in the reference project.

2.3 Reference project at Filborna

Within this Master Thesis a reference project, in the form of a planned *HT-BTES*, is to be used as an analysis basis from which modelling studies are to be performed. The planned *HT-BTES* is located at *Filborna*, in *Sweden*, and is to be connected to the thermal process at the cogeneration plant located there. The cogeneration plant uses incineration of waste in order to produce electricity, which secondarily yields thermal energy production. The cogeneration plant currently provides district heating for approximately 48 000 recipients in *Helsingborg*, and 10 000 recipients in *Ängelholm* (Öresundskraft 2019 A). Complementing the existing thermal production at the cogeneration plant with a *HT-BTES* would allow for seasonal storage of excess thermal energy produced during low demand. The storage process is secondarily used

as a cooling method for the thermal process for excess thermal energy, hence eliminating other costly methods for cooling.

The design aspect mainly given focus in this Master Thesis is the thermal performance perspective, focusing on the insulation aspects entailed for top insulation design. The insulation design perspective entails geometrical parameters as well as considerations of insulation materials. In this Master Thesis, the material alternatives to be analysed are: locally produced slag gravel, foam glass, expanded clay, and extruded polystyrene.

2.3.1 General design of the planned HT-BTES at Filborna

The conceptual system design for the reference project is presented in *Figure 2.2*. This shows the principle setup for charging (left) and extraction (right). It is from this outline that the modelling is to originate.

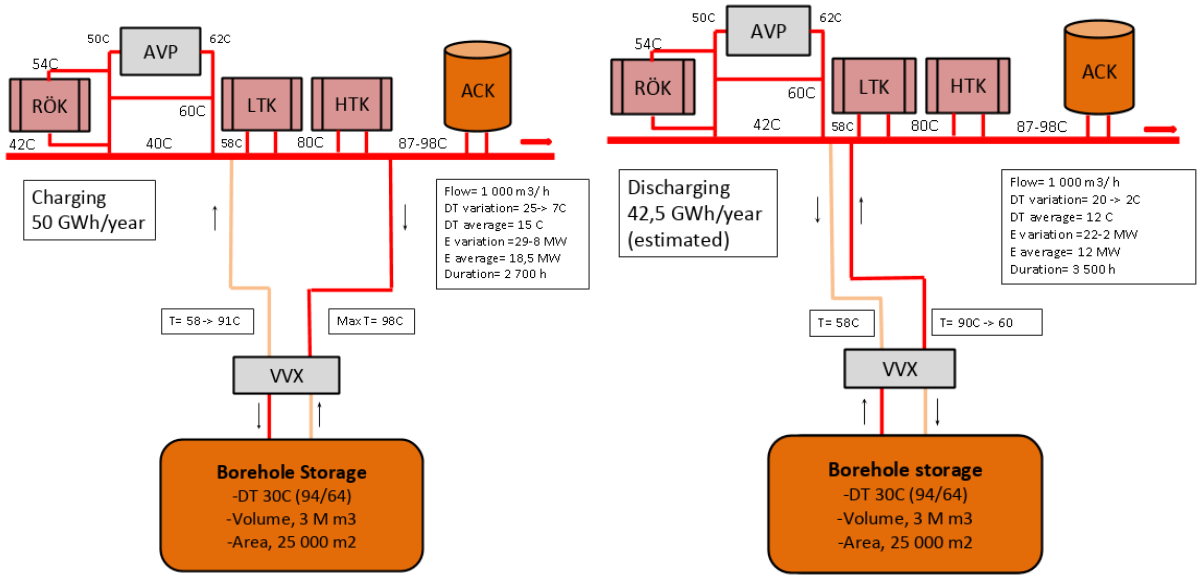

Figure 2.2 – Principle illustrations of charging and extraction circuits. Left: charging. Right: extraction.

The thermal storage acting as a reference for modelling and analysis has the general design parameters as presented in *Table 2.1*. These show the general dimensions of the storage, as well as the overall system design parameters.

Table 2.1 – General design of reference storage at Filborna

Borehole design parameters	
1500 boreholes 120 m deep 101.6 mm outer diameter	The boreholes are to be equipped with a bottom plug yielding a hermetically closed (air tight) system. These boreholes are equipped with *Coaxial Borehole Heat Exchangers* (*BHE*), and filled with water, making them thermally active along their total length
Storage and system design parameters	
Cylinder design 3 000 000 m^3 90 m cylinder radius	Connecting the vertical boreholes to the thermal process of the cogeneration plant is a horizontal pipe system made up of rubber pipes, connecting to an intermediate heat exchanger, alternatively an additional heat pump. This system allows for thermal energy to be stored, or extracted from the storage.

The segments connecting the thermal processes of the cogeneration plant to the thermal storage consists of a horizontal pipe system. This horizontal pipe system is to mainly be placed on top of the thermal storage, yielding that the top insulation of the storage also is used for insulation of the horizontal pipe system. The insulating layer is conceptual to be separated from other materials by geotextiles and is to be enclosed in an impermeable canvas to prevent moisture infiltration.

2.3.2 Description of field site

The thermal storage is to be located in the vicinity of the cogeneration plant at *Filborna*, as seen in *Figure 2.3*. *Figure 2.3* shows the two testing boreholes, for which thermal response tests and geologic conditions were investigated.

Figure 2.3 – The left figure shows the location of the storage. The right picture shows the two testing boreholes circled in red, and the area for the storage volume circled in yellow. (Öresundskraft Kraft & Värme 2018)

From tests performed in the proceedings to this feasibility study, the general geologic conditions of the field area could be stated. These are presented in *Figure 2.4* showing three main layers, gypsum, till and sedimentary bedrock.

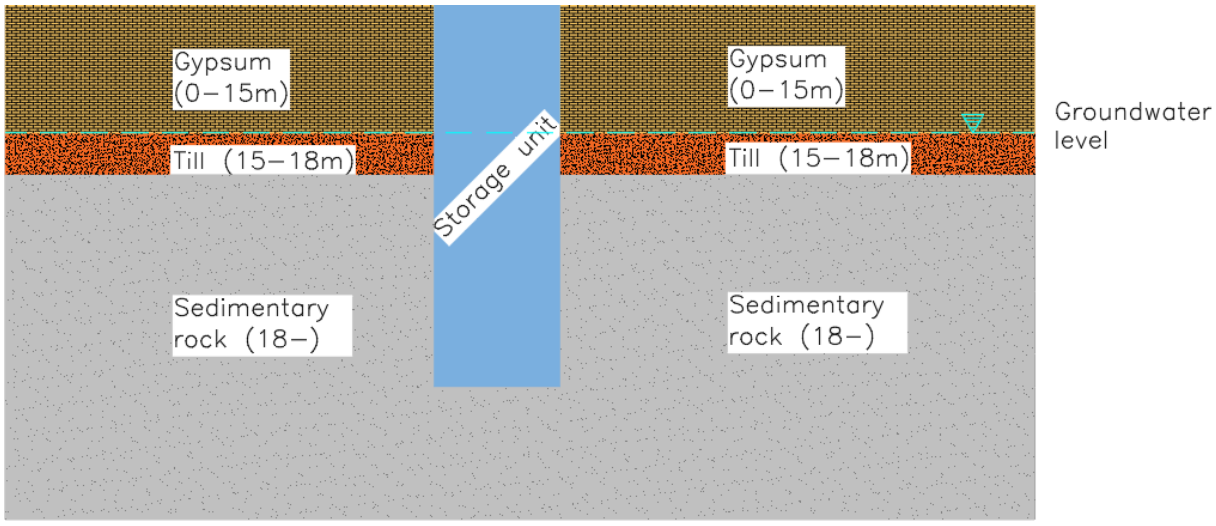

Figure 2.4 – Geologic model for ground conditions at reference project.

The gypsum layer, with a thickness of approximately 15 m, is a consequence of the field site being a former gypsum deposit. Underlying the gypsum deposit is a till layer, within which the groundwater level is found at a total depth of 16 m. The groundwater level shows no annual variations, but in the later determination of material properties, the till layer is assumed fully saturated throughout its thickness. This assumption is based on the common clay content in till, which common for the landscape of *Skåne*. Underneath the till layer there is sedimentary bedrock, which will make up most of the thermal storage volume. The bedrock was evaluated by Sweco in 2005 as part of a study aiming to map the geologic, and hydrogeological, conditions of the *Filborna* area. The sedimentary bedrock in the general area is in Swedish named "Höganäsformationen", which was formed in a coastal environment during the Jurassic era, approximately 200 million years ago. The bedrock mainly consists of sandstone, siltstone and claystone, which is present to a depth of approximately 250 meters. The storage volume will hence be located entirely in this formation. The "Höganäsformationen" is followed by "Kågerödsformationen" consisting of unsorted layers of sandstones and clays, deposited in a dry desert-like landscape approximately 220 million years ago. In some of the topmost parts of the geology a formation called "Döshultsledet" can be found, it is made up of coarse sandstones, siltstones and claystone. The hydrogeological conditions are stated as very varying in the investigation as porosities and presence of fissures are very varying, yielding hydraulic conductivities ranging from values of $3 \cdot 10^{-3}$ m/s to $6 \cdot 10^{-6}$ m/s. The groundwater level of the *Filborna* region was found to be at its highest around where the storage is to be located, which yields that the groundwater flow is directed away from the storage (SWECO 2012).

As can be illustrated in *Figure 2.5* from the CALP-test, a major fissure-zone is present in the local area where the storage unit is planned to be constructed at *Filborna*. The zone is located at a depth of 41 metres below the ground surface in UB1 and 35 metres below the ground surface in UB2. Another fissure-zone is located at 87-93 metres in UB1 and 91-96 metres in UB2 below the ground surface and is identified as the zone where sandstone and shales encounters. The condition of the bedrocks top is unknown as a feed supply pipe is installed in the boreholes.

The material properties of each layer are presented in *appendix A*, where the focus is kept to thermal properties.

The average temperature in the sub-terrain was tested in borehole *UB2* (bottom red circle in *Figure 2.3*). The results showed an average temperature of approximately 10 degrees, as seen in *Figure 2.6*. A noticeable deviation can be identified at the depth of 61 metres *in Figure 2.6*, this is noise in instrument and hence should be neglected during the evaluation of the results.

Topography wise the field area shows a slope towards the north-east/south-east. When regarding vegetation, the field site shows mainly grass growth with no significant growth of trees or other heavy vegetation, making for no major challenges for construction from this perspective.

Regarding the surrounding industry and buildings, no significant obstacles for construction can be identified as the field site is secluded from settlements and industries, see *Figure 2.3*. The construction hence mainly only needs to regard the everyday activities of the cogeneration plant which should not impose any great hinders.

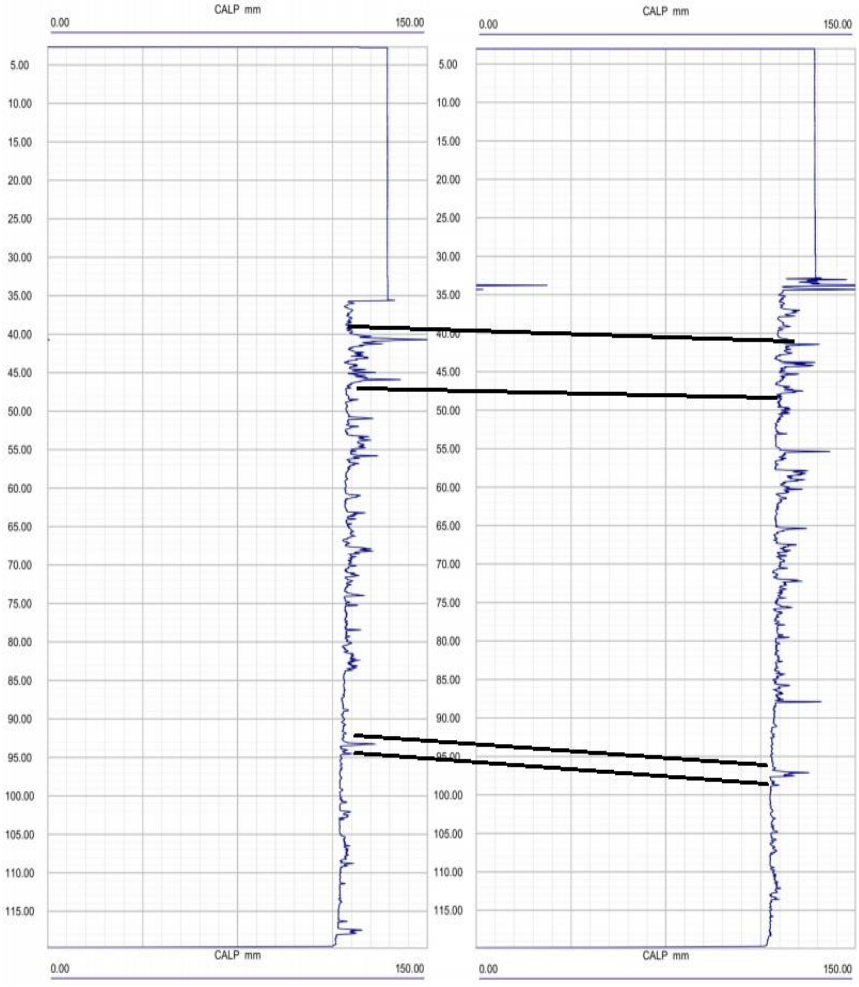

Figure 2.5 – CALP results for measurements of borehole diameter in UB1 and UB2. (Öresundskraft Kraft & Värme 2018)

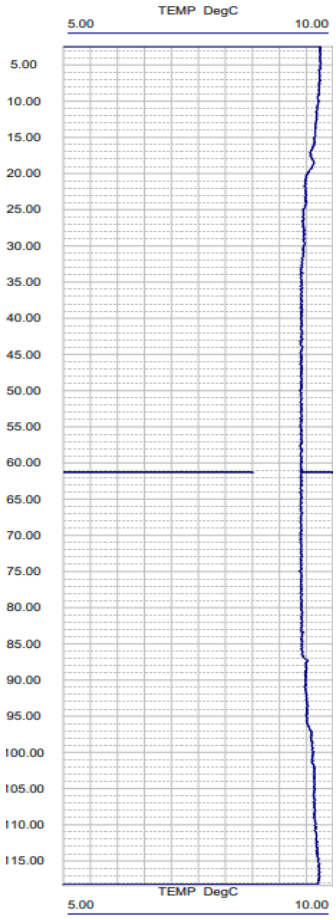

Figure 2.6 – Temperature variation in borehole UB2. (Öresundskraft Kraft & Värme 2018)

2.4 Existing thermal energy storage projects

Thermal energy storage applications can be found more or less throughout the world. In order of adding to the knowledge base of this Master Thesis, these applications are analysed from economic, environmental, and design perspectives. These are to be implemented when analysing system design, thermal performance aspects, as well as being a basis for conclusions of this Master Thesis.

2.4.1 Thermal energy storage in Emmaboda - Sweden

The *HT-BTES* at *Emmaboda* was taken into operation in 2010 and is used as a mean of reducing external heat dependency of the manufacturing plant (Nordell et al. 2016), and provide heating for 850 consumers (Emmaboda Energi & Miljö AB 2018). The storage is placed in granodiorite bedrock, with a groundwater level two metres below the top of the boreholes (Nordell et al. 2016). Design wise the storage consists of 140 boreholes, which are 150 m deep, divided into sections from which thermal energy can be injected or extracted separately. Each borehole is equipped with an open coaxial *Borehole Heat Exchanger* (*BHE*), with rotational flanges at the bottom, and internal and external spacers every 10 metres. The storage temperature is between 40 and50 ℃, which is a consequence of that the supply heat rarely exceeds 50-55 ℃. One reason for the feeding temperature to the storage being in this span is most likely due to the *BHE* design of using extruded polypropylene (PPE PN10) (Nordell et al. 2016) which has a temperature resistance up to 80 ℃ (Abrahamsson & Milesson 2013). The system is equipped with a heat pump unit in order to increase the return temperature to the facility during discharge as well as the efficiency of the system (Nordell et al. 2016).

The insulation aspect of a thermal storage is directly relatable to the thermal efficiency of the storage, i.e. how much of the injected thermal energy that is able to be extracted. The thermal storage is insulated with 40 cm of foam glass, which reduces the theoretical losses from 70.1 kW/m^2 to 26.3 kW/m^2, showing the importance of top insulation. The insulation is placed directly on top of the storage, not extending beyond the outer boundary of the storage volume. The overlay of the storage has the material sequence of soil, geotextile, foam glass, geotextile and sand. Within the sand layer, the horizontal pipe system is located (Nordell et al. 2016).

The project in *Emmaboda* brings forward the importance of preheating for bringing up the average temperature of the storage, and its surroundings. Resulting in reduced thermal losses when the storage is in full operation. One aspect brought forward as important to consider when utilizing a heat pump is the balance between electrical costs for the pump, and the supply temperature, if reaching for higher temperature of the return water in relation to the storage temperature (Nordell et al. 2016).

2.4.2 Thermal energy storage in Okotoks - Canada

In *Okotoks, Canada,* a *HT-BTES* has been in operation since 2007, as part of heat supply for environmentally friendly housing projects (R-2000 housing). The *HT-BTES* is loaded via solar collectors and is made up of 144, 35 metres deep, boreholes equipped with U-tube heat exchangers. The boreholes are connected in a series of six, and energy is injected centrally in the storage and extracted at the outer boundaries. Complementing the main *HT-BTES*-system is a short term buffer storage for dealing with thermal energy peaks (Sibbitt et al. N.D.).

The storage and the horizontal pipe system is insulated with 20 cm of polystyrene, which itself is covered by topsoil and placed on 40 cm graded sand (Sibbitt et al. N.D.).

The thermal performance of the storage was evaluated during the first five years of operation, during which the fourth year showed the greatest ratio between extracted and charged thermal energy, 54 %. (Sibbitt et al. 2012). From studying the system model, it was acknowledged that the location of the storage highly contributes to the end result regarding the efficiency of the storage. This relates to parameters for the subsurface that determines the efficiency, examples of these are: thermal conductivity, permeability, saturation level, and hydraulic gradient. (Catolico et al. 2015). *Sibbitt et al.* (2012) stressed that further investigations were needed in order to verify where, and how, the thermal losses occur. This in order to improve the future effectiveness of the storage. *Sibbitt et al.* (2012) further declare that the thermal performance of the storage will increase until a steady state has been reached.

2.4.3 Thermal storage in Germany

In *Germany* thermal energy storage can be seen as quite prominent as a lot of work within the field has been done. One analysis relating concepts of thermal storage to economic values was performed by *Mangold & Schmidt* (N.D.). Their work concluded in the results presented in *Figure 2.7*, where investment per cubic water equivalent was compared to the storage volume in cubic water equivalents. The figure shows that the investment cost in relations to storage volume is relatively low for *Borehole Thermal Energy Storage* (*BTES*) compared with *Pit Thermal Energy Storage* (*PTES*) and *TTES*. The relationship is further based on information found for the projects at *Dronninglund*, *Gram* and *Vojens* in *Denmark*.

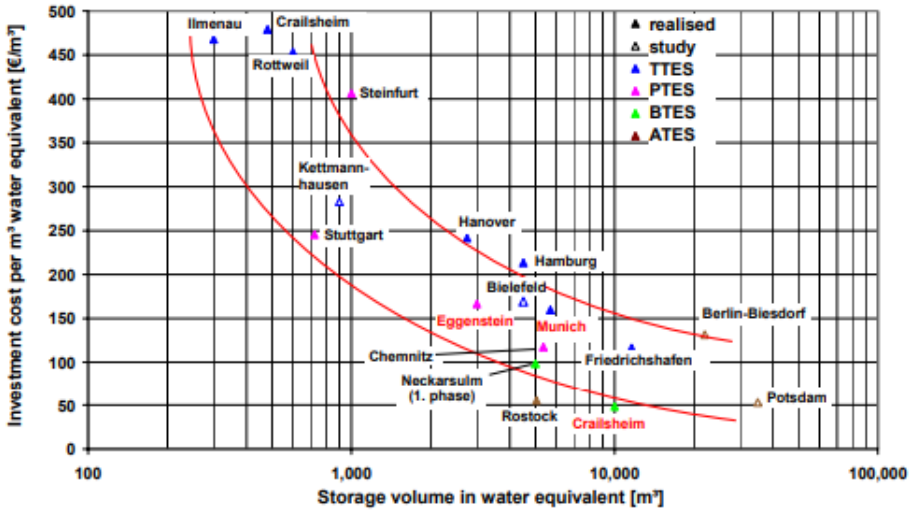

Figure 2.7 – Relation between investment cost and storage volume for different concepts of thermal energy storage. (Heidemann, Müller-Steinhagen & Ochs N.D.)

BTES - Crailsheim Germany

The *BTES* in *Crailsheim* is a solar generated thermal storage with both a diurnal and seasonal storage systems. Due to highly permeable zones found in the upper five metres of the geologic profile a protective and grouting material with low thermal conductivity casing was installed

for the topmost part, in order to minimize thermal losses. The rest of the boreholes were filled with grouting material with high thermal conductivity (Mangold et al. 2007).

Insulation wise the storage was covered by 50 cm of foam glass, and in the middle of the insulating layer, the horizontal pipes were installed in order to minimize losses upwards and downwards from this part of the system (Mangold et al. 2007).

PTES in Munich Germany

The *PTES* in *Munich* was insulated using foam glass at the side walls, at the bottom (20 cm), and on top of the storage (70 cm). The choice of foam glass for bottom insulation was based in its high stability against static pressure. In order to protect the insulation from moisture, vertical drainage was installed (Mangold & Schmidt N.D.).

Experimental concept of pit heat storage from Stuttgart

At the University of *Stuttgart*, Institute of Thermodynamics and Thermal Engineering (ITW), an experimental study of *PTES* was conducted, with the aim of analysing material suitability with regards to moisture permeability and insulating capacity. The study further entailed analysis of the relation between moisture content and thermal conductivity for foam glass and expanded clay, two materials considered for insulation of thermal storages (Heidemann et al. N.D.).

When analysing the results derived from the pilot project it was found that the storage did not perform in accordance with what was expected from modelling, due to the thermal losses exceeding the expected values. The reasons behind the deviation from the original design were brought forward as a combination of multiple parameters. One parameter which may have affected the results was that temperature changes were not included in the design, as well as a lack of insulation beneath the storage. One further parameter that is mentioned as a possible source of error is the lack of information and knowledge regarding design and material properties. These include boundary conditions such as groundwater flows, stratifications and thermal conductivities of materials (Heidemann et al. N.D.).

When analysing the results for the moisture-thermal conductivity relation it was clear that dependency between moisture content and thermal conductivity was present, both for foam glass and for expanded clay. These results are presented in *Figure 2.8* and clearly show that an increase in moisture content causes an almost exponential increase in thermal conductivity as moisture and temperature increases. This shows the need of drainage and protection for the insulating layers from moisture in order to maintain desired thermal properties (Heidemann et al. N.D.).

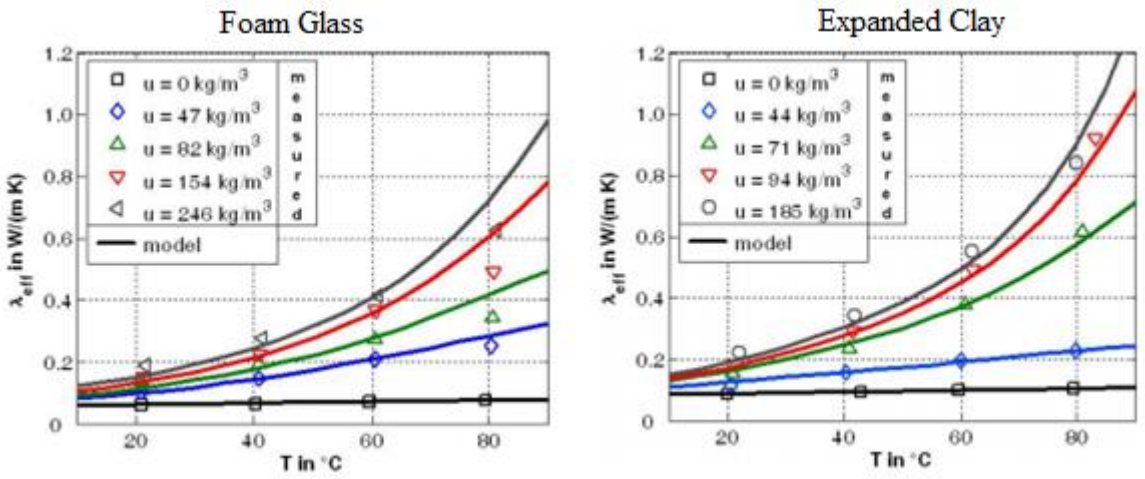

Figure 2.8 – Thermal conductivity of foam glass (left) and expanded clay (right) with regards to moisture content. 50kg/m³moisture content corresponds to approximately 5 volumetric-% for both materials presented in this figure. (Heidemann et al. N.D.)

BTES in Neckarsulm

The *BTES* in *Neckarsulm* is a solar charged storage with a volume of 20 000 m^3, which is an expansion from previous 4300 m^3. The storage configuration consists of 168 double-U-pipes in 30 m deep boreholes. When considering thermal losses in the design of the storage, the depth was limited in order to consider for groundwater movement, and the presence of dolomite layers (having a high thermal conductivity). The storage volume is located in sedimentary rock, consisting of different clay- and limestone. In order to deal with thermal peaks, buffer storage is used (Hahne et al. 1999).

Insulation of the *BTES* was done with 20 cm of extruded polystyrene, extending in a four-metre radius from the boreholes. The insulation was thereafter covered by 2-3 metres of refilled ground material (Hahne et al. 1999).

From the initial design of 4300 m^3, it was noticeable that the heat exchange was not sufficient, as much energy stayed embedded in the bedrock. Advantageous for borehole storage is the possibility of expansion by adding further boreholes, which is why the initial design was just expanded rather than creating a new storage (Hahne et al.1999).

When analysing the system, the results pointed towards that permeable materials show a dry-out effect due to increased temperatures, an effect not prominent for impermeable materials (Hahne et al. 1999). This effect yields the possibility of better maintaining the thermal properties of a permeable insulating layer as the moisture content reduces, and the thermal conductivity follows the same trend, a conclusion drawn from accordance with the results derived from the project in *Stuttgart-Figure 2.8*.

Another factor brought forward by the project was the perspective of the thermal conductivity of the storage itself. Having a greater thermal conductivity within the storage allows for a greater transfer of energy and hence greater possibilities for storage of larger volumes of energy. Although from a charging perspective this might seem beneficial, from a thermal performance perspective it allows for greater thermal losses due to conduction to the surroundings. There

needs to be a balance between the two factors when designing the storage. The experimental study pointed towards the aim of deriving as low as possible return temperatures in order to charge as much energy as possible as a mean of deriving a more efficient heat exchange process (Hahne et al. 1999).

Simulations showed that an increased duct diameter would yield greater heat transfer capacity (Hahne et al. 1999).

2.4.4 Thermal energy storage in Denmark

In *Denmark* the concepts of *Pit Thermal Energy Storage (PTES)* and *High Temperature Thermal Energy Storage (HT-BTES)* are used for thermal storage, the *HT-BTES* concept is found in *Brædstrup*, and the *PTES* concept in *Marstal*, *Dronninglund*, *Gram*, and *Vojens*.

HT-BTES in Brædstrup

In *Brædstrup* a *HT-BTES* was built as a pilot project for the design of commercial distribution of thermal storages. The thermal storage consists of 48 boreholes, connected in series of six boreholes per series, and equipped with double U-tube heat exchangers. The depth of the boreholes was set to 45 metres, in order to avoid interference with the groundwater, which yields the risk of causing significant thermal losses due to groundwater flow. The storage is charged from the centre, and extractions are made in the peripheral parts (PlanEnergi 2013).

The storage is placed in soil and insulated using mussel shells, covered by geotextile - a drainage matt - gravel - and 50 cm of soil. The insulation layer is divided into two layers (25 cm each) with an intermediate sheet of a semi permeable foil to avoid the effect of convection. The moisture content in the insulating layer has varied from 100-80 % from top to bottom, a condition which has been stable throughout the last two years of monitoring (Sørensen & Schmidt 2018).

The insulating material choice regarded the charging temperature and the humidity and was based on experience derived from a previous project in *Crailsheim* (see *section 2.4.3*). Key aspects were that the material should not absorb or retain water, have a low cost, and have a load carrying capacity of more than 30 kN/m^2, for which the mussels (λ=0.112 [W/mK]) were found fulfilling (PlanEnergi 2013).

From the modelling phase in the project, it was concluded that having boreholes in series will result in higher pressure drops, which in turn results in the reduced maximum allowed temperatures in the pipes. This will affect the efficiency of the storage as higher pressure drops will increase the energy demand of the pumps. Connecting boreholes in parallel will result in lower pressure drops, too low of a pressure drop results in difficulties to obtain a uniform flow (PlanEnergi 2013).

PTES in Marstal

In *Marstal* a *PTES* was built, based on a *TRNSYS* system design, with storage temperatures ranging from 17-85 degrees. The storage was kept moisture tight, and insulated with 24 cm of PE-insulation. The insulation was covered with a drainage matt, with the aim of allowing for

ventilation in order to drive out moisture from the insulating layer. This in order of maintaining thermal properties of the insulation, and avoiding water damage (Sørensen & Schmidt 2018).

The thermal efficiency (thermal losses/capacity) of the storage reached 48 %, which was close to the results expected by the *TRNSYS* system design. Providing an investment value of 0.44 €/kWh ≈ 4.4 SEK/kWh (Sørensen & Schmidt 2018).

PTES in Dronninglund

The *PTES* in *Dronninglund* was designed similar to the *PTES* built in *Marstal*. The storage though showed a much reduced thermal efficiency (thermal losses/capacity) of 19 %, which although yielded a very similar investment/capacity-ratio of 0.43 €/kWh (Sørensen & Schmidt 2018).

PTES in Gram Denmark

The project in *Gram* was mainly a mean of increasing the share of solar heating from 16 % to 61 %, which shows the environmental benefits possible with the method. In this project, the price of heat production is shown with an estimated price of 40 €/MWh (State of Green 2018).

PTES in Vojens Denmark

In *Vojens* the world's largest *PTES* was built. The storage aided in achieving more than 50 % of the annual heat production is from solar power. It had a temperature restriction of 80 degrees in order to increase the lifespan of the liner used, bringing the aspect of durability into perspective (State of Green N.D.).

2.4.5 Conclusions and experiences from similar projects

As can be noted from the applications of thermal energy storage these vary largely in design and concept, but with a joint idea of storing a surplus for utilization during a deficit of thermal energy.

The relation between moisture and thermal conductivity brought up in the project in *Stuttgart* (*section 2.4.*3) is one of the key aspects to be implemented in this Master Thesis. It further stresses the importance of limiting moisture in the insulating layers, as well as the importance of drainage. Both for reducing losses and for deriving durability of the system.

The project at *Marstal* (*section 2.4.4*) showed the possibility of designing the storage system using *TRNSYS*, yielding simulated results similar to practical ones. Providing validity to the usage of the *TRNSYS* software for use in the project application of *HT-BTES* analysis.

One factor brought up as problematic is the groundwater aspect. Groundwater flows risk causing excessive thermal losses, a factor which needs to be taken into consideration in the design stages. Similar to this problem is the risk of the presence of highly conductive zones, which also may yield additional thermal losses. These two factors show the importance of good geologic knowledge when designing the thermal storage system.

3 Theory

In order to validate results from the sensitivity study, a theoretical background is to be used as a reference for the validity of the derived results. Hence the theoretical background to the thermal storage process and thermal modelling is presented.

3.1 Thermal process

The thermal process, which is the base of the concept of thermal energy storage, is a complicated process combining global (large-scale) heat flows with local processes surrounding the ducts (boreholes). The large scale heat flows are three-dimensional processes making up the fundamentals of the thermal process. These large scale heat flows are determining for the thermal losses from the storage along with material properties of the material within and surrounding the storage volume (Hellström 1989).

The thermal process governing the concept of thermal energy storage is presented in the following chapter. Starting from the heat transfer from heat carrier fluid to storage volume, followed by the thermal process within the storage itself. To this main theory, secondary aspects are integrated which are hard to quantify or define in exact theory, and hence taking a secondary role.

3.1.1 Transfer of energy from carrier fluid to storage

The storage volume is given thermal energy from a heat carrier fluid passing through the heat exchangers to the bottom of the boreholes, transferring its thermal energy to the storage volume on its way upwards back to the horizontal pipes. As long as a temperature difference is present between the carrier fluid and the surrounding volume heat transfer will take place. In order to create a storage with good thermal efficiency and capacity, it is important that the heat transfer from the heat carrier fluid to the storage volume is efficient. The amplitude of the transfer will depend mainly on the fluid flow rate and the thermal resistance from fluid to the storage volume. If all transient conditions in the heat carrier fluid can be neglected, the equation for heat balance for the heat carrier fluid may be written as *Eq. (1)* (Hellström 1989).

$$C_f q_{fp} \frac{dT}{ds} + \alpha_p (T_f - T_a) = 0 \tag{1}$$

Alternatively

$$C_f q_{fv} \frac{dT}{ds} + \alpha_p (T_f - T_a) = 0 \tag{2}$$

Where

i) C_f equals to volumetric heat capacity of carrier fluid [J/(m^3 K)]
ii) dT/ds denotes the temperature deviation along a flow path increment [°C/m]
iii) q_f equals carrier fluid flow rate [m^3/s]
iv) T_f is the carrier fluid temperature [°C]
v) α is the heat transfer coefficient between the surroundings and the fluid [J/(s m K)]
vi) T_a equals the temperature of the surrounding ground in each point [°C]
vii) The index p denotes a heat balance per unit length of pipe, whilst the index v denotes a heat balance per volumetric unit of the storage volume.

Another factor governing the heat transfer is the damping effects that are present in the solution, a damping factor can be defined as *Eq. 3* (Hellström 1989).

$$\beta = e^{\frac{-\alpha_v V}{C_f Q_f}} = e^{\frac{-\alpha_p L_p}{C_f Q_f}} \quad (3)$$

Where

i) V denotes the storage volume [m^3]
ii) Q_f is the total flow rate [m^3/s]
iii) L_p is the total length of pipe [m]
iv) α_v denotes the heat transfer coefficient when regarding volume [J/(s m^3 K)]
v) α_p denotes the heat transfer coefficient when regarding pipe length [J/(s m K)]

From the expression for damping the outlet temperature from the storage may be written as *Eq. 4* (Hellström 1989).

$$T_{fout} = \beta \cdot T_{fin} + (1 - \beta) \cdot T_a \quad (4)$$

Where

i) T_{fin} denotes the inlet temperature [°C]

The total injected effect (q) to the storage volume can now be written using the results from *Eq. 4* (T_{fout}) as *Eq. 5*, which represents an energy balance of a fluid (Hellström 1989).

$$q = C_f Q_f (T_{fin} - T_{fout}) \quad (5)$$

This can be written as *Eq. 6*, which is applicable for temperature variations along the flow path of the heat carrier fluid (Hellström 1989).

$$q = \frac{C_f Q_f}{V} \cdot (1 - \beta) \cdot (T_{fin} - T_a) \quad (6)$$

3.1.2 Thermal properties governing the thermal process

On a general plane heat transfer is governed by *Fourier's law*, see *Eq. 7* (Thermopedia 2011). This equation shows the parameter dependency of the heat transfer.

$$q = -\lambda \cdot \frac{dT}{dx} \quad (7)$$

Where

i) q denotes the heat transfer [J/(s m^2)]
ii) λ denotes the thermal conductivity of the material. [J/(s m °C)]]
iii) dx denotes the distance over which the temperature difference dT is present. [m]
iv) dT denotes the temperature difference over the distance dx. [°C]

Heat transport in soils is governed by a number of mechanisms for the transferal of thermal energy. These mechanisms are mainly (see *Figure 3.1*):

- Conduction in solids (1)
- Conduction in air (2)
- Radiation between particles (3)
- Diffusion of water vapour (4)

- Convection in pore air (5).

These mechanisms are themselves influenced by the material properties of density, porosity and water content of the material (Johansen 1977).

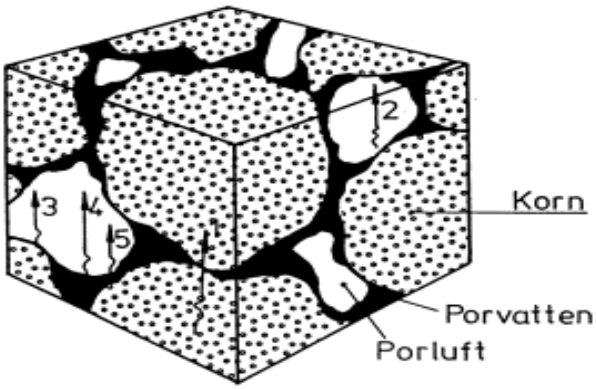

Figure 3.1 - Mechanisms for heat conduction in soil and rock. 1. Conduction in solids. 2. Conduction in air. 3. Radiation between particles. 4. Vapour diffusion. 5. Convection in pore air. Porluft-Pore air, Porvatten-Pore water, Korn-Grain (Sundberg 1991).

The aspect of diffusion is also something brought forward by *Johansen* (1977) as this is caused by variations in water vapour pressure in the pores of a material. The water vapour diffusion in the air is determined by Fick's law which is influenced by both moisture and temperature variations. Together the aspects of moisture end temperature tend to yield a larger diffusion in moist soils than that obtained when only considering diffusion in a gas. Diffusion of water vapour will contribute to heat transport in the form of latent heat exchanged during vaporization and condensation, thus yielding increased thermal conductivity for increased diffusion. The diffusion itself is as mentioned temperature and vapour pressure dependent. The vapour pressure has an exponential increase with temperature yielding potential for rapid increases in thermal conductivity with increasing temperatures.

Forced convection due to currents in the material will yield possibilities for increased heat transport which also is present for free convection which is dependent on the upward motion of water, due to density changes with temperature. If porous materials are not protected from water infiltration, this can yield flow circulation in the layer (as illustrated in *Figure 3.2)*, resulting in unwanted, accelerated heat transport, *Johansen* (1977). In order to limit the effects of convection impermeable layers can be used, something which was implemented in *Brædstrup* as a semi impermeable foil was placed in the middle and on top of the insulation layer (PlanEnergi 2013).

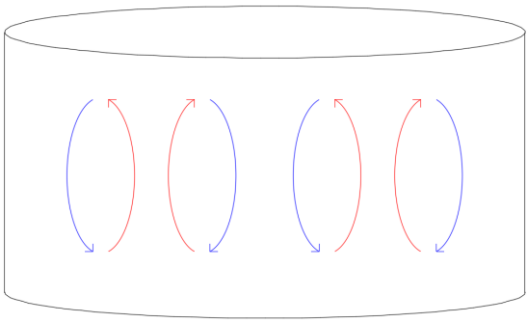

Figure 3.2 – Convection in medium.

At temperatures of around 0 degrees, conduction is the dominating mechanism for heat transport in a material, for materials with high water content the latent heat released from phase shifts in water is of great importance. From 0-25 degrees conduction is still the dominating mechanism if not convection is to become dominant in highly permeable materials. The concept is also applicable between 25 and 95 degrees with convection taking a larger role in permeable materials (Sundberg 1991 and Johansen 1977).

The main properties that are of interest for heat conduction, and storage, are thermal conductivity and specific heat capacity. The thermal conductivity is highly dependent on the density, water content, and mineral composition of a material. When water is present within a material it takes up space otherwise filled by air, and increases the contact between the particles, yielding higher thermal conductivity as water is a better conductor than air. Larger porosities tend to yield lower thermal conductivities as less direct conduction takes place. The mineral composition is highly influential as it governs the properties for conduction in the solids. In soils, the aspect of frozen and not frozen water is also an affecting factor, where frozen soils tend to yield higher thermal conductivities than unfrozen ones. Also, the heat capacity tends to be lower for frozen soils compared to unfrozen ones. (Sundberg 1991) Further aspects of this brought forward by *Carslaw & Jaeger* (1959) is that the thermal conductivity changes with temperature, making for a more complicated process.

Also, time variant thermal properties are possible due to shifts in the parameters above or other time dependent factors (Clarke & Hamdhan 2010).

A further aspect that is influential on the thermal properties of a material is the presence of anisotropy, it could be in the form of material layers or fracture zones (Sundberg 1991). Fracture zones can themselves conduct water risking greater thermal losses in a thermal storage, this represents forced convection due to groundwater flow and may have a serious effect on the thermal conductivity and is heavily dependent on the permeability (Johansen 1977). Another aspect of thermal conductivity is temperature. Increased temperatures tend to yield lower thermal conductivities in rock, but increased values in unsaturated soils (Sundberg 1991).

From the information above it can be identified that in order to derive exact thermal properties for large volumes many tests would have been needed. Hence the approach of choosing a representative material volume is required, from which the properties can be derived (Sundeberg 1991).

In the reference project at *Filborna*, a sedimentary bedrock makes up the majority of the thermal storage. As brought up by Sundberg (1991) the porosity of the bedrock can vary greatly and since a lack of tests limits the knowledge of individual layers a representative storage volume is chosen for which thermal properties are derived via thermal response tests.

3.1.3 Local thermal process

The main problem for the analysis of the thermal problem is the interaction between the local thermal processes and the global thermal process including the storage and the surrounding ground. As a consequence of this, a detailed description of the local thermal process is needed in order to obtain the right amount of injected and extracted heat to/from the total system. The heat transfer is governed by the fluid temperature in the heat exchangers, the heat transfer properties and the temperature in the ground surrounding the duct (Hellström 1989).

Area of influence

The analysis of the local thermal process is based upon the premise that each duct is designated an area of influence (A_P), within which the heat exchange from the duct will have an impact. This area is itself dependent on the spacing between the boreholes (B), from which an influential radius can be calculated as shown in *Eq. 8* (Claesson et al. 1985).

$$r_1 = 0.525 \cdot B \tag{8}$$

Where

i) B denotes the borehole spacing [m]

The region within which the local thermal process is assumed influential is assumed to be within the region of $r_b \leq r \leq r_1$, where r_b denotes the outer radius of the heat exchanger pipe and r the radial distance from the centre of the pipe (Hellström 1989).

Temperature variations – Initial stages

The initial temperature variations around one heat exchanger are the same as for if being placed in an infinite surrounding. After a certain time influence from the surrounding heat exchangers will have an effect and the temperature process changes character. The temperature in the ground region assigned to one specific heat exchanger is named as local average temperature (Claesson et al. 1985).

The heat flow from the heat exchangers to the surrounding ground is dependent on the temperature differences as well as the thermal resistance between different sections. This is the basis of analysis for the thermal process relation. When analysing the analytical solution for a constant effect from the heat exchangers a solution as presented in *Figure 3.3* (T_c denotes the average temperature in the medium before storage) is derived. This shows the characteristic temperature variations in the cylindrical region surrounding the heat exchangers when no influence from surrounding heat fields caused by heat exchangers is affecting the local region (Claesson et al. 1985). T_c denotes the initial temperature for the region around each pipe. The influence of the outer boundary of each borehole, denoted r_1, can be neglected during the initial stages of the heat transfer. In the time of the first period, no interaction between boreholes is

accounted for. During these phases, the heat transfer can be seen as acting in an infinite surrounding and the solution is given as a heat transfer in a solid medium (Hellström 1989).

As mentioned the effects from surrounding heat fields can be neglected as long as no thermal transfer takes place over the boundary of the influenced cylinder. The time it takes for the solution to change character, in other words until the heat transfer across the outer boundary (R1) no longer can be neglected, is approximated by *Eq. 9* below yielding the time after which the character changes (Hellström 1989).

$$t_{lim} = \frac{0.2 \cdot r_1^2}{a} \tag{9}$$

Where

i) $a = \lambda / C$ [m^2]
ii) λ denotes thermal conductivity [W/(m K)]
iii) C denotes volumetric heat capacity [J/(s m^3 K)]

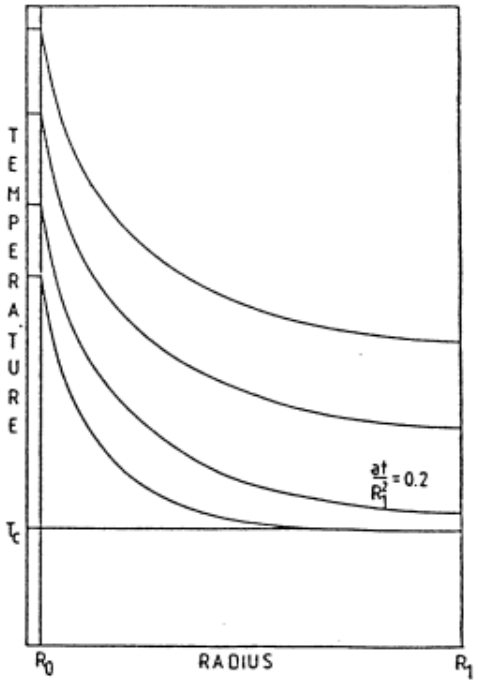

Figure 3.3 – Temperature profile for the local solution (Hellström 1989)

Temperature variations – Steady-flux conditions

Steady flux entails a constant transfer of energy. The temperature increase is given by the following expression (*Eq. 10*) as a linearly increasing temperature at the outer boundary after the initial character process is done (Hellström 1989).

$$T_m(t) = \frac{q \cdot t}{\pi \cdot C \cdot r_1^2} \tag{10}$$

Where

i) q denotes the heat injection rate [J/(s m)]
ii) t denotes the time [s]

When the heat-flux in each point constant in time we have reached a steady-flux regime. The fluid temperature is in the steady-flux segment is given by *Eq. 11* (Hellström 1989).

$$T_f(t) \cong T_m(t) + \frac{q}{2 \cdot \pi \cdot \lambda}\left(2 \cdot \pi \cdot \lambda \cdot R_b + \ln\left(\frac{r_1}{r_b}\right) - \frac{3}{4}\right) \tag{11}$$

Where

iii) R_b denotes the total thermal resistance per unit length of the pipe, between fluid and ground at r_b [(s m K)/J]

The heat injection becomes proportional to the temperature difference between the temperature of the fluid (T_f) and the mean temperature of the storage volume (T_m) as the following (Hellström 1989).

$$\frac{q}{\pi \cdot r_1^2} = \frac{\lambda \cdot (T_f - T_m)}{l^2} \tag{12}$$

Where the characteristic heat transfer length between the fluid in the pipe and the surrounding ground is given by the following (Hellström 1989).

$$l = r_1 \cdot \sqrt{\frac{1}{2} \cdot \left(\ln\left(\frac{r_1}{r_b}\right) - \frac{3}{4} + 2 \cdot \pi \cdot \lambda \cdot R_b\right)} \tag{13}$$

3.1.4 Global process

The global process is essentially the combination of the interaction of heat conductivity problems within and outside the storage volume and how these interact. (Hellström 1989)

The global solution is based on a model of the storage volume and a sufficient segment of the surrounding area. The model is designated thermal properties, volumetric restrictions, duct information, insulation and temperature data. Thermal conductivity and volumetric heat capacity are properties representing the thermal properties of the ground. Within the storage volume itself, the properties are assumed homogenous throughout the entire storage volume. Outside the storage volume, the ground is stratified after geologic conditions where each layer is designated individual properties (Hellström 1989).

Apart from the ground conditions the top of the storage is of great importance for the global process, especially when considering shallow *Borehole Thermal Energy Storages* with a large top influence area. Here insulation may be placed and time varying temperature is to act (Hellström 1989).

Complicating the process is the anisotropic conditions present, making models more complicated than if a homogenous material would be present. This aspect may be considered by the storage volume being modelled as one homogenous material in order to simplify calculations. But in order to get good results from this, it is needed that the boundary conditions stated are representative of the actual ones (Hellström 1989).

Thermal properties

Thermal properties which can be modified for the model are thermal conductivity and volumetric heat capacity. In the currently existing *DST-model*, a homogenous storage volume is presumed. Hence an average value for both of these parameters is given. For the ambient ground, the properties may vary for multiple horizontal layers, note that no inclination concerning the horizontal layers can be modelled for the ground surrounding the storage (Hellström 1991).

Volumetric restrictions

The total volume, and its shape, is of interest when determining the maximum capacity of the storage and the losses. The shape of the storage unit will determine the effective surface which will affect the heat exchange with the surrounding ground. In order to achieve the most effective surface of a volume, a spherical profile is the most favourable shape to mimic. For a storage unit with vertical borehole, this is not possible to obtain, hence a cylindrical shape is the most effective shape (Hellström 1991).

Insulation

Insulation can be installed anywhere along the top surface of the storage and beyond its edges and along the sides of the storage unit all the way down to its bottom. Since the insulation layer is usually thin and represents a small part of the total volume in comparison with the rest of the components in the model. This is the argument behind that the simulation model only considers for thermal heat transfer through the insulation material and neglects its thermal capacity since its capacity is neglectable in the entirety of the storage.

Temperature

The thermal energy storage will be influenced by the surrounding temperatures, which are present as the ambient temperature of the air and the effect it has on the ground surface above the storage unit. The second heat source that will affect the store is the ground temperature. These two are dependent on each other if the thermal energy storage runs deep the contribution from the ambient air temperature variation will not to a large extent affect the store hence the ground temperature will have a greater influence.

Heat balance

The heat balance for a given cell in the mesh of the storage unit is simply described by the relations presented in *Eq. 14-15*. These equations describe the heat flows to a specific cell, based on a heat conduction parameter (K), and the temperature variation from previous cells (T). When the net flow to a cell is greater than zero the temperature in this cell will rise, and when the net flow is below zero the temperature in the cell will decrease. The temperature change is dependent on the volumetric heat capacity (C). In *Eq. 14-15* the radial (F_r), and vertical (F_z), heat flows are presented (Hellström 1989).

$$F_r(i,j) = K_r(i,j) \cdot [T(i,j-1) - T(i,j)] \quad (14)$$

$$F_z(i,j) = K_z(i,j) \cdot [T(i,j-1) - T(i,j)] \quad (15)$$

Where:

i) K_r represents the heat conductance between the radial cell (i-1,j) and (i,j)
ii) K_z represents the heat conductance between the vertical cell (i-1,j) and (i,j)

In order to calculate the temperature in a cell, two heat sources have to be considered, the contribution from the local problem (*section 3.1.3*), and the redistribution of heat within the storage due to the circulation of carrier fluid within the storage district loop. When considering the heat flows, the contributions from the heat source and boundary conditions the final temperature in a cell can be calculated via *Eq. 16* (Hellström 1989).

$$T(i,j)_{t+\Delta t} = T(i,j)_t + [F_r(i,j) - F_r(i+1,j) + F_z(i,j) - F_z(i,j+1) + Q_l(i,j) + Q_{sf}(i,j)] \cdot \Delta t / C(i,j) \quad (16)$$

Where:

i) Δt is the time step [s]
ii) $Q_l(i,j)$ denotes the net heat contribution from the local solution
iii) $Q_{sf}(i,j)$ denotes the net heat contribution from redistribution of heat due to circulation of heat carrier fluid within the storage

3.1.5 Steady-flux problem

Heat injection/extraction for long periods of time is a central process in the thermal analysis of *BTES*. The thermal properties remain constant once one takes the interaction between boreholes into account when the injection/extraction rate is constant over long periods of time. This implies that the deviation between local mean temperature, and carrier fluid temperature, is constant, and a steady-flux state has been reached (Hellström 1991).

Steady-flux solutions are derived from a visualisation of a two-dimensional plane, which is perpendicular to the pipe direction. The solution will be dependent on the type of heat exchanger and if there are multiple channels interacting with each other. The aspect of multiple channels is most interesting when using U-tube solutions for the heat exchangers since multiple U-tubes can be installed in one borehole. This multiple channel aspect is also highly influential when U-tube solutions are used in soil, due to the possibility of a close arrangement. The process will also consider for temperature variations of the carrier fluid along its flow path due to heat exchange with the surrounding storage volume (Hellström 1991).

The steady-flux analysis only considers the distribution of thermal energy within the boundaries of the storage unit. This due to that after a certain point in time the surrounding ground will have a constant temperature, yielding minor constant, or no, exchange with the storage unit (Hellström 1991).

The heat flow will as a consequence become constant over time, yielding linear behaviour of temperature decreases and increases, due to constant behaviour between the fluid temperature, the average local temperature and the heat injection/extraction rate according to the relation presented in *Eq. 17* (Hellström 1991).

$$T_f - T_m = q\, R_{sf} \quad (17)$$

Where:

i) T_f is the fluid temperature [°C]
ii) T_m is the average local temperature [°C]
iii) q is the heat injection/extraction rate [J/(s m)]
iv) R_{sf} is the thermal resistance between the heat carrier fluid and the storage [(K s m)/J]

The temperature of the heat carrier fluid will vary along its flow path, due to heat exchange with the surrounding storage unit. Along the vertical of the heat exchangers, there will be a point where the temperature of the downwards flow is the same as the temperature of the upwards flow. Because of the difference in direction, this phenomena risks generating a reduction in efficiency of the heat exchange with the surrounding, due to an interaction between the up and downward flows. This phenomenon has been documented by *Hellström* (1991) for the case when a coaxial heat exchanger is used. The relation for the interaction between flow channels is expressed as *Eq. 18-19* (Hellström 1991).

$$T_{f1}(z,t) = T_{f1}(0,t)f_1(z) + T_{f2}(0,t)f_2(z) + \int_0^z T_b(\varsigma,t)f_4(z-\varsigma)d\varsigma \tag{18}$$

$$T_{f2}(z,t) = -T_{f1}(0,t)f_2(z) + T_{f2}(0,t)f_3(z) - \int_0^z T_b(\varsigma,t)f_5(z-\varsigma)d\varsigma \tag{19}$$

Where:

i) $f_1(z) = e^{\beta z}[\cosh(\gamma z) - \delta \sinh(\gamma z)]$
ii) $f_2(z) = e^{\beta z}\frac{\beta_{12}}{\gamma}\sinh(\gamma z)$
iii) $f_3(z) = e^{\beta z}[\cosh(\gamma z) + \delta \sinh(\gamma z)]$
iv) $f_4(z) = e^{\beta z}\left[\beta_1\cosh(\gamma z) - \left(\delta\beta_1 + \frac{\beta_2\beta_{12}}{\gamma}\right)\sinh(\gamma z)\right]$
v) $f_5(z) = e^{\beta z}\left[\beta_2\cosh(\gamma z) + \left(\delta\beta_2 + \frac{\beta_1\beta_{12}}{\gamma}\right)\delta\sinh(\gamma z)\right]$
vi) $\beta_1 = 1/\left(R_1^{\Delta}C_fV_f\right)$
vii) $\beta_2 = 1/\left(R_2^{\Delta}C_fV_f\right)$
viii) $\beta_{12} = 1/\left(R_{12}^{\Delta}C_fV_f\right)$
ix) $\beta = \frac{\beta_2-\beta_1}{2}$
x) $\gamma = \sqrt{(\beta_1+\beta_2)^2/4 + \beta_{12}(\beta_1+\beta_2)}$
xi) $\delta = \frac{1}{\gamma}\left(\beta_{12} + \frac{\beta_1+\beta_2}{2}\right)$
xii) $R_1^{\Delta} = R_{fao} + R_p' + R_c$
xiii) $R_2^{\Delta} = \infty$
xiv) $R_{12}^{\Delta} = R_{fc} + R_p' + R_{fai}$
xv) C_f denotes the thermal heat capacity of the fluid [J/(m^3 K)]
xvi) V_f denotes the volume of the fluid [m^3]

xvii) T_b represents the temperature of the ground outside the borehole wall at each node in the mesh surrounding the duct [°C]

In the calculation process presented above, the R components ($R_1^{\Delta}, R_2^{\Delta}\ and\ R_{12}^{\Delta}$) denote thermal resistances. These are dependent on the convective heat transfer resistance, where R_{fc} is the resistance between the fluid in the heat exchanger pipe and the surface of the inner heat exchanger pipe. R_{fai} corresponds to the resistance between the fluid in the borehole pipe outside the heat exchanger and the surface of the outside material of the heat exchanger. R_{fao} represents the resistance between the fluid in the borehole pipe outside the heat exchanger and the borehole casing. The R_p' represents the resistance of the heat exchanger, or the borehole pipe, depending on which thermal resistance is to be calculated. R_c denotes the contact resistance between the borehole liner and the borehole wall.

The reason why the thermal resistance parameter $R_2^{\Delta} = \infty$ is because there is not a direct connection between the flow channel in the heat exchanger and the borehole wall, which implies that the β_2 factor can be neglected in the temperature calculations.

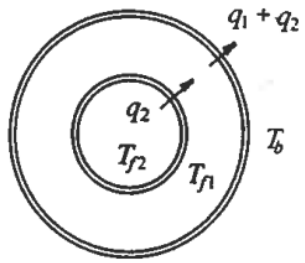

Figure 3.4 – The heat exchanger is constructed using two pipes with an air gap between them in order to insulate the pipe to minimize the interaction between the downwards flow and the upwards flow (Hellström 1991).

The steady-flux problem is used in the modelling process to implement redistribution of heat within the storage volume due to the circulation of the carrier fluid during constant injection/extraction rates. This gives information regarding temperature fields around each pipe. Unlike the local thermal problem presented in *section 3.1.3*, the steady-flux problem depends on temperatures in each individual cell, while the local problem depends on the mean temperature in the sub-region. The temperature for an individual cell can be calculated using *Eq. 20* for each time-step considering the precondition mentioned regarding constant injection/extraction rates (Hellström 1991).

$$T(x, y, z, t) = T_{sf}(x, y, z) + \frac{qt}{C_T} \tag{20}$$

Where

i) T_{sf} represents the temperature of the spatial coordinates [°C]
ii) q is the total heat injection rate to the region of interest [J/(s m^3)]
iii) C_T describes the heat capacity of the region [J/(m^3 K)]

There will be no heat flux over the boundaries of the local region around each borehole, this due to symmetry, this is illustrated in *Figure 3.4*. During the steady-flux problem, the net energy which is contributed to each sub-region in the global problem from the steady-flux part is zero. This is described via the calculation path (*Eq. 21-24*) below (Hellström 1991).

For a region, V, the following expression can be written for the thermal heat capacity.

$$C_T = \int_V C(x,y,z)\, dxdydz \tag{21}$$

The expression for temperature over time in each cell can be rewritten using the equation for general heat balance with constant thermal properties $\nabla^2 T = \frac{1}{a}\frac{dT}{dt}$ to *Eq. 22* (Hellström 1991).

$$\nabla^2 T_{sf} = \frac{Q}{\lambda C_T / C} \tag{22}$$

The heat capacity (C) can be set constant, and for the steady-flux problem, the net heat flow will be set to zero, whereas *Eq. 23* applies (Hellström 1991).

$$\int_V C(x,y,z) T_{sf}(x,y,z) dxdydz = 0 \tag{23}$$

For cases where the heat capacity is constant, *Eq. 23* (above) can be simplified to *Eq. 24*, which concludes that the average temperature flux of a steady-flux problem is zero (Hellström 1991).

$$\int_V T_{sf}(x,y,z)\, dxdydz = 0 \tag{24}$$

3.1.6 Super positioning of temperature components

The temperature at a given point is given as a superposition of a global solution, a steady-flux solution around the nearest pipe and a local radial solution (Hellström 1989).

$$T = T^k_{g,i,j} + T^k_{l.j'} + T^k_{s,f,j'} \tag{25}$$

3.1.7 Secondary effects of the thermal process

The thermal behaviour of the storage may secondarily be affected by site-specific factors. One factor brought forward by *Hellström* (1989) is groundwater flows. This factor is dependent on the porosity of the material, and fractures and fissures in rock materials, yielding potential for substantial thermal losses. According to *van Myers* (Hellström 1989), groundwater flows as low as 50 mm/day yield the risk of substantial effects on the efficiency of an underground thermal energy storage. Hence reducing measures may be required if groundwater flows are of this magnitude or larger. Another factor having potential effects on the thermal behaviour of the storage is the presence of water in the ground, due to saturated material showing natural convection due to the density dependency on the temperature of the water. This effect is dependent on the type of material and its' porosity, as the material properties (porosity and permeability) limit the possibility for convectional flows of water within the ground. This effect

will be influential on the thermal storage if the permeability exceeds approximately 10^{-12} m^2. Natural convection will though be hindered by the presence of horizontal impermeable layers, such as clay, solid rock, and other none permeable layers. Presence of water will also influence the thermal properties of materials. Low water content is to strive after in the unsaturated zone of the storage since an increased content of water will act negatively on the thermal properties. Hence the capacity and efficiency of the storage will decrease (Hellström 1989).

The effect of the heat capacity of the carrier fluid is a factor which often can be neglected (Claesson et al. 1985).

3.2 Thermal modelling

The main segment of this Master Thesis entails the creation of a simulation model of a thermal storage facility which can be used for analysing the system design with regards to alterations of parameters affecting the efficiency and performance aspects of a thermal energy storage. It is from this model that results are to be derived upon which the further analysis of optimization of design and cost is to be performed. For this thermal modelling, the *TRNSYS* software was used. This software allows for simulations of transient heat problems, which conforms to the desired properties of such a program.

3.2.1 Transient thermal modelling

The modelling is performed within the *TRNSYS* program which uses *types* (modules) for the representation of different parts in a storage system, such as pumps, pipes and heat exchangers. These *types* use a multitude of inputs, giving them desired properties, and are linked together as a mean of deriving a system in which a component is dependent on output information from a previous component.

When designing a *TRNSYS* model of a thermal storage, one of the key components is the *type* representing the thermal storage itself. This component derives its properties from a *Duct Ground Heat Storage Model* which is described by *Hellström* (1989 & 1991).

Parameter dependence of thermal storage design

The depth of the storage relates to the extent to which the boundary conditions at the top of the storage needs to be taken into account. Deeper storage can neglect variations in boundary conditions in the surface, but for shallow storage, these need to be taken into account. A change in water content will though influence the performance of layers with regards to thermal properties. Minor variations in thermal properties are neglectable as long as they are not close to a duct, as the latter will affect the local thermal transfer process (Hellström 1989).

Thermal modelling using g-function

The analytical method to solve this kind of problem is split into two problems, short-term and long-term. The short-term performance of a borehole field is handled using the duct storage model made by *Hellström 1991* (Biancucci 2015).

The long-term performance of a borehole field is modelled using the cylindrical heat source by *Carslaw & Jaeger* (1959), which is built upon the first model *Infinite Line Source* made by *Ingersoll* in *1954*. In order to make the model conform better to reality, *Eskilson* introduced the

g-function in the 1980s, which is a dimensionless thermal response factor. The function is defined by the relation presented in *Eq. 26*. This function addressed the problem the previous model had regarding heat transfer in the radial direction from boreholes, as well as to deal with short time responses. The function contributes to the calculation of the thermal response of the symmetrical borehole field with regards to the influence of surrounding boreholes and the ground (Biancucci 2015).

$$Tb(t) = Tg + \frac{q(t)}{2\,\pi\,\lambda} \cdot g\left(\frac{t}{t_s}, \frac{r_b}{H}, \frac{B}{H}, \frac{d}{H}\right) \tag{26}$$

Where

i) Tb is the average borehole wall temperature [°C]
ii) Tg is the temperature of the undisturbed ground [°C]
iii) q(t) is the heat extraction [W/m]
iv) λ is the thermal conductivity of the ground [W/(m K)]
v) $g\left(\frac{t}{ts}, \frac{rb}{H}, \frac{B}{H}, \frac{d}{H}\right)$ is the g-function which is dimensionless

The g-function is dependent on the relation between t/t_s where t_s is the characteristic time of a borehole field, r_b which is the borehole radius, B which denotes the distance between the boreholes, d that is the active borehole length of the storage unit and H which is the total length of the borehole (Biancucci 2015).

The computation of the g-function has later been remodelled in order to simplify it, reduce calculation time, and improve it a number of times. One of the changes which had the most impact on the result was to utilize the mean temperature along the length of the borehole instead of the temperature at its centre. A greater emphasis has also been placed on the transition between short- and long-term thermal responses (Biancucci 2015).

3.3 Potential environmental effects of the thermal storage

As a concept, *BTES* is seen as environmentally beneficial, but there are still environmental implications. When analysing the whole system of a *BTES*, factors such as energy demand for pumps and other necessary components needed in order to run the system will have environmental effects. This adds an energy demand to the system, whilst the thermal process itself will have environmental implications, mostly on the groundwater (Malmberg 2017).

3.3.1 Potential effects on groundwater from BTES

As a large amount of thermal energy is to be stored in the ground, this brings the possibility of a temperature rise in the groundwater. This could yield the risk of affecting the microbiology in the groundwater (Malmberg 2017).

York et al. (1998) performed a study at *Richard Stockton College* to assess the impact of thermal injection into a 130 m deep borehole. From the study, a growth in the total amount microorganisms when the temperature increased was observed. It was also detected for sites where no increase in the total amount of microorganisms occurred, that there were some changes in the biodiversity of organisms which strengthens the proclamation that fluctuation of temperature in the groundwater affects the microorganisms (York et al. 1998).

While a later study made by *Bonte et al.* (2011) made a different conclusion after their research. According to this study, no significant growth in microbial biomass was detected. However, a greater variety of species were found, suggesting that it is due to the fact that some organisms flourish in environment and temperatures where others do not. That there are other reasons why the quantity of organisms does not noticeably increase, that it is highly dependent on factors like nutrition and oxygen (Bonte et al. 2011).

A similar study was performed in France by *Garnier et al.* (2011) during the same time period as *Bonte et al.* (2011) performed theirs. The results from this study were that no increase in bacterial activity as an effect of thermal injection/extraction was observed. This strengthens the conclusions made by *Bonte et al.* (2011) regarding the effects on growth of microorganisms with increased temperatures, but questions the claim that the diversity of organisms changes.

3.3.2 Potential environmental risks from implementing a heat pump

If a heat pump is to be installed to complement the storage unit, in order to increase the efficiency of the planned *BTES*, it is of importance to identify the environmental effects it may have and not just the increase in efficiency and amount of energy which can be extracted. One must identify how much energy the heat pump requires to operate as well as if there is a potential risk if there will be a malfunction in the machine. One key aspect to keep in mind when determining which heat pump to use when discussing potential environmental risks, is the refrigerant medium component used in the device. There are two main aspects when discussing refrigerant fluid, it is the Global Warming Potential (*GWP*) and Ozone Depleting Potential (*ODP*) for the fluid. Currently, both of these kinds of refrigerants are slowly being replaced by fluids with lower, or zero, *GWP* and *ODP* with other new synthetic refrigerants. Since the newer mediums have not been tested in the same range as the older their consequences on the environment is often unknown. Hence there will be an unpredictable risk using these mediums as potential risks for leakage and spill are present (Forsén 2005).

4 Insulation approach to thermal energy storage

Central to the aim of this Master Thesis is the analysis of how the insulation aspect is to be approached when designing *High Temperature Borehole Thermal Energy Storages*. This insulation aspect is mainly comprised of two perspectives, the first entails insulation design, and the second regards the choice of insulating material. The design perspective mainly regards how the thermal storage is to be insulated with regards to top insulation. While the design perspective analyses how layers are to be placed and geometrically designed, the material perspective relates to the properties which this insulating layer is to possess. This material perspective is approached from an investigatory perspective where the reference project at *Filborna* and the reference projects presented in *2.4* are used for finding material alternatives for analysis. Both perspectives of the insulation aspect aim towards finding an optimized solution with regards to thermal performance, as well as economic and environmental parameters.

4.1 Insulation design

The insulation design perspective of *borehole thermal energy storage* mainly entails the design of the top insulation layer. Secondarily this perspective includes insulating methods, not related to top insulation, used for reducing thermal losses from a *borehole thermal energy storage*. The top insulation is external insulation (placed outside/on top of the storage volume), whilst the secondary insulation aspects can be both internally, and externally, placed.

4.1.1 Top insulation design

Top insulation is the common denominator for insulation placed on top/around the storage volume. There are mainly two conceptual design alternatives for top insulation, which are presented in *Figure 4.1*. Design alternative A consists of a horizontal insulating layer of homogenous thickness placed on top of the storage volume, this may extend beyond the outer boundary of the surface of the storage if this is desired. Design alternative B is made up of a homogenous horizontal layer being placed on top of the storage volume, and which "folds down" along the outer boundary of the storage volume (Hellström 1989).

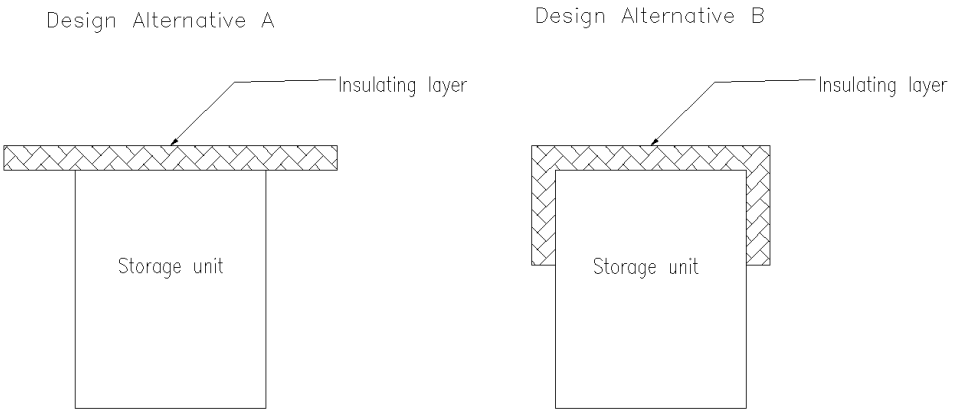

Figure 4.1 – Alternatives for top insulation. Alternative A shows a horizontal insulation layer with a certain width and thickness. Alternative B shows the insulation being designed to "fold" down the sides of the storage volume to a certain depth.

Understandable from the design alternatives presented in *Figure 4.1* design alternative B comes with additional constructional challenges, when compared to alternative A. In this Master

Thesis design alternative A was investigated. A reason why alternative B is ruled out comes from the preconditions, as well as the additional excavation work needed for alternative B. For a storage of the size as in the reference project this work would have to be very substantial in order to fully enclose the desired segment of storage volume. This would be very cost and time demanding, as well as requiring for a more complicated design for the vertical insulation, as vertical placement of material requires sequential filling if the thickness is to be kept constant to save on material.

In order for the top insulation to maintain its insulating properties, and derive sufficient durability, the aspect of moisture protection is brought forward as critical in several of the existing projects. The project in *Stuttgart* (*2.4.3*) showed that increased moisture content tends to yield an increase in thermal conductivity of a material, hence reducing the insulating properties. In *Brædstrup* (*2.4.4*) it is presented that if not insulated from moisture properly, the moisture contents will risk becoming very high in the insulating layers. The alternatives used for moisture protection could be identified as very varying between different projects. In *Brædstrup* and *Marstal* (*2.4.4*) a drainage matt was used, with the aim of providing ventilation of moisture from the insulating layer. While in most other projects the layers were separated by geotextiles from other material. It can be assumed that it was relied on that the coarseness of the materials would drain excess water, as well as that the dry-out effect (as seen in *Neckarsulm 2.4.3*), due to increased temperatures, would reduce moisture content in the material. In the reference project at *Filborna*, an impermeable matt is to be placed around the insulating material, in order to prevent moisture infiltration. This solution is heavily dependent on the property of none-permeability of the matt, and prevention of moisture from entering the layer during the construction stages, which otherwise risks trapping moisture.

4.1.2 Secondary insulation aspects

Secondary aspects identified having a significant effect on the thermal performance of the storage comes from the projects in *Brædstrup* (*2.4.4*) and *Crailsheim* (*2.4.3*). In *Brædstrup* the borehole depth was limited, as not to be in contact with the groundwater. Something brought forward in the projects as a potential risk for additional thermal losses. From the project in *Crailsheim*, the problem of highly conductive zones in the ground was brought forward. These showed potential for additional thermal losses as energy was conducted away from the storage more easily.

Groundwater flows

Hellström (1989) states that groundwater flows as low as 50 mm/day risk causing substantial thermal losses. Hence this needs to be considered for in the modelling, and evaluation of thermal storages where this is present. (*3.1.7*)

In order to limit the thermal effects of groundwater flows it is brought forward in the project in *Brædstrup* (*section 2.4.4*) that the borehole depth can be limited. Something which entails shallower storage, for which the effects are evaluated in the sensitivity study of this thesis.

There are methods for reducing groundwater flows, such as injection. The effects of this is unknown as no implementation of injection methods in thermal energy storage can be found in the litterature.

Highly conductive zones

When highly conductive zones are present, they risk diverting thermal energy away from the storage at a higher rate than predicted for the storage volume material. In order to limit the effects from this, it is brought forward by *Mangold et al.* (2007) that a protective casing can be used, as in the *Crailsheim* project (*2.4.3*). This casing insulates the borehole at the segment of high conductivity, hence reducing the thermal loss effects at this point by not having direct heat exchange with the highly conductive zone.

Remarks on secondary aspects

Identifiable in the secondary aspects brought forward is that they require high knowledge of geological, and hydrogeological, conditions. As this information is very site dependent only conceptual solutions can be presented. Neither in the reference project at *Filborna* information to a sufficient extent can be found regarding the geological or hydrogeological conditions. This limits the project to excluding these aspects from the feasibility study included in this Master Thesis, hence only considering them on an analytical plane.

4.2 Insulating material

The material analysis entails the investigation of suitability, and thermal performance, of material alternatives for top insulation design. This analysis aims to provide a basis for the analysis of thermal performance in relation to material properties. By implementing a material perspective economic and environmental aspects can be integrated into the thermal performance analysis, broadening the analysis.

Possible material alternatives were identified from the existing projects (*2.4*), as well as from preconditions given for the reference project at *Filborna*. These material alternatives include: Slag gravel (preconditions from *Filborna*), foam glass (used a lot in thermal storage in *Germany-2.4.3,* and *Emmaboda-2.4.1*), expanded clay (investigated in the project in *Stuttgart, 2.4.3*), and polystyrene (used in *Neckarsulm, 2.4.3,* and *Okotoks, section 2.4.2*). In the following, the materials identified are analysed regarding insulating properties, which are to be implemented in the modelling of the reference project at *Filborna.*

4.2.1 Slag gravel

Slag gravel is a material alternative given in the preconditions for the reference project at *Filborna*. Slag gravel is a bi-product from the incineration process used for energy production at the cogeneration plant at *Filborna*. The material analysed in this Master Thesis comes from the cogeneration plant at *Filborna*, where the reference storage is to be located. The desire to use this material for insulation is based in its current limited possibility of use, as well as since it is a locally produced bi-product it would, in this case, be practically without cost. As a consequence of the variations in incinerated material, the material properties of the slag gavel show great potential for variance (see *appendix B*). The thermal property evaluation of this material is performed by thermal conductivity tests, complemented with a sieving test and a minor water absorption test.

Thermal properties of slag gravel

The variances in material properties of the slag gravel are identifiable from the performed thermal conductivity tests, see *appendix B.* These variances may be related to granular

distribution, see *appendix C*, as well as material composition, due to variances in incinerated material.

The main alternatives for insulation using slag gravel, as given by preconditions, were the "3-6" and "6-24" samples. The "0-3" sample was to be used for the embedding of the horizontal pipe system. The sample of "3-6" showed a thermal conductivity of 0.29 [W/m K], and the "6-24" sample showed a thermal conductivity of 0.35 [W/m K], see *appendix B*. This gave the range of thermal conductivity that was to be used for further analysis of the thermal performance of the storage if insulated with slag gravel.

$$\lambda_{slag} = 0.29 - 0.35 \left[\frac{W}{m \cdot K}\right] = 1.04 - 1{,}26 \left[\frac{kJ}{h \cdot m \cdot K}\right]$$

These values do not account for the influence of thermal conductivity dependency due to water content or temperature. As all samples were tested during naturally moist conditions, these values should be used with caution, as thermal conductivities may increase if high moisture contents or temperatures, in analogy with the results from *Stuttgart* (*section 2.4.4*), are present.

Secondary aspects of slag gravel

The insulating suitability of the slag gravel is a central part of this Master Thesis, as the utilization of the material alternative shows potential for environmental and economic benefits. This as the current utilization is limited due to uncertainties in material content, see *appendix D* for example of material content.

The sieving test results presented in *appendix C* show a granular distribution of the materials coherent to sandy gravel ("3-6"-sample, 3-6 mm) and gravel ("6-24"-sample, 6-24 mm). Gravel which has a fractional setup showing draining properties and little capillary rise (Statens Geotekniska Institut 2019). Which ought to decrease the risk of any free water staying in the material. The granular distribution also yields the possibility of a relatively great air content if the layer is designed properly. Air having great thermal insulating potential would hence benefit the insulating properties.

The moisture absorption test presented in *appendix E* shows that both slag samples show potential for moisture absorption, which in analogy with the project from *Stuttgart* (Heidemann, et al. N.D.) shows the potential of change in thermal properties due to moisture.

Economic aspects of slag gravel

The economic gains with slag gravel would come from that the material is already owned by the cogeneration plant, and hence has no material cost, nor any greater transportation costs as the storage is located within the vicinity of the plant. This yields that the material cost can practically be set as zero in the economic analysis.

Environmental aspects of slag gravel

Slag gravel is a material produced from sorting the bi-product (slag) from the incineration of household waste. Scrap is removed from the slag and the rest is sorted after granular size, which is then called slag gravel. The slag is commonly alkaline with pH-level of 9.5-11.5 since it will contain a lot of metals, mainly aluminium, iron, calcium and potassium, but also mercury and arsenic are found at lower levels. (Bjurström et al. 1999). An example of this can be found in *appendix D* for slag gravel from *Filborna*.

At the current time, there is no specific legal framework for using slag gravel, hence it cannot be used outside the specific deposit site without a permit or sold commercially. There are environmental regulations that concern the content of example, mercury and arsenic where there are limitations to what is an acceptable amount if the material is to be used as a building material (Arm et al. 2016).

Both mercury and arsenic are known to be harmful to humans. These concentrations, therefore, have to be investigated in each specific case as not to exceed regulation limits.

Currently, there is no general authorization for using slag or slag gravel in *Sweden* as a building or insulation material. Though *Norrköping Energi* has authorization for using their slag product as filling material within the municipality. It has for example been used as filling at *Norrköping* bay (Bjurström et al. 1999).

In *Malmö*, slag gravel has been used as a replacement for gravel as the base course at SJs service terminal at *Malmö Central Station*. Before it could be used it had to be stored over a certain time period in order to lower the pH-level, content of heavy metals, and other substances by oxidation (Bjurström et al. 1999).

But as the planned storage at *Filborna* is to be located within the boundaries of the waste dump these regulations do not apply. This as the leaching water is controlled and hence no contamination risk is present.

4.2.2 Foam glass

Foam glass is manufactured from recycled glass, which is heated together with an activator in order of deriving a porous glass material (Olofsson 2014). The material can be seen used in several applications of thermal energy storage, as seen in the existing projects (*2.4*).

Thermal properties of foam glass

From the project, in *Stuttgart*, the thermal properties of foam glass were identified as heavily dependent on the moisture content, and temperature, see *Figure 2.8*. In order to derive representative thermal properties for the material one must put trust in that the material will maintain the thermal properties declared by the manufacturer, and also trust in that the moisture protection will over time help to maintain these properties. The moisture, and temperature, dependency induces uncertainties in the results and analysis, which hence are to be approached with caution.

In the reference project at *Filborna*, the thermal properties of the foam glass material are given by the manufacturer *HASOPOR*, see *appendix F*. These declared thermal properties further strengthens the bond between thermal conductivity and moisture content of the material. The thermal conductivity of the dry material is given as 0.110 [W/m K], which increases to 0.145 [W/(m K)] at a water content of 25 %. In the analysis, the higher of the two values will be used, as this corresponds to the worst case scenario of the two, when considering declared values.

$$\lambda_{Foam\ glass} = 0.145 \left[\frac{W}{m \cdot K}\right] = 0.52 \left[\frac{kJ}{h \cdot m \cdot K}\right]$$

Secondary aspects of foam glass

The declared material properties presented in *appendix F* show a potential water absorption of 30 weight-% after 28 days, and 50 weight-% after 68 weeks. These properties show a "short term" absorption close to the declared thermal conductivity value at 25 weight-%. The long-term absorption exceeds this by a large margin which points towards the need of moisture protection of the material as to keep thermal properties. This desire for moisture protection is further stressed by *Eriksson & Hägglund* (2007) in order to maintain desired material properties.

When comparing the foam glass material to alternative insulating materials *Eriksson & Hägglund* (2007) brings forward the advantage of not requiring an even surface for placement of the insulating material, something which is needed for i.e. extruded polystyrene alternatives. The durability of foam glass is to be seen as quite good as this is both relatively persistent to freeze cycles, as well as being chemically neutral (Eriksson & Hägglund 2007). This aspect of foam glass gives a durability positive factor to the usage of foam glass.

Economic aspects

In the reference project the material of foam glass is an external material which is needed to be transported to the field site. The cost of the material is within the project given as 571 SEK/m^3.

Environmental analysis of foam glass

Eriksson & Hägglund (2007) brings forward the environmentally positive aspect of reusing existing materials, in this case, glass, hence eliminating needs for new production of materials limiting both resource and energy needs. The product of foam glass in *Sweden* is made of finely crushed recycled glass which could not be used for outer purposes, which adds to the environmental benefits (Olofsson 2014).

The material does not degrade over time, hence there are good possibilities to reuse the material without the need for greater purification processing. The process of manufacturing the material from raw material to the finished product has a global warming potential as it is a high heat demanding process, approximately 7.8 kg of carbon dioxide is emitted for each cubic metre foam glass produced (EDP International AB 2017).

4.2.3 Expanded clay

Expanded clay is a product made from clay burnt at high temperatures in a rotary kiln where the temperature reaches up to 1200 °C. Due to the rotation of the kiln, small aggregates are formed which then expands because of the high temperatures they are exposed to. In this process, the aggregates get a porous core and a solid ceramic husk (Boudaghpour & Hashemi 2008).

Thermal properties of expanded clay

As for foam glass, it was identifiable from the project in *Stuttgart* (*Figure 2.8*) that the thermal properties of expanded clay are heavily moisture and temperature dependent. From the material properties presented by the manufacturer (*appendix G*), a great potential for moisture absorption can be identified for the material, which further induces uncertainties into the results and analysis. The thermal properties presented by the manufacturer show a thermal conductivity of

0.18 [W/(m K)] at 50 % moisture content, which corresponds to the highest declared value and is to be used in the future analysis.

$$\lambda_{Expanded\ clay} = 0.18\ \left[\frac{W}{m \cdot K}\right] = 0.65\ \left[\frac{kJ}{h \cdot m \cdot K}\right]$$

Secondary aspects of expanded clay

When considering expanded clay as an alternative for insulation, it is convenient as a levelled surface is not required for placement of the material since it comes in the form of aggregates, in analogy with the positive aspect presented for foam glass.

Expanded clay is a material that has been around for approximately 100 years, hence is a material which has been investigated thoroughly and its properties are well documented (LECA N.D.). The durability of the product is seen as very good as it has a lifespan of 50-100 years. This due to it being ceramic, and having a chemically inert husk, which creates a protection against both freeze cycles, heat, chemical exposure, and pressure from loading (Boudaghpour & Hashemi 2008 and LECA 2015). This also allows for the material to be reused if desired, which is an environmental positive for the material alternative (Boudaghpour & Hashemi 2008).

Economic aspects of expanded clay

In the reference project, the material of expanded clay is an external material which has to be brought in. An approximate price of 550 SEK/m^3 is found from analysing current retail prices.

Environmental analysis of expanded clay

As the aggregates only consist of clay, the risk of contamination due to leaching is reduced as no greatly harmful components are part of the material. (Boudaghpour & Hashemi 2008). This durability aspect is further strengthened by *LECA* (2015, N.D) who claims that the material is not naturally decaying. The perspective from *LECA* has to be taken with caution though as this is a manufacturer of the product.

However, the process of producing the product demands a lot of energy because of the high temperatures needed. This has to be taken into account when analysing the environmental effects the material has. Since the operation of the mining process, as well as the burning process, uses mainly non-renewable energy sources which emits CO_2 that contributes to global warming (Jonsson 2013).

As the material is not locally produced it would have to be transported to the field site, which yields additional environmental impact from transports.

4.2.4 Extruded polystyrene

Extruded polystyrene (commonly called XPS-Styrofoam) is an insulation material made from the polymer polystyrene (in liquid phase) combined with hydrocarbons which are then moulted/cast. The final product is a stiff foam with a closed pore system, which yields low permeability as well as some load carrying capacity (Masse Modin & Sundberg 2012).

Thermal properties

The thermal conductivity of extruded polystyrene materials is found from analysing manufacturers. This analysis showed a thermal conductivity of approximately 0.029 [W/m K], in accordance with material properties presented in *appendix H*.

$$\lambda_{Extruded\ polystyrene} = 0.029\ \left[\frac{W}{m \cdot K}\right] = 0.1\ \left[\frac{kJ}{h \cdot m \cdot K}\right]$$

This value does not account for effects of moisture in the material, a factor which potentially may yield significant effects on the thermal properties, as seen for the other alternatives.

Secondary aspects of polystyrene

The material is seen as durable over time with regards to degradation in nature. (Finja 2019)

As the material is not in aggregate form it needs an even surface for placement, something which will yield additional construction costs.

Economic aspects of polystyrene

The price of polystyrene within the reference project is set as 700 SEK/m^3s from analysing retail prices from several manufacturers, as well as assuming a cost reduction of approximately 30 % when buying in bulk.

Environmental analysis of extruded polystyrene

The material is an oil based product, which is a none-renewable source. This fact is the most profound argument against the usage of polystyrene as a material (Rogers 2015).

This type of material contains chlorofluorocarbons (CFC) which is a substance that contributes to ozone-depleting and is also a greenhouse gas (Naturvårdsverket 2016).

XPS Styrofoam is classified as hazardous waste and needs to be handled professionally and with care, it cannot be normally deposited since then there is a risk of the CFC substances to leach out into waters and cause contamination. Hence there are negative effects using the material and extra caution must be taken when dealing with the material, especially during future maintenance where the risk of contamination is highest if the material is not kept intact (Naturvårdsverket 2016).

The CO_2-emissions for producing the material can be assumed similar to the ones for producing expanded polystyrene, which is 2.6 kg CO_2/kg EPS (Boustead 2015).

Future studies must also be done regarding degradation of the material as the material will be used in a constant moist condition which could have a big impact on the lifespan of the material as well as the insulation properties. This would increase the requirement of maintenance and add to the total cost as both the material will need to be replaced and handled correctly.

4.2.5 Final thermal analysis of material alternatives

From the experimental project in *Stuttgart* (*2.4.3*), it can be identified that the materials foam glass and expanded clay both show tendencies of increasing thermal conductivity by increasing moisture content. This is further strengthened by the theoretical background for heat transfer in soils *3.1.2* where an increased water content shows a greater heat transfer due to water diffusion,

and hence higher thermal conductivity. This thermal behaviour could be assumed to be true for all insulation materials identified and hence needed to be taken into consideration in the later analysis.

5 Methodology of modelling and analysis

Central to the aim of this Master Thesis is the modelling, and analysis, of a *High Temperature Borehole Thermal Energy Storage* system. The modelling is performed in *TRNSYS*, which is a simulation tool used for modelling of transient thermal systems. As the nature of the study is investigatory, as are feasibility studies, this is approached by performing a sensitivity study for system parameters. From the sensitivity study an evaluation of the parameter effect on thermal performance can be implemented. These sensitivity studies make up the basis for the thermal performance analysis, which is to be complemented with an economic study, as well as a secondary environmental evaluation. The outline of method is listed below, where the methodology segments are gone through in a chronological order of implementation.

- Modelling of thermal storage system in *TRNSYS*
- Methodology for sensitivity study
- Economic analysis of *HT-BTES* design

The basis of method and analysis is presented for each separate section. It is also from the outline presented in these segments that the discussion will originate.

5.1 Modelling of thermal storage system in TRNSYS

The *TRNSYS* software allows the user to create transient flow systems, from which a multitude of thermal, and system, data can be derived. In this Master Thesis one main system, denoted *system A*, is modelled based on the reference project at *Filborna*. It is from this model that the general perspective will be lifted from the results.

Problematic for the usage of *TRNSYS* for modelling and simulation, is that the mathematical base of simulations is described as a "black box", giving room for concern. But as the software was implemented with good results in the project in *Marstal* (*section 2.4.4*) the program is deemed credible.

5.1.1. System modelling

The system which was to be modelled is conceptually presented in *Figure 2.2* corresponding to the reference project at *Filborna*. Conceptually the system consists of two intersecting loops, the intersection is made up of a heat exchanger. The first loop connects the thermal process of the cogeneration plant to the heat exchanger, the thermal process of the cogeneration plant being the source of thermal energy for charging of the thermal storage. The second loop connects the heat exchanger with the thermal storage, making up the central part of the model. The TRNSYS model for this is presented in *Figure 5.1* and component descriptions presented in *Table 5.1*.

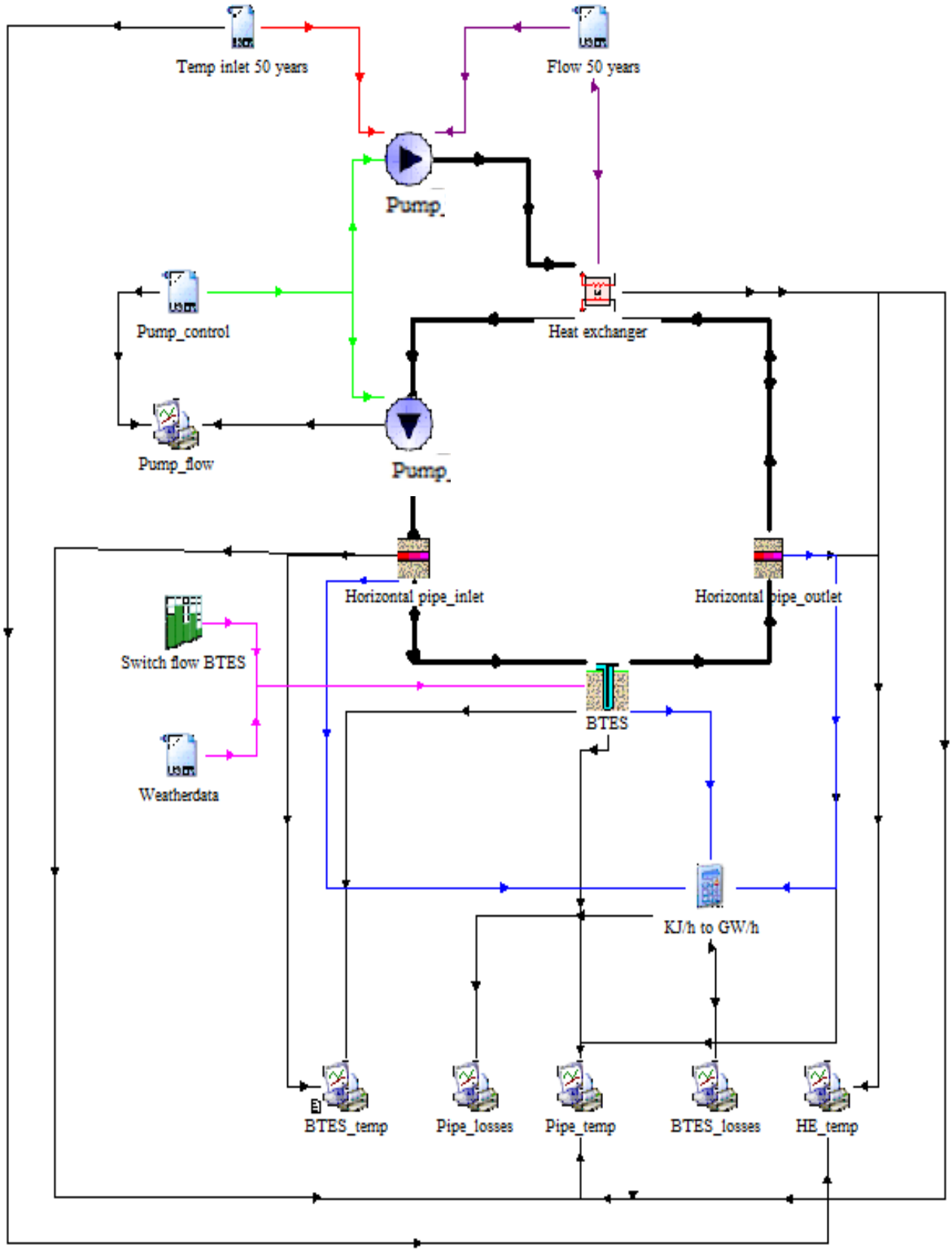

Figure 5.1 – Thermal storage system. Component descriptions are found in Table 5.1.

Table 5.1 – Component descriptions for TRNSYS models

Type		Description
	*Type 9a (Weatherdata, Flow 50 years, Pump_control, Temp inlet 50 years)*	The type 9a is used for input data to the model. In the models presented above the type 9a is used for adding weather data to the system.
	*Type 14h (Switch flow BTES)*	The type 14h gives in data to the system for used defined periods in time. This is used for flow regulations and temperature regulations of the load, and discharge, temperatures.
	*Type 65b (Pump_flow, BTES_temp, Pipe_losses, Pipe_temp, BTES_losses, HE_temp)*	The type 65d is used for deriving output data and plot this data.
	*Type 91 (Heat exchanger)*	The type 91 represents the heat exchanger. This performs a heat exchange which always runs from the warmer to the colder side.
	*Type 114 (Pump)*	The type 114 represents a pump and is used to circulate fluid.
	*Type 557d (BTES)*	The type 557d represents a vertical tube-in-tube ground heat exchanger, which represents the thermal storage. This component includes the DST-model.
	*Type 952 (Horizontal pipe_inlet, Horizontal pipe_outlet)*	The type 952 represents the horizontal pipe system located on top of the *Borehole Thermal Energy Storage*.
		Other types
	*Equation (kJ/h to GWh)*	The equations used in *TRNSYS* are not given a unit number. These equation components use user-defined in data and user-defined equations to yield out data.

Modelling of system from cogeneration plant to heat exchanger

The thermal process at the cogeneration plant is in the reference project both source, and recipient, of thermal energy, dependent on if the storage is being charged or extracted from. A principle illustration of the section from the cogeneration plant to heat exchanger can be seen in *Figure 5.2*. This process is in the reference case simplified as set inlet flows and temperatures

to the heat exchanger. This is a consequence of that the thermal process at the cogeneration plant expands beyond the knowledge basis of this Master Thesis.

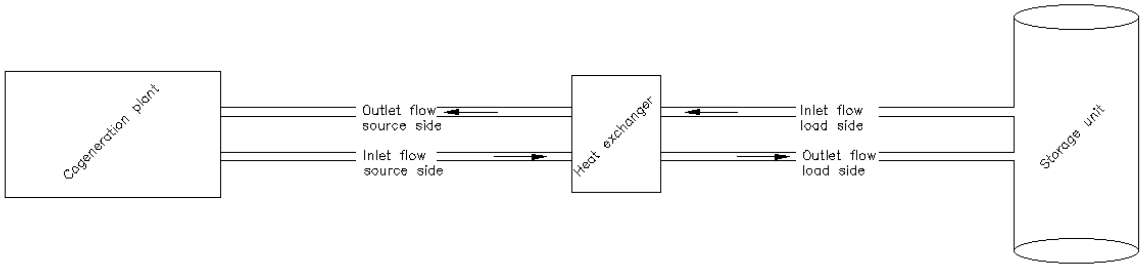

Figure 5.2 – Principle schematic sketch of flow system from cogeneration plant to storage unit, via heat exchanger.

The flow is set to work according to a periodic schedule. During periods of discharge and extraction, the flow is set to 1000 [m^3/h] and set to zero during non-operational periods. This periodization can be seen in *Figure 5.3*. Similarly, the temperatures of the carrier fluid were periodically divided where the temperature during charging was set to 98 [°C], and to 58 [°C] during discharging. At all other times, the temperature was set to zero.

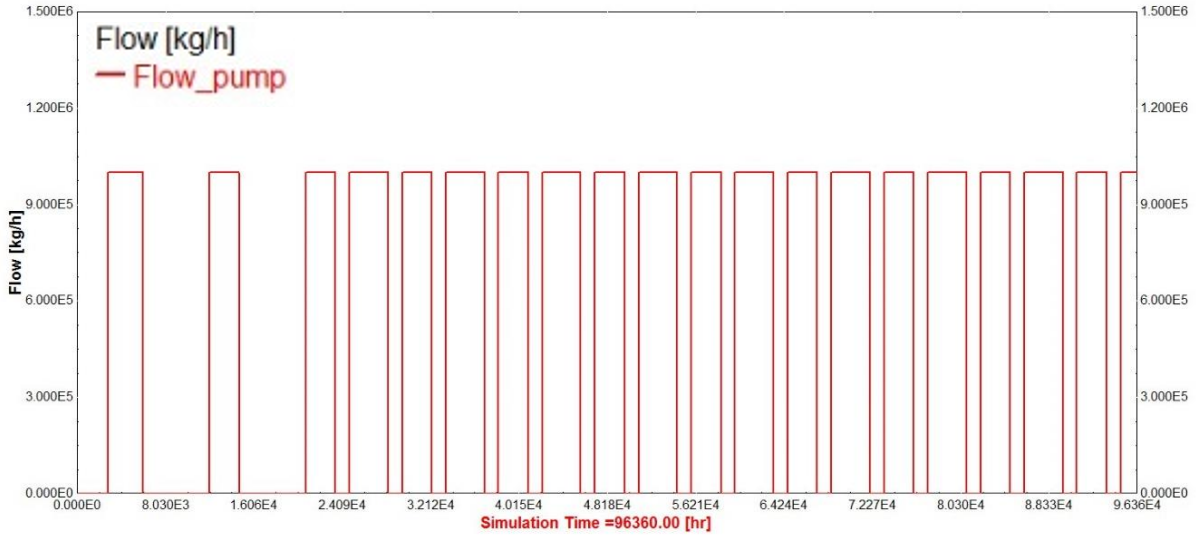

Figure 5.3 - Flow chart during the first 10 years of operation. Starting from January 1st.

It is from the in- and outlet flows of the heat exchanger that the amount of thermal energy charged (put into the storage system loop) and extracted can be calculated. These energy quantities are calculated via an energy balance for the carrier fluid going to and returning from, the heat exchanger. The equation (Sarbu & Sebarchievici 2018) for this is presented below and has to be integrated over time in order to derive the total amount of energy charged/extracted.

$$E_{Stored/Extracted} = \rho \cdot V \cdot C_f \cdot (T_{fout} - T_{fin}) \cdot t \qquad (27)$$

Where

i) ρ – Density of carrier fluid [kg/m^3]
ii) V – Flow of carrier fluid [m^3/h]
iii) C_f – Specific heat capacity of carrier fluid [kJ/(kg, K)]
iv) T_{fout} – Outlet temperature of the heat exchanger on source side [°C]

v) T_{fin} – Inlet temperature of the heat exchanger on source side [°C]

vi) t – Duration of the storing/extraction period [h]

Example: In order to shine light upon the magnitude of the energy amounts that can be stored the following example is put forward for a system design as the one illustrated in *Figure 5.2*. Based on *Eq. 27* and with the following parameter values an example of the charged amount of energy is shown. The carrier fluid is assumed to be water (C_p=4.2 [kJ/(kg K)]), with a flow of 1000 [m^3/h], as in the reference project. The charging temperature is set to 98 [°C], and the return temperature is set as approximately 80 [°C] (from simulation example presented in *Figure 5.4*). Over a charging period of 2700 hours this yields the following amount of charged energy: $E_{Charged} = 10^3 \cdot 10^3 \cdot 4.2 \cdot (98 - 80) \cdot 2700 = 204\,120\ GJ = 56.7\ GWh$

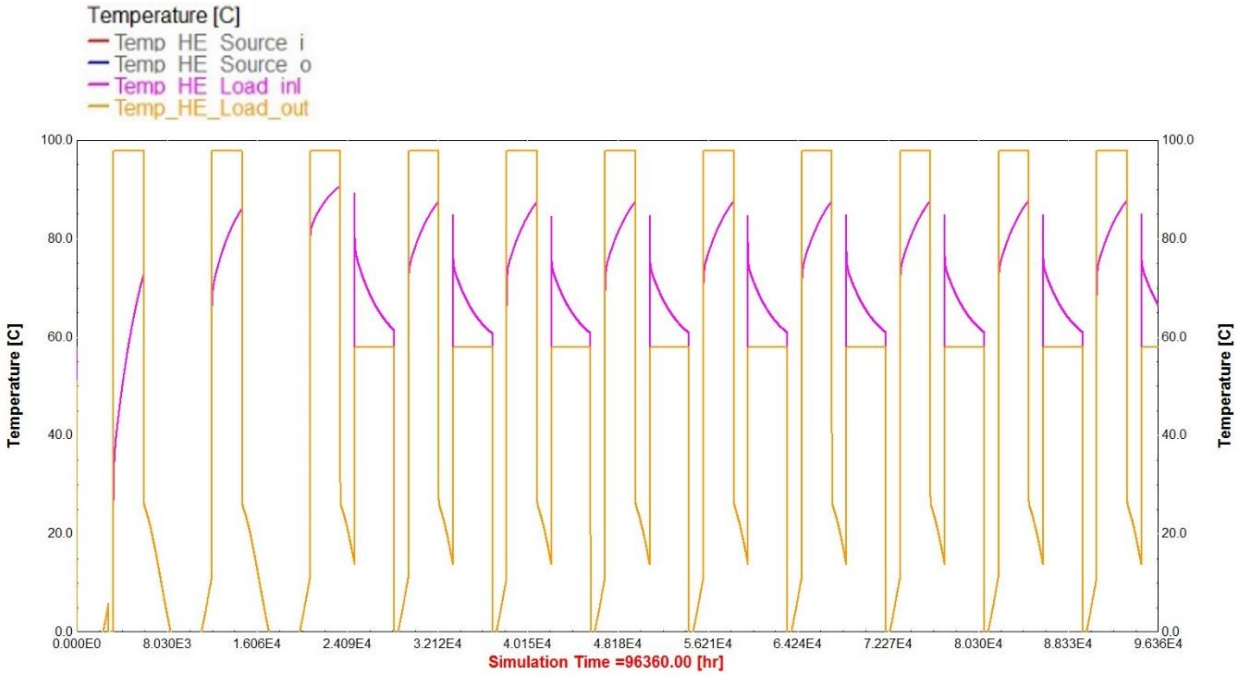

Figure 5.4 – Example simulation of thermal performance of storage during a time period of 11 years.

Modelling of system from heat exchanger to thermal storage

The heat exchanger connects to the BTES via a horizontal pipe system. This horizontal pipe system consists of none insulated rubber pipes, hence an external insulating layer is needed. The conceptual loop is illustrated in *Figure 5.5*. The pipe system is mainly to be placed on the surface of the storage (see *Figure 5.6*), which has the consequence that the top insulation of the storage secondarily acts as insulation for the horizontal pipe system. The pipe system is modelled as two separate components, one entering the thermal storage, and the other exiting the storage. The assumed length of each component is 7000 m when considering the number of boreholes, the distance between boreholes, and number of boreholes in series. This length aspect is heavily influential on the amount of thermal losses from the pipe system and will hence be included in the later sensitivity study. Principle design parameters for the horizontal pipe system is presented in *appendix I*.

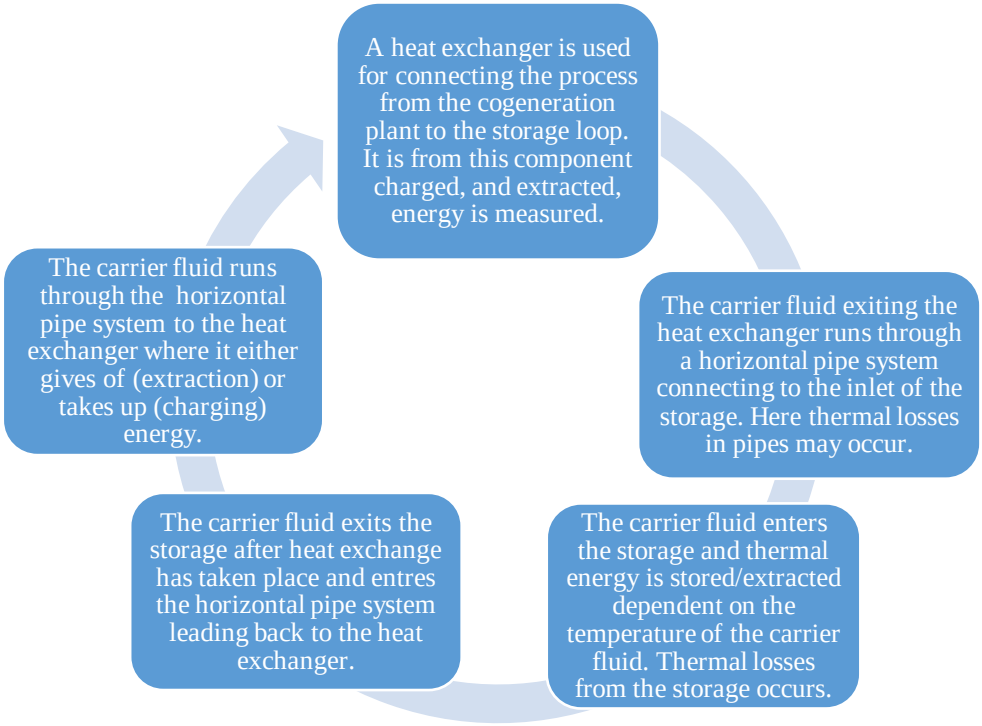

Figure 5.5 – Illustration of thermal storage process for thermal energy storage illustrated in Figure 5.2.

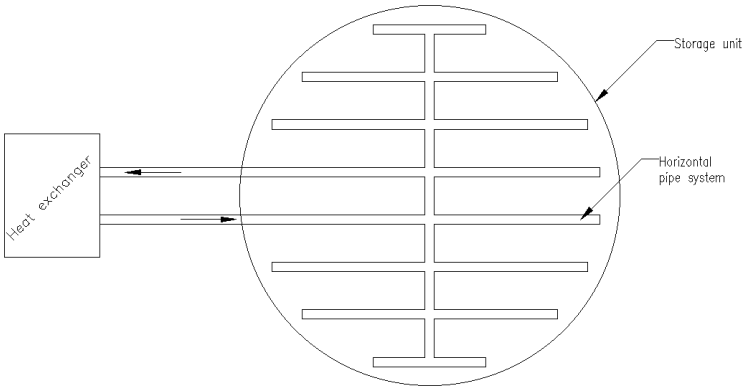

Figure 5.6 – Principle sketch of horizontal pipe system

Modelling of the thermal storage

The thermal storage is modelled in accordance with the *DST-model* presented in *appendix J*. This model includes geologic parameters within, and outside, the storage volume. As well as borehole parameters and level of detail for the simulations. The geologic model was presented in *section 2.3.2*, and has properties in accordance with *appendix A*. In *TRNSYS* the storage volume itself is modelled as one homogenous material, which has to be assigned material properties corresponding to those of the whole storage volume (gypsum, till and bedrock), see *appendix A*. From the component representing the storage volume, denoted "BTES", in *Figure 5.1*, the thermal losses from the storage, average storage temperature, and outlet temperatures, were derived.

Modelling of external parameters

The air-temperature-component was derived as an average hourly temperature from weather data given by *SMHI* (2019) for *Helsingborg* for the time period 1995-2018.

Component dependency

Within the models, the internal dependencies between components are represented by links. These ensure that output data from a previous component is given as input to the following component, creating a closed system of dependencies. An example of this can be seen in *Figure 5.7*.

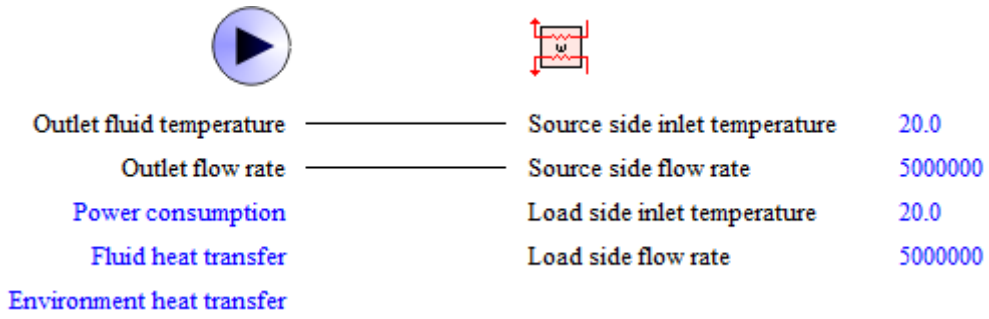

Figure 5.7 – Example of link between components, in this case pump to heat exchanger

5.1.2 Simulation outline

The simulations performed on the modelled storage included one charging, and one extraction, period during each yearly cycle. The first three years only charging took place, acting as a preheating period. This as to increase the temperature of both the storage itself, as well as the surrounding ground. The charging period was set as acting over 2700 hours, whilst the extraction phase lasted during 3500 hours. In the reference project the charging period is set from May-September, and the extraction period from November-March.

When analysing the thermal performance of the thermal storage the parameters of interest are: charged energy, extracted energy, thermal losses from storage, and thermal losses from the horizontal pipe system.

i) Charged energy: Corresponds to the amount of energy put into the storage loop during one charging period. This is to account for thermal losses and extracted thermal energy.
ii) Extracted energy: Corresponds to the energy extracted from the storage during one extraction period, which can be used for external purposes.
iii) Thermal losses from storage: Corresponds to the thermal losses from the storage itself.
iv) Thermal losses from the horizontal pipe system: Corresponds to the thermal losses from the horizontal piping system connecting the storage to the heat exchanger.

The results derived from the *TRNSYS* models are based on the values for the tenth year of operation. This is motivated by that the results derived at point in time are deemed stable enough for interpretation of thermal performance during full operation. An example of this can be seen in *Figure 5.8* and *Figure 5.9*. These figures show data variation for the different parameters of interest in this Master Thesis over the time period of ten years.

All thermal performance data is derived as integration of performance over time, where the time corresponds to the charging/extraction period. For exemplification of this *Figure 5.9* shows thermal losses over 10 years of operation. When integrating over one year the total annual losses are derived, the same principle is used for the other thermal properties.

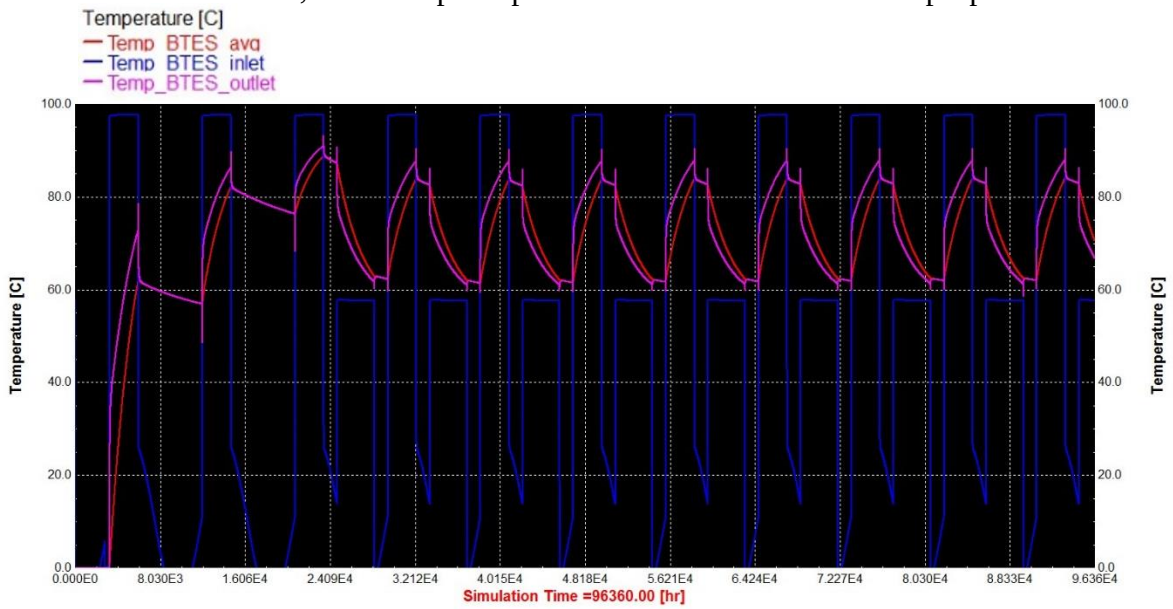

Figure 5.8 – Example of thermal response in the BTES during the first ten years of operation.

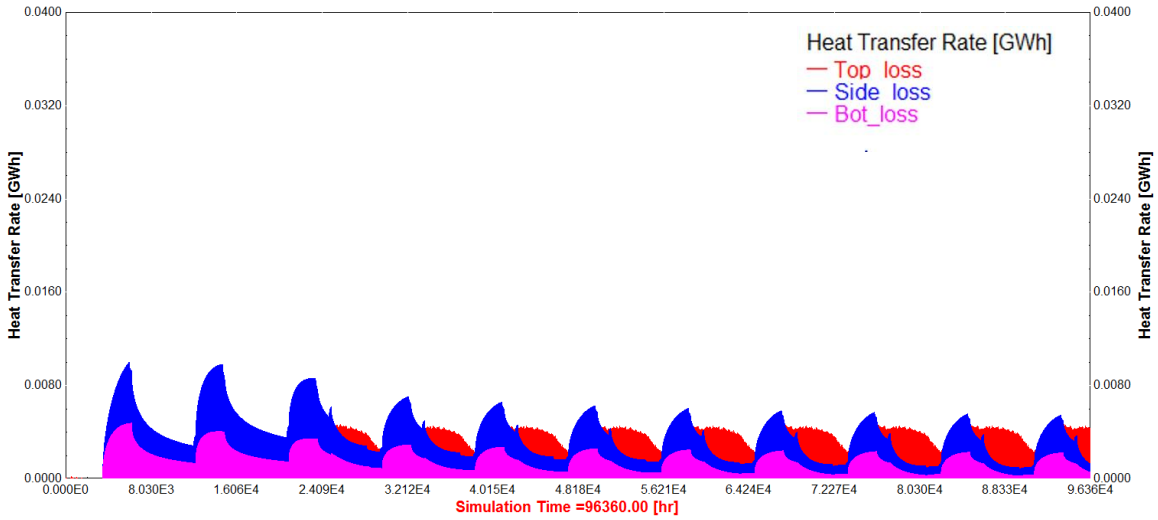

Figure 5.9 - Example of thermal losses over time. When integrating one charging/extraction year the losses during this are derived.

5.2 Sensitivity study

The modelling using *TRNSYS* is performed as a sensitivity study, where parameter analysis is performed from a reference outline. The original outline corresponds to the *Duct Storage Model,* and horizontal pipe model presented in *appendix J* and *I*. These correspond to the original plan of design for the reference project at *Filborna*, and are performed for the original system, *system A*. The sensitivity study originates from the desire of deriving an optimized solution when regarding thermal performance. This optimization is mainly considering thermal insulation aspects but also entails varying parameters of the storage design parameters.

Within this Master Thesis emphasis is on the thermal performance of *HT-BTES* from an insulation perspective. This by using the reference project at *Filborna* as a basis for simulation models. The aspect of thermal performance analysis a feasibility study, which concludes the use of a sensitivity study. The sensitivity study itself is divided into two parts, one regarding design parameters of the storage itself, whilst the other deals with the insulation aspect.

5.2.2 Methodology of sensitivity study

From the *DST-model* presented in *appendix J* for the thermal storage, parameters were methodically varied. This as to show the dependency between thermal performance and the design parameter. The parameters analysed when regarding storage design are listed below, for which "length of horizontal pipe system" originates from *appendix I* instead of *appendix J* as the others. These parameters were deemed as central to the system design and hence chosen for the study, giving room for uncertainties as other key parameters may have been overseen.

- Storage volume
- Borehole depth
- Borehole radius
- Gap thickness (distance between borehole casing and the bedrock wall where for example water can accumulate)
- Header depth (depth between the top of the borehole and the water level inside the borehole system)
- Number of boreholes
- Number of boreholes in series
- Efficiency of heat exchanger
- Length of horizontal pipe system

Analysis of insulation design

When considering the insulation aspect of *HT-BTES,* the model aspects analysed are: Thermal conductivity of insulation, insulation thickness, and insulation width. The parameter of insulation width is approached in the same manner as for storage design parameters, originating from the *DST-model* presented in *appendix J*. The parameters of thermal conductivity and insulation thickness both need to be considered in the models for the horizontal pipe system and storage volume. This as the pipe system is to be placed on top of the storage volume and hence have the same insulation. The thermal conductivity aspect ranges from a value corresponding to that of polystyrene, to the one of water. This as a fully saturated material is assumed to show thermal properties equal to those of water. The range is motivated by the

moisture dependency of thermal conductivity as presented in the project in *Stuttgart* (*section 2.4.3*).

Insulating material perspective

When implementing the material aspect into the thermal performance regarding insulation design one must relate the choice of material to a corresponding thermal conductivity. When this is done one can compare material alternatives with regards to thermal performance in relation to thermal conductivity of insulation, as well as insulation thickness. In the reference project, the material alternatives were presented in *chapter 4*, within which corresponding thermal properties were presented. Complementing the thermal performance aspect of the material analysis is an economic and environmental analysis, which regards the choice of insulating material.

The analysis of thermal performance is to include: charged energy, extracted energy, thermal losses from storage, and thermal losses from the horizontal pipe system. The thermal performance is further evaluated via thermal efficiency, which is defined as seen below. The results are based on the tenth year of operation, which includes three preheating years. This, as it is at this point, noted that the variations between years are minor with regards to derived results.

$$Thermal\ efficiency = Degree\ of\ efficiency = \frac{Extracted\ energy}{Charged\ energy}$$

5.3 Economic analysis of HT-BTES design

As brought forward by *Nordell* (2000), one main area of concern when it comes to designing *Borehole Thermal Energy Storages* is finding economic profitability of utilization. In the following the integration of the economic aspect into the design optimization is gone through, this as a mean of finding value within the design aspect *HT-BTES*. This economic perspective is divided into aspects of value derived from the storage, and cost aspects of investment, operation, and maintenance. In the following segments, these aspects are implemented into the analysis of thermal storage design.

In order to achieve the possibility of profitability for the thermal storage the value of the stored thermal energy must be greater at the point of extraction, than the value when stored.

5.3.2 Value of thermal energy

The value of the thermal energy that is extracted is dependent on if this energy is assigned a value of electrical equivalent, or a corresponding value for district heating. If the energy is to be used in the electrical generating process this is to be assigned an equivalent electrical value, whilst it is to be assigned a district heating value if used for this purpose. In the reference project at *Filborna*, it is assumed that the stored energy is to be used for district heating. But as to have a further basis for analysis an equivalent electrical value is also presented, showing the dependency of thermal energy value.

In the reference project energy is assumed to have no value during charging, as it comes as an excess of thermal energy from the electricity producing process at the cogeneration plant. This thermal energy would otherwise have been needed to be removed by other means of cooling.

Hence an economically beneficial factor as it acts as cooling as well as a heat source depending on the time of year.

District heating value of thermal energy

When the thermal energy is to be used for district heating the extracted energy can be designated a value corresponding to the energy price of the district heating provider at the time.

Under the assumption that the energy has no value during the charging period, the thermal energy in the reference project at *Filborna* can be assigned a value of 704 kSEK/GWh during the discharging period. The district heating value derived from an agreement from 2018, applicable from 2019 until 2021, and assumed corresponding to future price levels (Öresundskraft 2019 B).

Electrical value of thermal energy

When assigning the thermal energy, a value equivalent of electrical energy an exchange rate between thermal and electrical energy equivalents is needed. This exchange rate is assumed to 1:1, as no further information is given in the preconditions. In other words one GWh of thermal energy corresponds to one GWh of electrical energy.

From an electrical perspective, the energy will have a value dependent on the discharging period, see *Figure 5.10*. The equivalent electrical value hence needs to take the annual variations into consideration, which in the reference project at *Filborna* is performed by analysing the energy prices from the energy provider *Öresundskraft* over the extraction period. The equivalent electrical price is set as a mean value during the discharging months (November-March), which corresponds to an average of 450 kSEK/GWh.

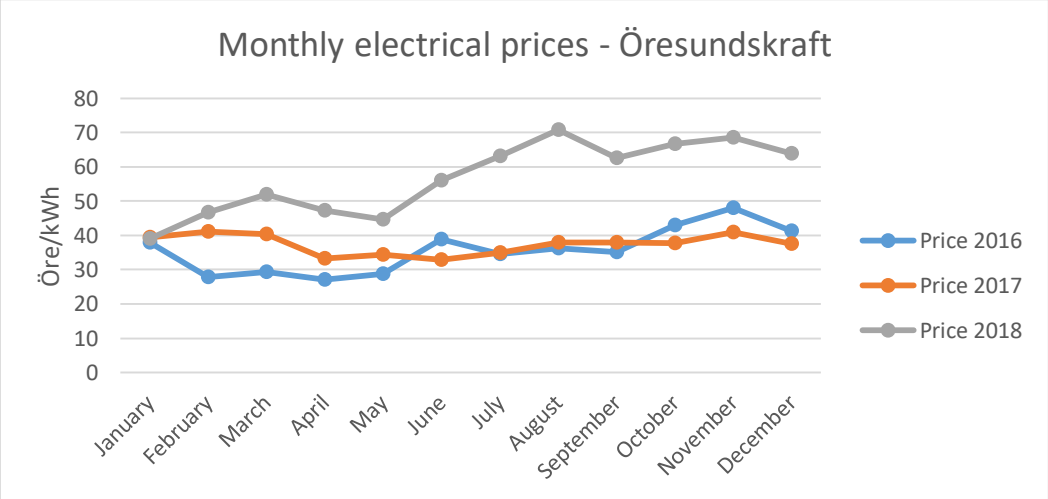

Figure 5.10 – Electrical prices from the energy provider Öresundskraft (2018)

By using the value of equivalent electrical value for the stored energy the extracted energy can be transferred into a total value derived from a storage period. This value needs to cover investment costs over time, as well as maintenance costs, in order to yield profitability of the storage.

5.3.3 Cost aspects of BTES

The cost approach to a thermal energy storage is a multi-aspect perspective, which is very project specific. In this Master Thesis emphasis is put into the following aspects.

- Material costs for insulation
- Investment costs
- Electrical demand of system
- Maintenance costs

Out of these, only the material cost aspect is directly implementable in the economic evaluation. This as the other aspects are very site dependent and hence not quantifiable from a general perspective. The material costs are volume dependent, and hence depend on the chosen design. Investment and maintenance depend on the system design, as does electrical operation costs. Hence only the material perspective is to be implemented in a general sense, from a basis of relating this to the reference project in the following.

The electrical demand of the system comes from pumps, possibly a heat pump (*system B*), and other flow regulating components. In the economic analysis this aspect is integrated as just the energy demand of pumps, and heat pump in *system B*.

The investment cost of the system is unknown, and hence only integrated into the economic analysis as a mean of having a profit margin which can cover this over time, something which is brought into the analysis perspective in the results. The same approach is used for the maintenance aspects of the system.

5.3.4 Implementation of economic perspective in thermal analysis

The economic perspective is implemented in the thermal analysis by assigning the extracted thermal energy a value corresponding to the one for district heating (*section 5.3.1*). This is based on that the thermal energy is to complement the thermal process in the reference project. From this value, the cost aspects need to be subtracted, leaving a value margin which is to cover for investment costs. If there is no margin after subtracting the costs, the system is not economically beneficial.

In the reference project, and in the later analysis, the thermal energy will be assigned the value for district heating. By then looking at the tenth year of operation, which is deemed sufficient for low deviations of results between years, an extracted energy value can be calculated for each year of operation. This yearly extracted value is to cover for all cost aspects identifiable in the reference project, as well as leave margin for unforeseen costs and profit margins.

When solemnly comparing material alternatives on a basis of material investment cost, and yearly extracted energy value an equation system on the form $y=kx+m$ can be created where:

- y equals the remaining value
- k equals the yearly extracted value
- x the number of years
- m the material investment cost

This simple equation system allows for material comparison with regards to the two parameters of material cost, and yearly extracted value. The aspect of material cost is directly linked with insulation thickness, and the aspect of extracted energy is linked with thermal conductivity of

insulation. This yields that a comparison can be made between insulation materials with regards to both insulation thickness and thermal conductivity of insulation.

5.4 Comparative study with an alternative system with heat pump

If a heat pump was to be implemented in the thermal storage system, this for additional extraction, in analogy with what was used at *Emmaboda* (*2.4.1*). As the heat pump utilizes electricity for the transfer of thermal energy between mediums this induces a reduction of the value of the transferred amount of energy. This reduction is dependent on the value of the thermal energy compared with the electrical cost of transferring it, a factor which is dependent on the COP of the heat pump. A higher COP-value would yield that more thermal energy can be transferred per electrical unit.

The conceptual system design for the reference project is presented in *Figure 5.11*.

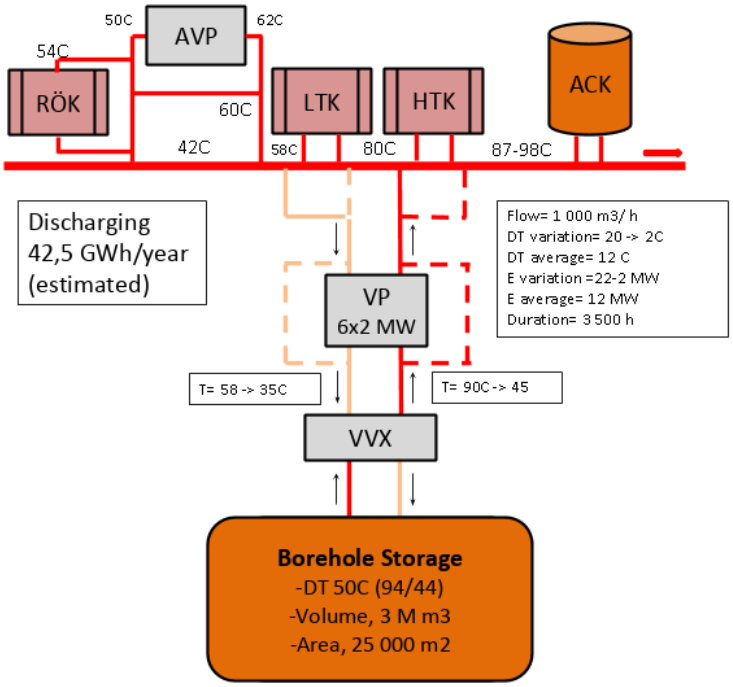

Figure 5.11 - Principle design of system including a heat pump in the reference project.

6 Results and analysis

The following chapter presents the simulation results derived from simulations in *TRNSYS*. The results are complemented with theoretical background and an analysis interpreting the results from both a general perspective, and from a perspective of the reference project at *Filborna*. The order of presentation of results is as follows:

- Results from sensitivity study of storage design parameters
- Results from sensitivity study of insulating parameters
- Implementation of cost analysis
- Environmental evaluation
- System validity

6.1 Sensitivity study of storage design parameters

The sensitivity study analysing the parameter influence regarding storage design is presented in the following section. This was performed in accordance with the methodology presented in section *5.2*, and shows thermal energy charged and extracted, as well as thermal losses from horizontal pipes and from the storage volume. The original outline corresponds to the *Duct Storage Model*, and horizontal pipe model presented in *appendix J* and *I*. The order in which the different investigated parameters are presented is shown below.

- Varying the storage volume
- Varying borehole depth
- Varying borehole radius
- Influence of gap between heat exchanger and borehole wall
- Influence of header depth
- Varying the number of boreholes
- Varying the number of boreholes in series
- Varying the length of the horizontal pipe system
- Varying the efficiency of the heat exchanger

6.1.2 Sensitivity analysis of storage volume

The results from varying the parameter of storage volume in the sensitivity study presented in *5.2.2* are presented in *Figure 6.1* and *Figure 6.2*.

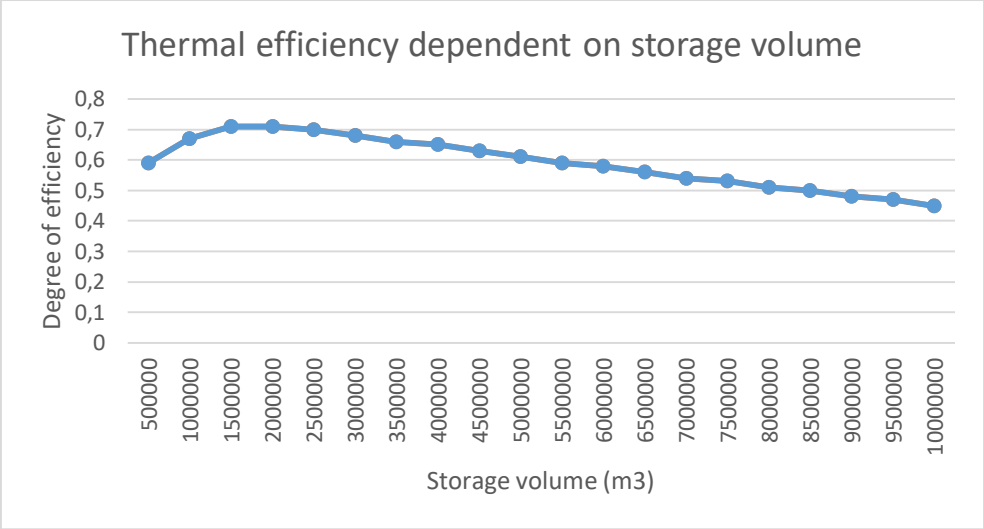

Figure 6.1 – Thermal efficiency dependent on storage volume.

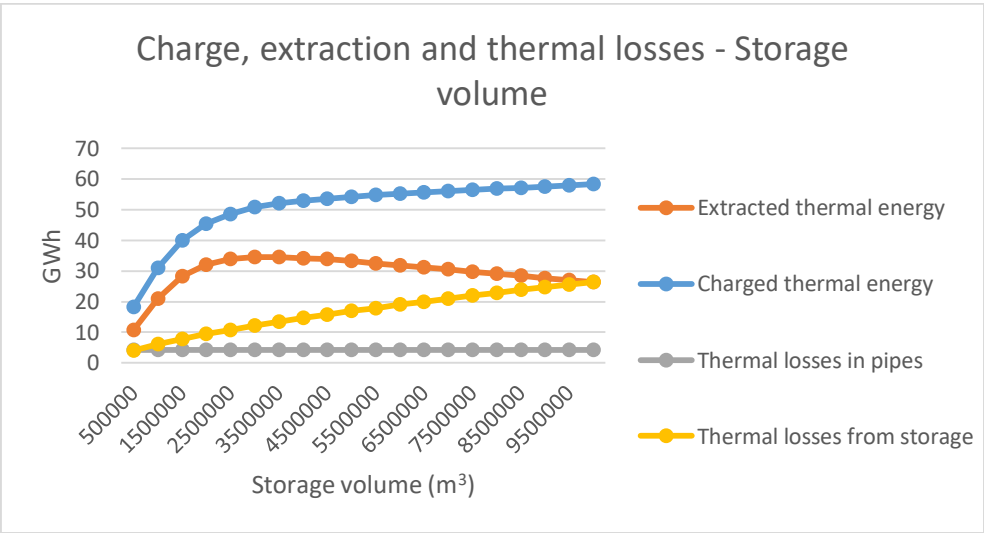

Figure 6.2 – Thermal performance dependent on storage volume.

Theoretical basis of results for variant storage volume

The thermal efficiency (*Figure 6.1*), and thermal performance (*Figure 6.2*), indicate a significant dependency of thermal performance in relation to storage volume. A theoretical explanation for this dependency can be found in the outline of the sensitivity study. As the volume increases, without any alteration of borehole or depth, so does the surface radius. Without changing the amount of boreholes the same amount now has to be evenly distributed over a larger area, hence increasing the borehole spacing (B). This has implications in both the heat transfer between carrier fluid and storage volume (*section 3.1.1*), as well as the local solution for thermal storage (*section 3.1.3*).

The impact on the heat transfer between carrier fluid and storage volume, see *section 3.1.1*, comes from *Eq. 3* and 6. A lowering of the damping coefficient (β), *Eq. 3*, will yield that a

greater amount of energy may be charged, *Eq. 6*. This explains the charging curve in *Figure 6.2*.

$\beta = e^{\frac{-\alpha_v V}{C_f Q_f}}$ → As V increases the damping coefficient (β) decreases.

$q = \frac{C_f Q_f}{V} \cdot (1 - \beta) \cdot \left(T_{fin} - T_a\right)$ → As β decreases, the transferred energy (q) increases. But an increase in V also decreases q, which from the results is outweighed by the decrease in damping factor.

Further explanation for the thermal performance presented in *Figure 6.2* can be found in the local solution, *section 3.1.3*. By utilizing *Eq. 8* and *10* the increased borehole spacing (B) is shown to yield a decreased average storage temperature (T_m). This yields that the temperature difference between carrier fluid and storage volume generally becomes greater. As this thermal gradient is the driving force behind the heat exchange a consequence of the greater gradient is that more energy will be transferred, and more energy will be transferred during charging. The opposite applies when extraction is desired as the difference becomes smaller and hence the heat exchange becomes less effective, and less energy is extracted.

$r_1 = 0{,}525 \cdot B$ → As B increases, so does r_1

$T_m = \frac{q \cdot t}{\pi \cdot C \cdot r_1^2}$ → T_m decreases as r_1 increases

An explanation for the increase in thermal losses from the storage, shown in *Figure 6.2*, is conceptually derived from the outer parameter of the storage. As the volume increases so does the length of the outer parameter of the storage, in other words the circumference increases. This yields for a greater area of heat exchange with the surrounding area, as well as a greater surface area acting as an area for heat exchange upwards.

The thermal losses in the horizontal pipe system were not greatly affected as no parameter regarding their properties were altered.

Analysis of thermal performance results for storage volume dependency

When analysing the thermal performance results in *Figure 6.1* and *Figure 6.2* the following statements can be made, regarding the dependency on storage volume. These results can further be implemented into a general perspective, as well as in the reference project.

- When regarding thermal efficiency, it can be concluded from *Figure 6.1* that a storage volume of approximately 1500000-2000000 m^3 would yield the maximum efficiency.
- From a cooling perspective the increased possibility of charging, see *Figure 6.2*, is seen as positive. This as the use of other cooling methods reduces.
- From an extraction perspective the increased volume (above 3000000 m^3), see *Figure 6.2*, yields a lowering of possible amounts of extracted energy. Hence it becomes more difficult to find economic profitability in the storage system.
- The thermal losses from the storage increase linearly, as the volume increases. Hence an acceptable amount of losses needs to be determined, as these correspond to lost economic value.

- In the reference project a storage volume of $3 \cdot 10^6$ m^3 was given in the preconditions. In *Figure 6.2* this corresponds to a charge of 50.7 GWh, and an extraction of 34.5 GWh, which is the highest possible value for the reference *DST-model* in *appendix J*. *Figure 6.1* shows this to yield a moderately high thermal efficiency.

6.1.3 Sensitivity analysis of borehole depth

The results from varying the parameter of borehole depth in the sensitivity study presented in *section 5.2* are presented in *Figure 6.3* and *Figure 6.4*.

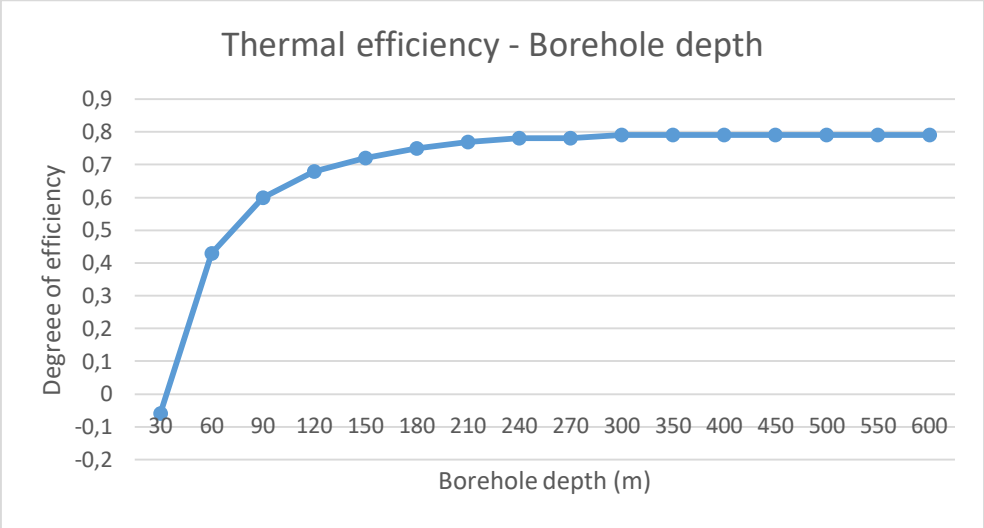

Figure 6.3 – Thermal efficiency dependent on borehole depth.

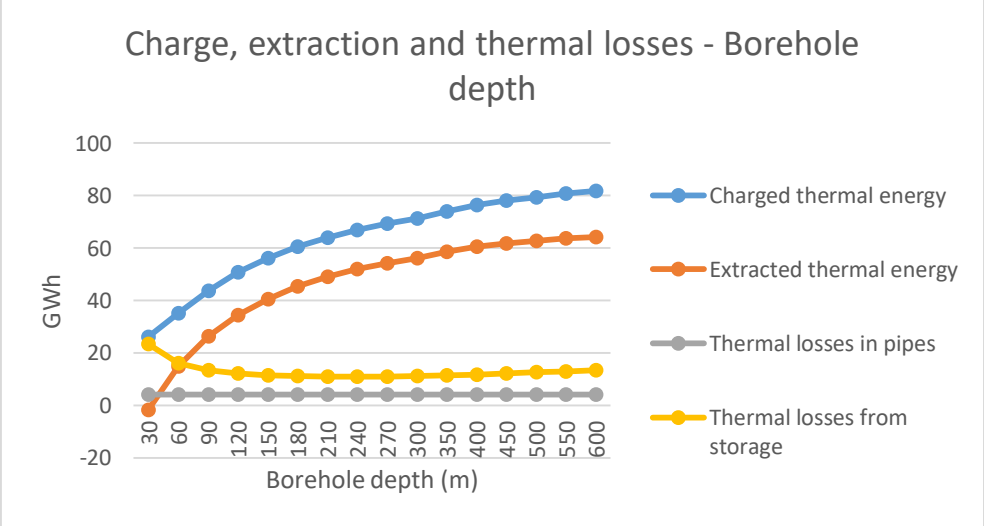

Figure 6.4 – Thermal performance of the storage for variant borehole depth.

Theoretical basis of results for varying the borehole depth

The variation of borehole depth alters the geometry of the storage volume in such a way that the cylinder varies in height and radius, as seen in *Figure 6.5*.

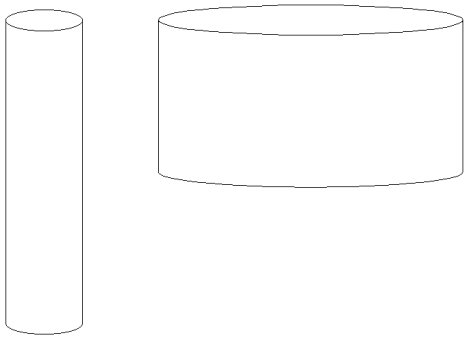

Figure 6.5 – Cylinder geometry dependent on borehole depth.

The increased depth will in accordance with *Eq. 3, section 3.1.1*, yield a lowered damping coefficient for heat transfer. This lowered damping coefficient will in accordance with *Eq. 6, section 3.1.1*, yield a greater thermal energy transfer between carrier fluid and storage volume. This explains for the results in *Figure 6.3* and *Figure 6.4*.

$\beta = e^{\frac{-\alpha_p L_p}{C_f Q_f}}$ → As L_p increases, β decreases

$q = \frac{C_f Q_f}{V} \cdot (1 - \beta) \cdot \left(T_{fin} - T_a\right)$ → A decrease of β yields an increased energy transfer (q)

The thermal extraction is dependent of the average temperature of the storage, which during discharge will be the driving force behind the extraction. When the volume and number of boreholes is constant but the radius decreases a smaller borehole spacing will be derived. By using *Eq. 8-10, section 3.1.3*, it can be shown that the average temperature increases, and hence also the possibility of thermal energy extraction, as seen in *Figure 6.4*. *Eq. 9* shows that the time before interaction between boreholes decreases, which explains for higher storage temperatures and better possibility of extraction.

$r_1 = 0{,}525 \cdot B$ → As B decreases, so does r_1

$t_{lim} = \frac{0{,}2 \cdot r_1^2}{\lambda}$ → As r_1 decreases, so does t_{lim}

$T_m = \frac{q \cdot t}{\pi \cdot C \cdot r_1^2}$ → As r_1 decreases, T_m increases

The thermal losses are according to *Nordell* (1987) explainable by the reduced influence of the top boundary conditions of the storage as borehole depth increases. The temperature variations on top of the storage are hence more negligible and will give less effect. The thermal losses will also be reduced as the increased depth alters the volume shape to a cylinder with a smaller radius, see *Figure 6.5*. This smaller radius yields a smaller circumference yields a smaller area over which exchange can take place with the surroundings.

Analysis of thermal performance results for borehole depth dependency

When analysing the thermal performance results in *Figure 6.3* and *Figure 6.4* the following statements can be made, regarding the dependency on borehole depth. These statements regard both general perspectives, as well as they are interpreted from a perspective of the reference project.

- It can be interpreted from *Figure 6.3* that an increased borehole depth yields a greater thermal efficiency. This without regards to thermal gradients, groundwater flows, and highly conductive zones. Factors which need to be taken into consideration when designing/analysing borehole thermal energy storages.
- The thermal performance results shown in *Figure 6.4* show that deeper boreholes are desirable from a charging, and extraction, perspective. A statement which is further strengthened by the thermal efficiency results in *Figure 6.3*.
- In line with the statement presented by *Nordell* (1987) that deeper boreholes yield lowered thermal losses from the storage, the results presented in *Figure 6.4* further strengthens this statement. Hence deeper boreholes are from a thermal perspective desirable. However, from an economic perspective the increased depth would come with increased costs and hence a balance must be found between investment cost and value of extracted energy.
- The thermal losses of the horizontal pipe system are not affected as no parameter regarding their properties were altered.
- Noticeable from the thermal performance figures are the initial negative performances. The explanation for this is theoretically unknown and hence to be analysed analytically. This might be due to the storage being very shallow and dependent on the upper boundary conditions which alter the set ground temperature of 10 degrees to a lower value more dependent on the surface temperature.
- In the reference project at *Filborna* a borehole depth of 120 metres was preliminarily chosen, which from *Figure 6.3* and *Figure 6.4* show not to yield the highest thermal efficiency, nor charged or extracted amount of energy. The thermal losses are though heavily reduced when comparing with shallower storages.

A secondary aspect brought forward by *Nordell* (2016) is the straightness of the boreholes. This aspect is not implementable in the *TRNSYS* model and can only be dealt with on a theoretical plane. The factor relates to practical deviations from theoretical preconditions and brings these deviations into light. If inclination occurs, this means that a reduction of depth takes place, hence reducing efficiency and potential amount of energy extracted. This also affects the interaction between boreholes as the spacing alters.

6.1.4 ***Sensitivity analysis of borehole radius***

The results from varying the parameter of borehole radius in the sensitivity study presented in *section 5.2* are presented in *Figure 6.6* and *Figure 6.7*.

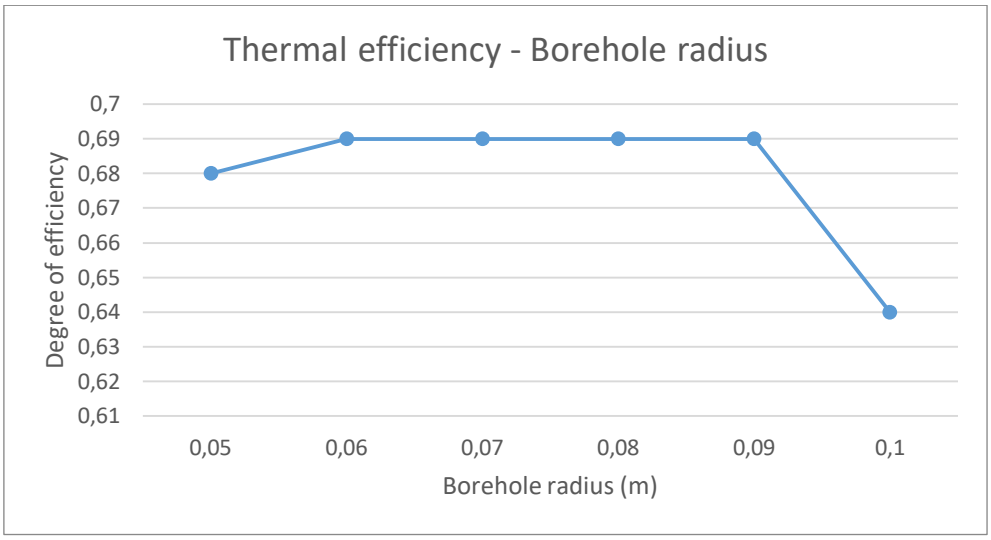

Figure 6.6 – Thermal efficiency dependent on borehole radius.

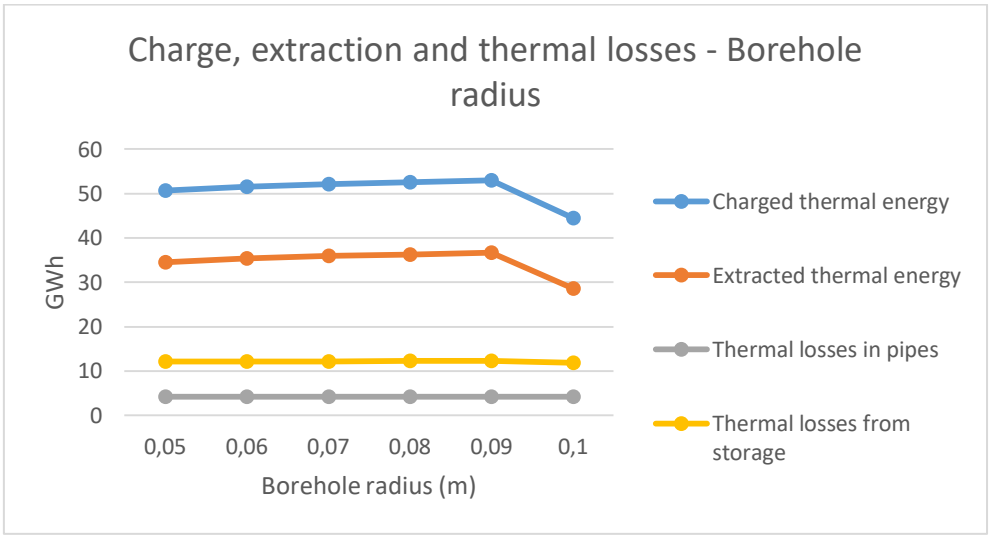

Figure 6.7 – Thermal performance of the storage for variant borehole radius.

Theoretical basis of results for variant borehole radius

As the radius increase, without altering the borehole depth, so does the heat transfer rate between the borehole and the storage volume, this as an effect of the boreholes area increases.

Since the thermal transfer is increased in general, this results in both more charged, and extracted, thermal energy for the system.

As mentioned in *section 3.2.1* the g-function is dependent on borehole radius, however its relation is unknown as the g-function is not fully described.

$$g\left(\frac{t}{t_s}, \frac{r_b}{H}, \frac{B}{H}, \frac{d}{H}\right)$$

Analysis of thermal performance results for borehole radius dependency

When analysing the thermal performance results in *Figure 6.6* and *Figure 6.7* the following statements can be made, regarding the dependency on borehole radius. These statements regard both general perspectives, as well as they are interpreted from a perspective of the reference project.

- It can from *Figure 6.6* be interpreted that an increase in borehole radius does not yield a greater thermal efficiency.
- The thermal performance results presented in *Figure 6.7* show that with increased borehole radius follows the possibility to charge, and extract, more thermal energy.
- Thermal losses from the horizontal pipe system, and the storage, can be concluded as independent of the borehole radius as these show no significant variation for the results presented in *Figure 6.7*.

From the results presented in *Figure 6.6* and *Figure 6.7* it is noticeable that the largest analysed borehole radius does not conform to the trend of the other data points. This deviation is in this study unexplainable, and further studies should be performed as to verify this uncertainty.

6.1.5 ***Sensitivity analysis of the influence of a gap between heat exchanger and borehole wall***

The results from varying the parameter of gap thickness in the sensitivity study presented in *section 5.2*, are presented in *Figure 6.8* and *Figure 6.9*. The gap thickness corresponds to a spacing between the casing of the borehole, and the borehole wall, which is assumed filled with water.

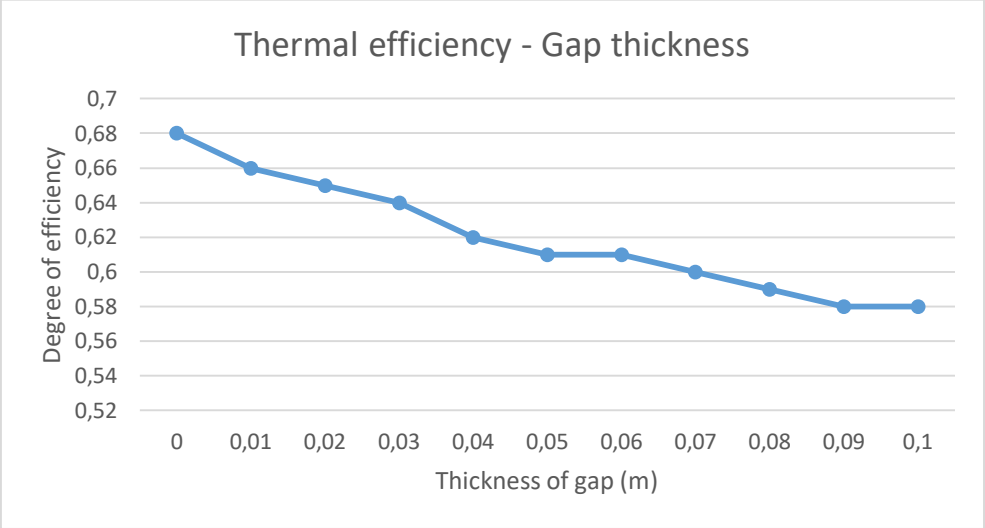

Figure 6.8 – Thermal efficiency dependent on gap thickness.

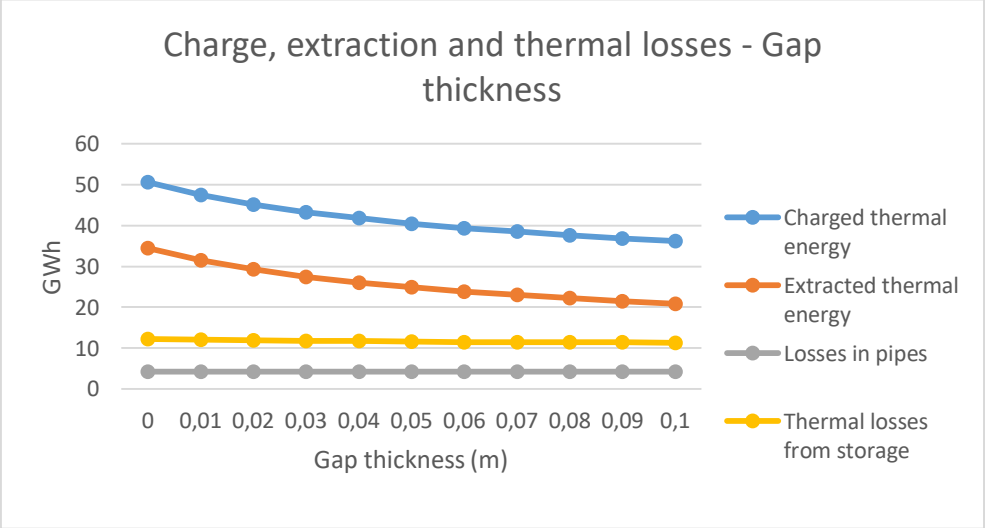

Figure 6.9 – Thermal performance of the storage for variant gap thickness.

Theoretical basis of results for variant gap thickness

The thermal response results are somewhat logical as the gap poses a further obstacle for the heat exchange between carrier fluid and storage mass. These results are hence somewhat explainable by the local solution, see *section 3.1.3. Eq. 11* shows that the thermal resistance per unit length of pipe (R_b) clearly has an effect on the transfer between carrier fluid and storage mass. If this resistance is to increase, the transfer would hence be affected.

$$T_f(t) \cong T_m(t) + \frac{q}{2 \cdot \pi \cdot \lambda}\left(2 \cdot \pi \cdot \lambda \cdot R_b + \ln\left(\frac{r_1}{r_b}\right) - \frac{3}{4}\right)$$

$\rightarrow If\ R_b\ increases, the\ fluid\ temperature\ T_f\ increases, hence\ a\ lower\ amount\ of\ heat\ has\ been\ transfered.$

This concept is further brought up in the steady-flux regime, see *section 3.1.5*, where *Eq. 17* further shows this effect as if the thermal resistance takes a larger portion of the relation between storage temperature and carrier fluid temperature. A higher temperature of the carrier fluid points towards that a reduced heat exchange has taken place.

$$T_f - T_m = q\ R_{sf} \leftrightarrow If\ R_{sf}\ increases\ T_m\ decreases\ if\ T_f\ is\ kept\ constant$$

Analysis of thermal performance results for dependency on gap thickness

When analysing the thermal performance results in *Figure 6.8* and *Figure 6.9* the following statements can be made regarding the dependency of gap thickness. Both general perspectives, and implementation in the reference project is to be made.

- *Figure 6.8* shows that an increased gap thickness yields a lowered thermal efficiency. Hence this is not a desirable phenomenon.
- Both the curve for charge and extraction in *Figure 6.9* show a decrease as the gap thickness increases. It is hence preferable to avoid a gap between casing and borehole wall from both a charging, and extraction, perspective.
- The thermal losses are not affected greatly for both storage and horizontal pipe system.
- The impact of this factor in practical results can only be implemented on a theoretical plane as it is not a factor which can be measured. Furthermore the factor cannot be foreseen and can hence only be implemented as an assumption in the simulation models, which is the case in the reference project where no gap is assumed.
- The gap is assumed to be filled with water as the majority of the boreholes are located beneath the groundwater level. Hence the thermal conductivity of the gap is assigned values corresponding to water. If the gap was to be made up of air this would yield greater effects as air has a lower thermal conductivity than water. Hence less energy would be able to be stored or extracted as the thermal resistance (R) would increase.

6.1.6 Sensitivity analysis of the influence of header depth

The results from varying the parameter of header depth in the sensitivity study presented in *section 5.2* are presented in *Figure 6.10* and *Figure 6.11*. When studying the influence of the parameter of header depth one must compensate the lowering of the header depth in the storage volume. A header depth of zero corresponds to surface level, while a header depth of five metres corresponds to the water level being 5 m below the surface. Making the heat exchangers thermally inactive for the topmost five metres, hence using the material where no heat exchange takes place as an insulating layer.

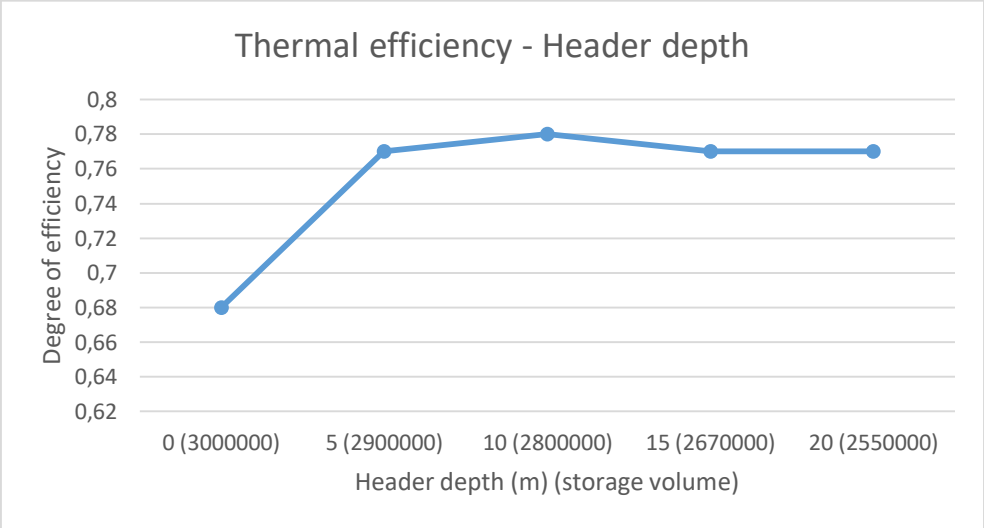

Figure 6.10 – Thermal efficiency dependent on header depth.

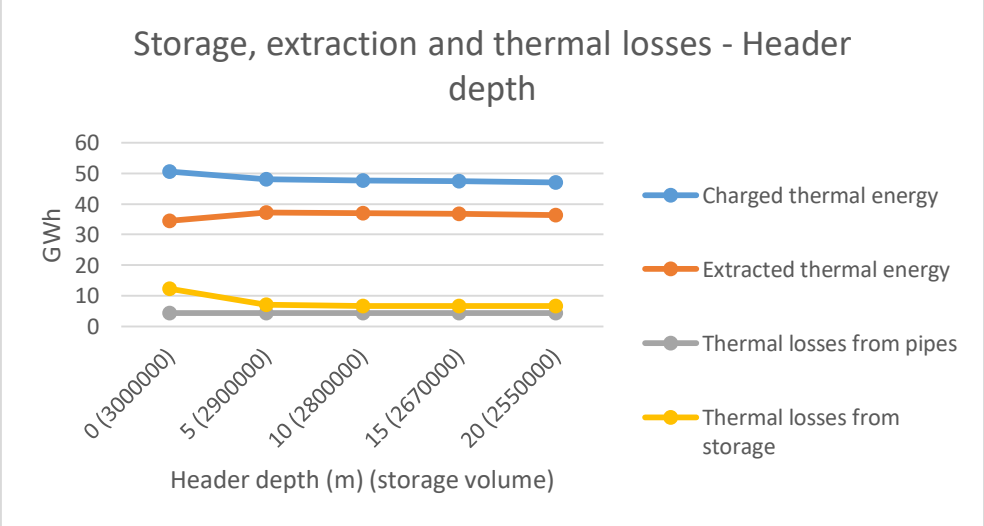

Figure 6.11 – Thermal performance of the storage for variant header depth.

Theoretical basis of results for varying header depth

The increased header depth yields that the topmost section, corresponding to the header depth, is thermally inactive. As a consequence of this, the topmost thermally inactive segment acts as an insulating layer, which will lower the thermal losses.

Analysis of thermal performance results for dependency on header depth

When analysing the thermal performance results in *Figure 6.10* and *Figure 6.11* the following statements can be made regarding the dependency of header depth. These both from general perspective, and from the perspective of the reference project, upon which the sensitivity study is based.

- The thermal efficiency presented in *Figure 6.10* show a peak of efficiency around 10 metres of header depth. But a significant increase overall from a header depth of 0 metres.
- From a charging perspective an increased header depth yields that less energy may be stored, which from a cooling perspective is negative.
- From an extraction perspective the increased header depth yields a small increase in possibility of extraction, which is positive from an economic perspective where value is found in this energy.
- The thermal losses from the storage are significantly reduced as the header depth increases up to five metres, after which the curve is practically none variant. It can be assumed that the decrease corresponds to top losses and that the "steady segment" of the thermal loss curve correspond to the side, and bottom, losses from the storage.
- The thermal losses from the horizontal pipe system are not affected.
- From an optimization perspective in the reference project a header depth around 5-10 metres show the greatest efficiencies and potentials for extraction. Hence this alternative system setup would be preferable. Questionable is if these effects would compensate for complications in design of the heat exchangers. As the effects do not deviate largely the simplest, most economic, design alternative should be promoted if no support can be found for economic profitability of a lowering of the header depth in the design.

6.1.7 ***Sensitivity analysis of the influence of the number of boreholes***

The results from varying the parameter of *number of boreholes* in the sensitivity study presented in *section 5.2* are presented in *Figure 6.12* and *Figure 6.13*.

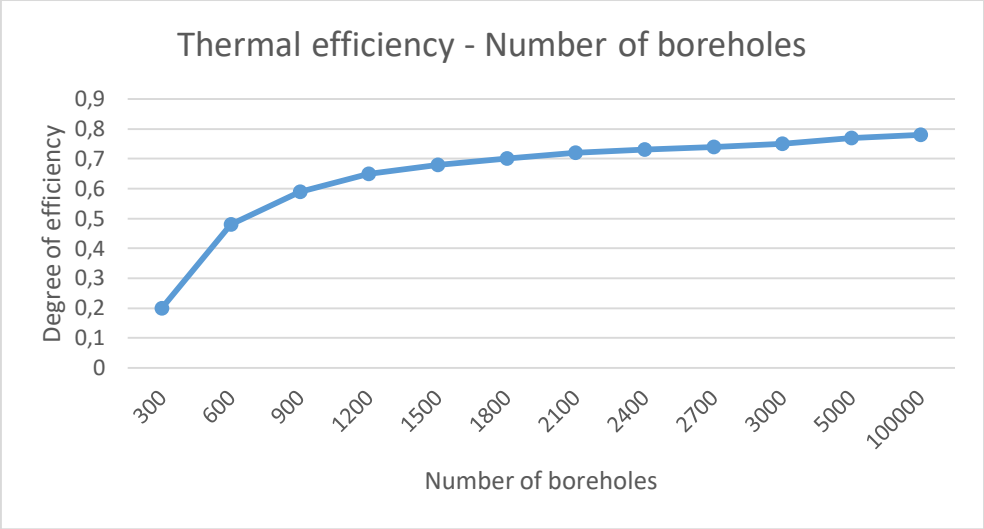

Figure 6.12 – Thermal efficiency dependent on the number of boreholes.

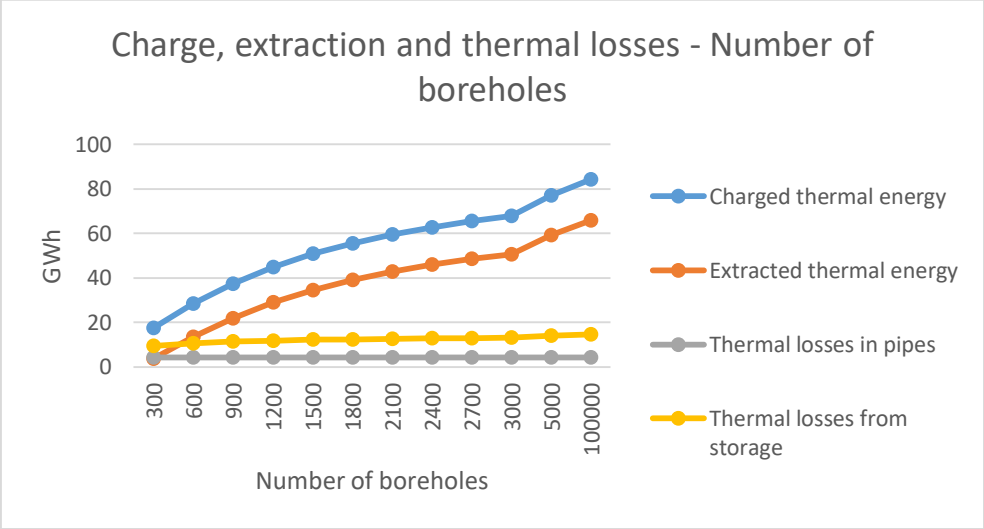

Figure 6.13 – Thermal performance of the storage for a variant number of boreholes. (Note that the last two values are of different scale than the rest of the data values)

Theoretical basis of results for varying number of boreholes

When varying the number of boreholes in a set volume this affects the borehole spacing. As the boreholes are to be evenly distributed in the storage volume an increased number of boreholes will yield a smaller spacing. This decreased borehole spacing (B) will in the local solution, *section 3.1.3*, yield that the average storage temperature increases, which via *Eq. 8* and *10* shows that an increased amount of thermal energy has been transferred.

$$r_1 = 0{,}525 \cdot B \rightarrow As\ B\ decreases\ so\ does\ r_1$$

$$T_m = \frac{q \cdot t}{\pi \cdot C \cdot r_1^2} \rightarrow T_m\ increases\ as\ r_1\ decreases$$

Analysis of thermal performance results for dependency on number of boreholes

When analysing the thermal performance results in *Figure 6.12* and *Figure 6.13* the following statements can be made regarding the dependency on the number of boreholes. From the sensitivity study, based on the reference project, both general and reference related perspectives are analysed.

- *Figure 6.12* shows that an increased number of boreholes, in a fixed storage volume, yields an increased thermal efficiency, as defined in *section 5.2*.
- *Figure 6.13* indicates that an increased number of boreholes, in a fixed volume, is positive from a charging and extraction perspective.
- The results for thermal performance presented in *Figure 6.13* show that no major influence on the thermal losses from the storage takes place. This can be assumed to be related to that the geometry does not change, only the average storage temperature, which could cause the minor increase in thermal losses from the storage.
- The thermal losses from the horizontal pipe system are not affected as no parameter regarding these was altered.
- In the reference project 1500 boreholes were planned for, which from *Figure 6.12* and *Figure 6.13* is not the most thermally beneficial option, but might be based in economic balance between construction cost and time, contra profitability.
- A larger number of boreholes are over all seen as positive, but this increase comes with an economic downside as more boreholes will yield greater investment costs. Hence a balance between investment and profitability is needed.

6.1.8 Sensitivity analysis of the influence of the number of boreholes in series

The results from varying the parameter of *number of boreholes in series* in the sensitivity study presented in *section 5.2* are presented in *Figure 6.14* and *Figure 6.15*.

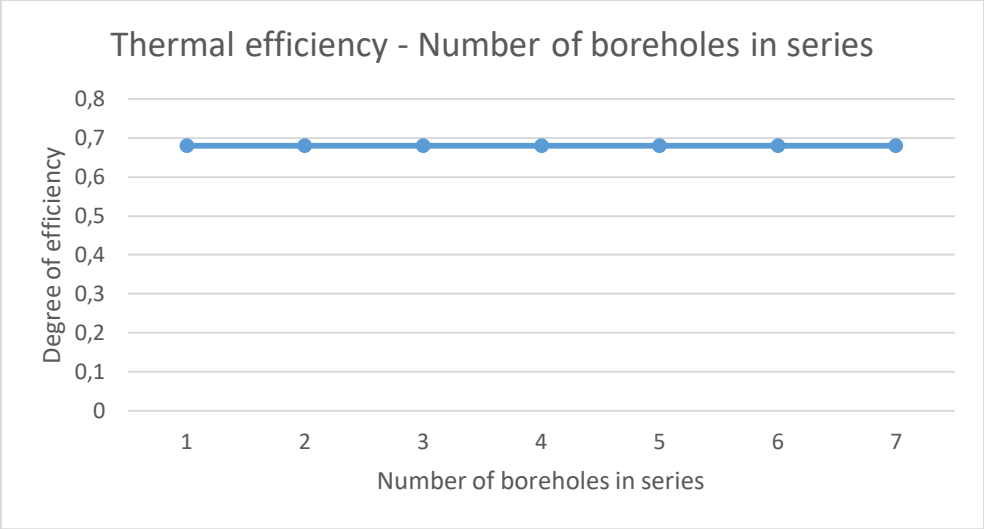

Figure 6.14 – Thermal efficiency dependent on the number of boreholes in series.

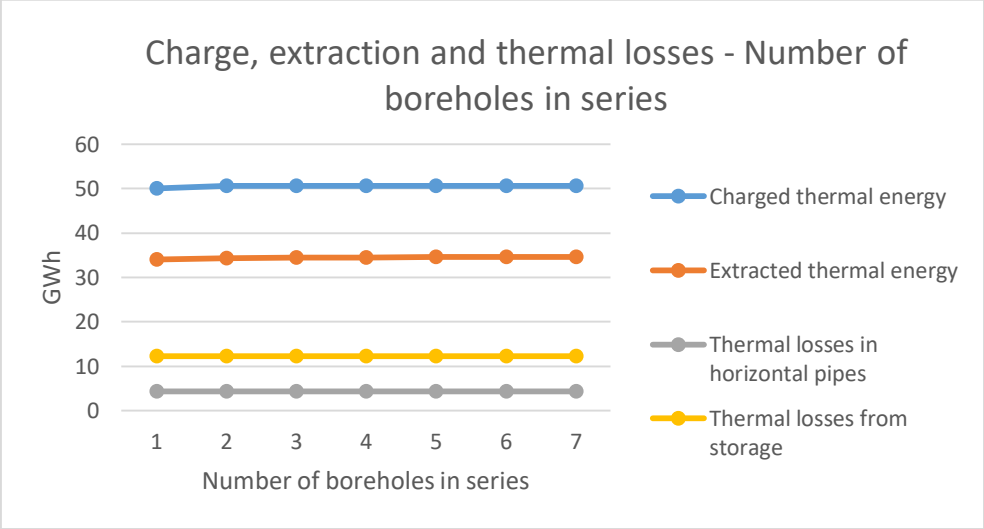

Figure 6.15 – Thermal performance of the storage for variant number of boreholes in series.

Theoretical basis of results for varying the number of boreholes in series

The theoretical basis for why the results don't vary, as shown in *Figure 6.14* and *Figure 6.15* is not found and can hence only be theoretically analysed in the following segment.

Analysis of thermal response results for dependency on number of boreholes in series

Why the results do not depend on the number of boreholes in series may be because the thermal exchange process becomes the same. The only alteration may be the problematics in design as a longer flow-path for the carrier fluid along with more boreholes would yield greater pressure drops in the pipe systems. Something not desirable because of this makes it harder to maintain a homogenous flow, a parameter not included in a further analysis.

6.1.9 ***Sensitivity analysis of the influence of the length of the horizontal pipe system***

The results from varying the parameter of *horizontal pipe length* in the sensitivity study presented in *section 5.2* are presented in *Figure 6.16* and *Figure 6.17*.

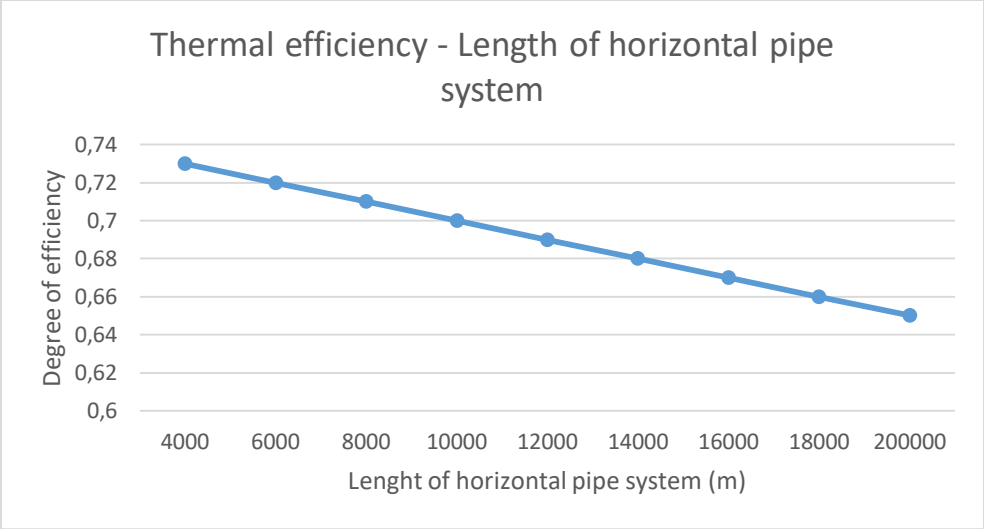

Figure 6.16 – Thermal efficiency dependent on the length of the horizontal pipe system.

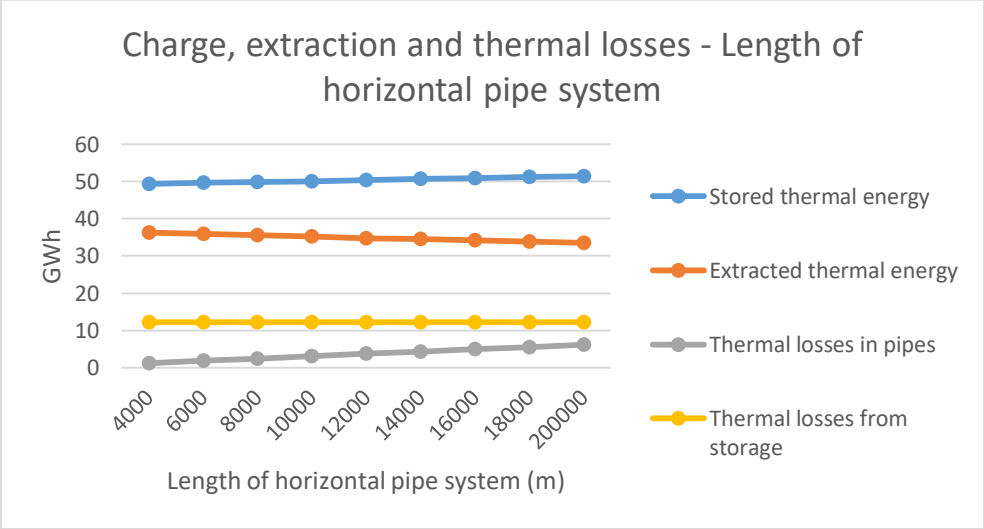

Figure 6.17 – Thermal performance of the storage for variant length of the horizontal pipe system.

Theoretical basis of results for varying the horizontal pipe length

The theoretical basis of the results derived in *Figure 6.16* and *Figure 6.17* is found in the concept of thermal losses from the horizontal pipe system occur. These losses are consequences of the heat exchange the horizontal pipes have with the surrounding area. Hence an extended length of pipe will increase the exposure time of the fluid in the pipe system, and the losses will increase. This is purely intuitively derived.

Analysis of thermal response results for dependency on number of boreholes in series

When analysing the thermal performance results in *Figure 6.16* and *Figure 6.17* the following statements can be made regarding the dependency on the number of boreholes.

- *Figure 6.16* shows that from a thermal efficiency perspective, a short as possible horizontal pipe system is desirable.
- *Figure 6.17* shows that the thermal performance of charge, extraction, and thermal losses are linear. As the charge is defined as the summary of all other parameters in *Figure 6.17* the linear increase is corresponding to the increase of thermal losses from the horizontal pipes. The increased losses in the horizontal pipes also yield that the extracted energy decreases as well as that the storage losses decrease as the average storage temperature decreases.
- In the reference project the horizontal pipe length is assumed. This sensitivity analysis shows the sensitivity of the system if an incorrect assumption is made, hence this parameter should be taken into consideration for the final design as not to cause unpredicted losses.
- Note that the charged amount of energy is measured from the heat exchanger and hence incorporates both the storage volume and the horizontal pipe system.

6.1.10 Sensitivity analysis of the influence of the efficiency of heat exchanger

The results from varying the parameter of *efficiency of heat exchanger* in the sensitivity study presented in *section 5.2* are presented in *Figure 6.18* and *Figure 6.19*.

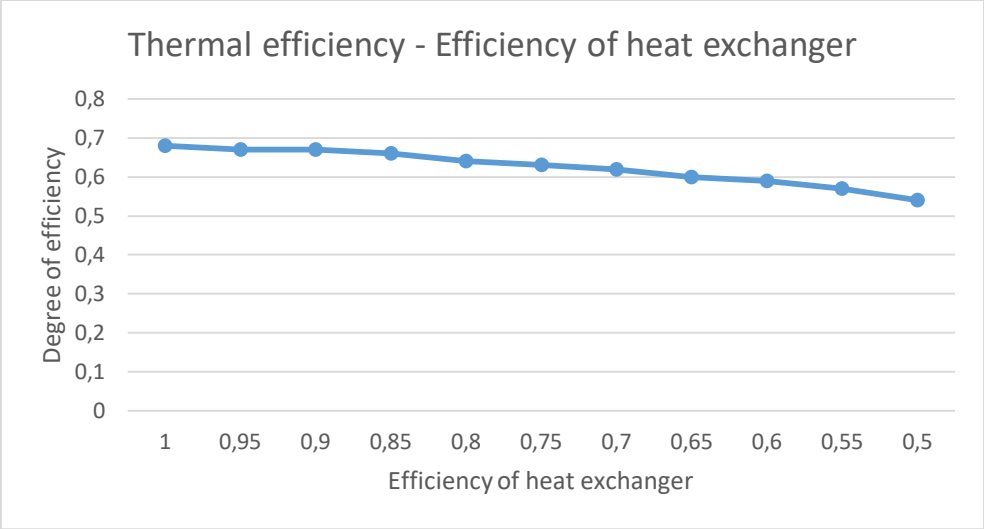

Figure 6.18 – Thermal efficiency dependent on the efficiency of the heat exchanger.

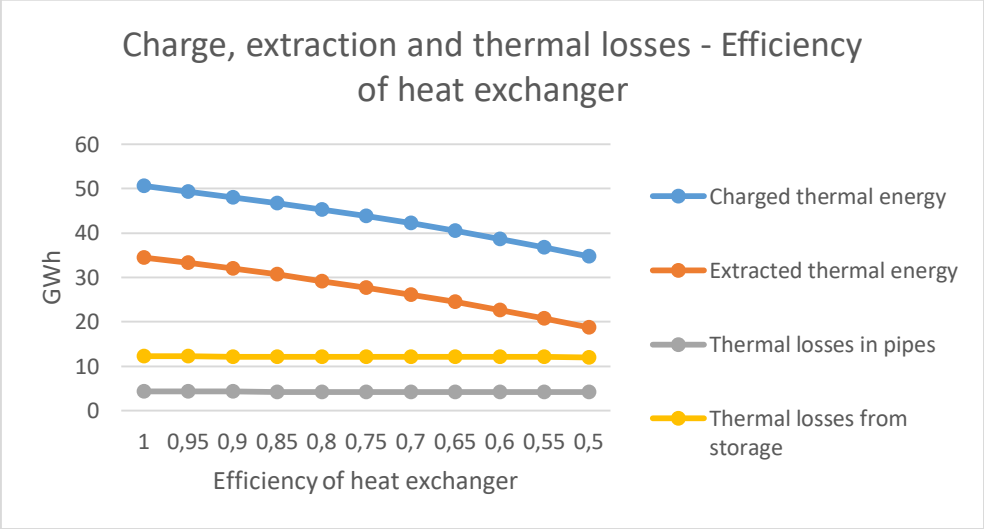

Figure 6.19 – Thermal performance of the storage for variant length of the efficiency of the heat exchanger.

Theoretical basis of results for varying efficiency of the heat exchanger

The results are logical as the efficiency of the heat exchanger relates to how much energy may be transferred from the thermal process of the cogeneration plant, to the loop of the thermal storage. As this efficiency decreases, so does the possibility of charging and extracting, as there is less energy in the system.

One interesting observation is though that the losses are constant and are independent of the efficiency of the heat exchanger. This seems questionable since the thermal losses should be lowered when the mean temperature of the storage decreases. Further investigations have to be executed in order to identify if there is a malfunction in the simulation tool or not.

Analysis of thermal response results for dependency on number of boreholes in series

When analysing the thermal performance results in *Figure 6.18* and *Figure 6.19* the following statements can be made regarding the dependency on the number of boreholes.

- *Figure 6.18* shows a decrease in thermal efficiency of the system as the efficiency of the heat exchanger decreases.
- The results in *Figure 6.19* show a decreased potential for charging and extraction as the efficiency of the heat exchanger decreases. This points towards that a knowledge of this efficiency is needed when the thermal system is modelled as the results may vary significantly.
- The thermal losses, as seen in Figure *6.19*, seem independent of the thermal efficiency.

6.2 *Analysis of insulation design*

The analysis performed in accordance with *section 5.2.1* regarding the analysis of insulation design yielded the results for insulation width, and the joint analysis results of insulation thickness and thermal conductivity of insulation as presented below.

6.2.2 ***Analysis of the influence of insulation width***

The results from varying the parameter of *insulation width (height fraction in TRNSYS)* in the sensitivity study presented in *section 5.2.1* are presented in *Figure 6.20* and *Figure 6.21*.

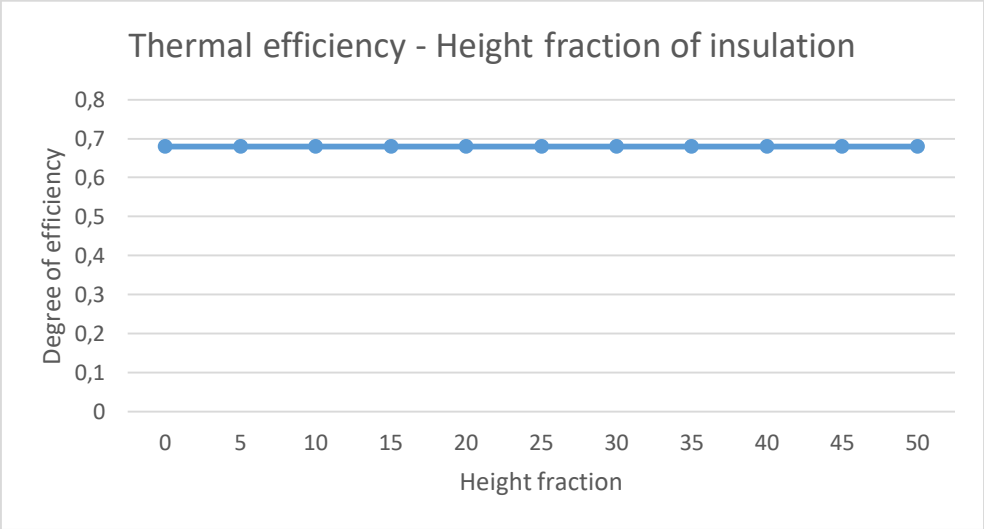

Figure 6.20 – Thermal efficiency dependency on insulation width beyond the storage outer perimeter.

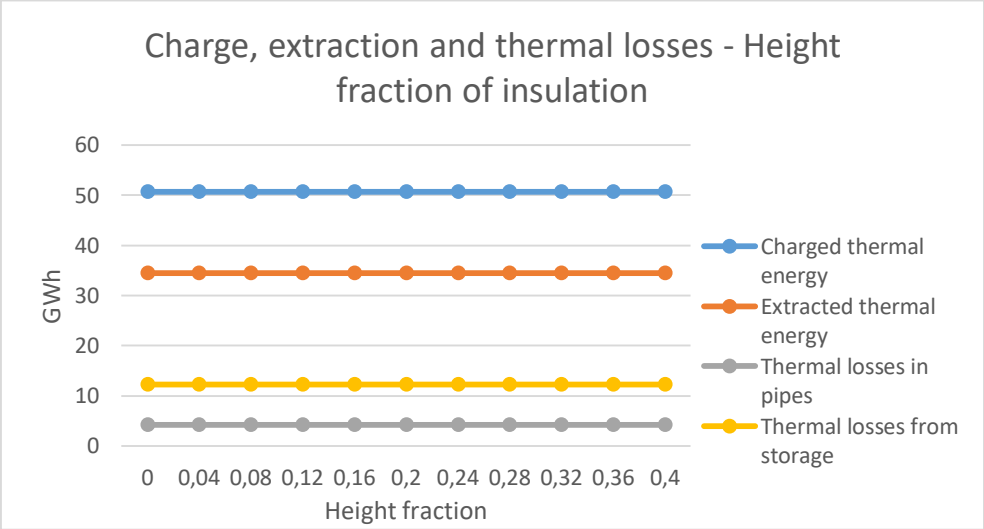

Figure 6.21 – Thermal performance of the storage for variating the extension of the insulation layer beyond the storage top horizontal boundary.

Theoretical basis for results of varying the width of the insulating layer

No theoretical basis was found for why the thermal performance was none-dependent on the insulation width. Hence only an analysis perspective can be used, as in the following.

Analysis of thermal response results for dependency of insulation width

The results presented in *Figure 6.20* and *Figure 6.21* indicate a little influence of insulation width on the thermal performance of the storage. Hence this can be restricted to solemnly cover the topmost part of the storage, which limits material use.

6.2.3 ***Joint analysis of insulation thermal conductivity and insulation thickness***

When analysing the insulation thickness along with the thermal conductivity of the insulating layer, results as presented in *Figure 6.22* - *Figure 6.26* are derived.

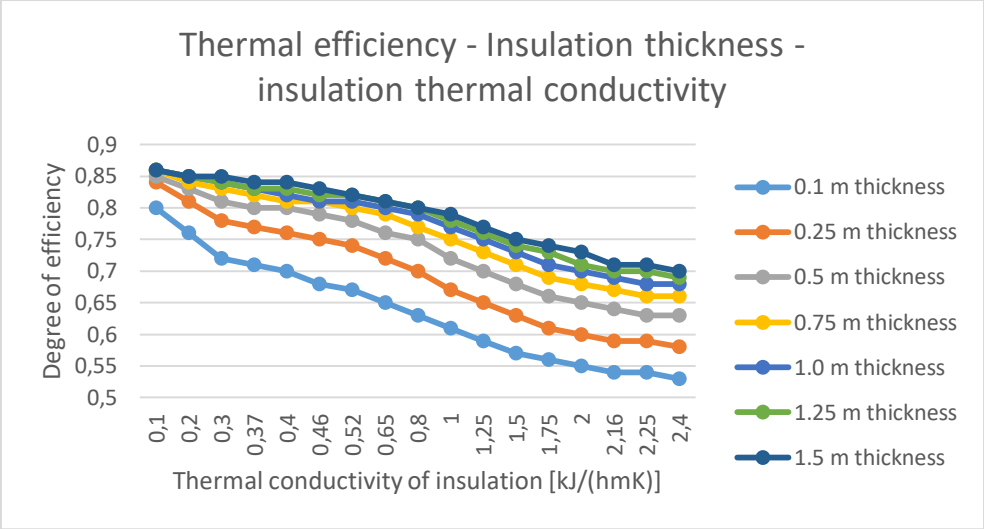

Figure 6.22 – Thermal efficiency dependent on the insulation thickness and its thermal conductivity.

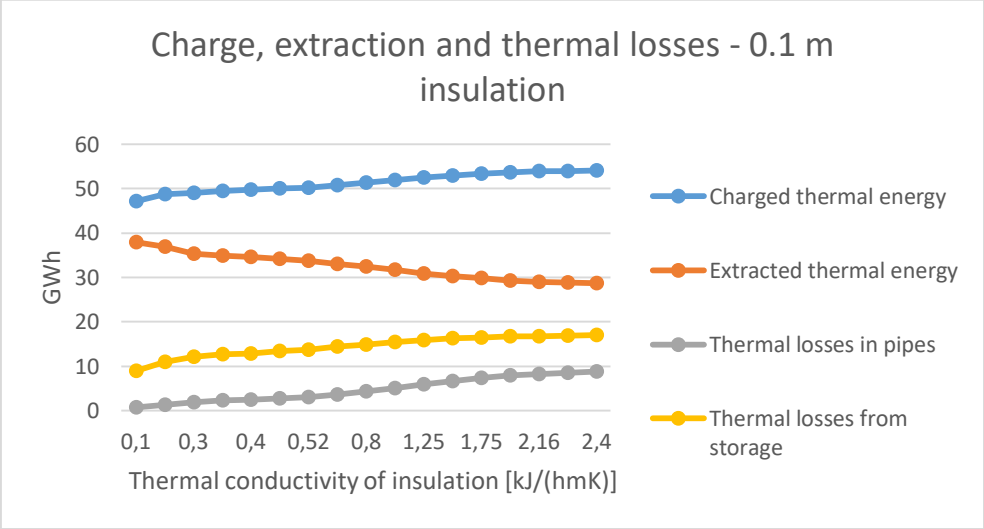

Figure 6.23 – Thermal performance of the storage for variant thermal conductivity for the insulation thickness of 0.1m.

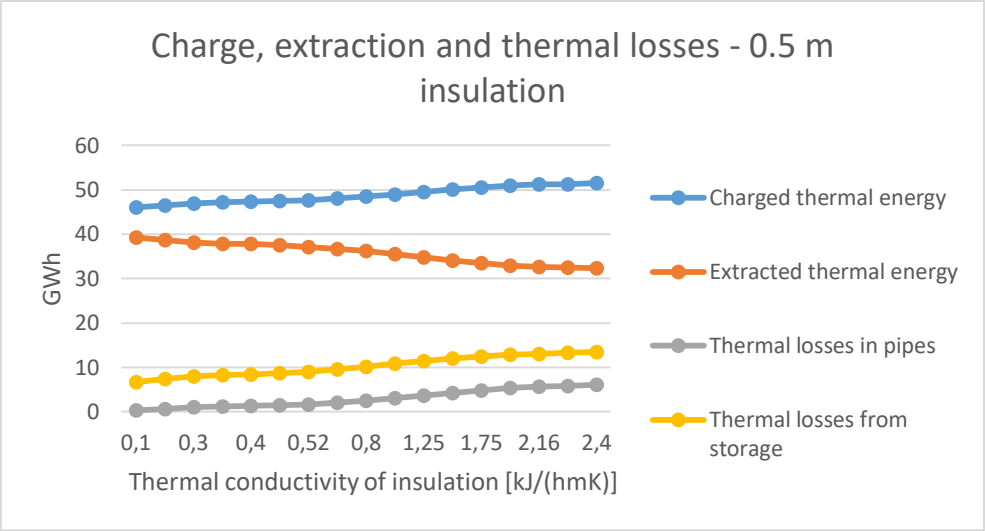

Figure 6.24 – Thermal performance of the storage for variant thermal conductivity for the insulation thickness of 0.5m.

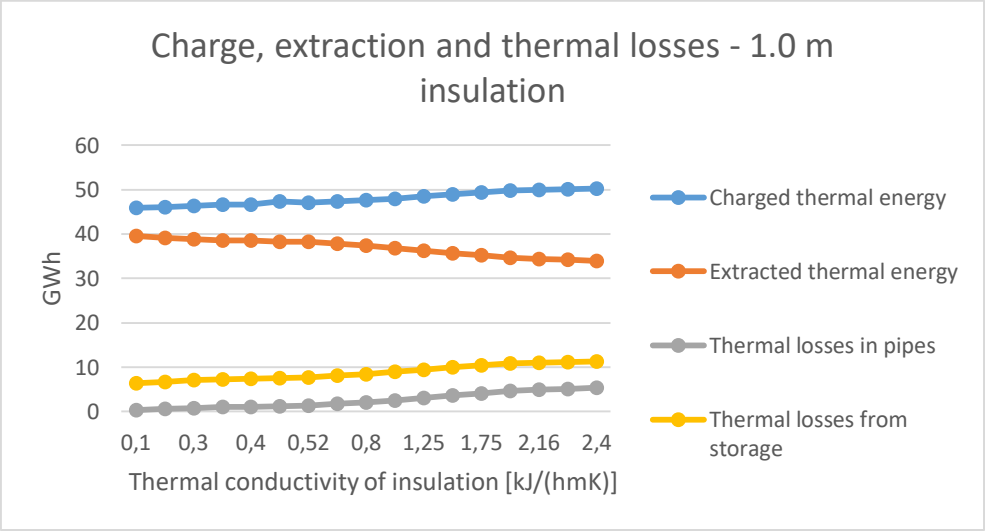

Figure 6.25 – Thermal performance of the storage for variant thermal conductivity for the insulation thickness of 1m.

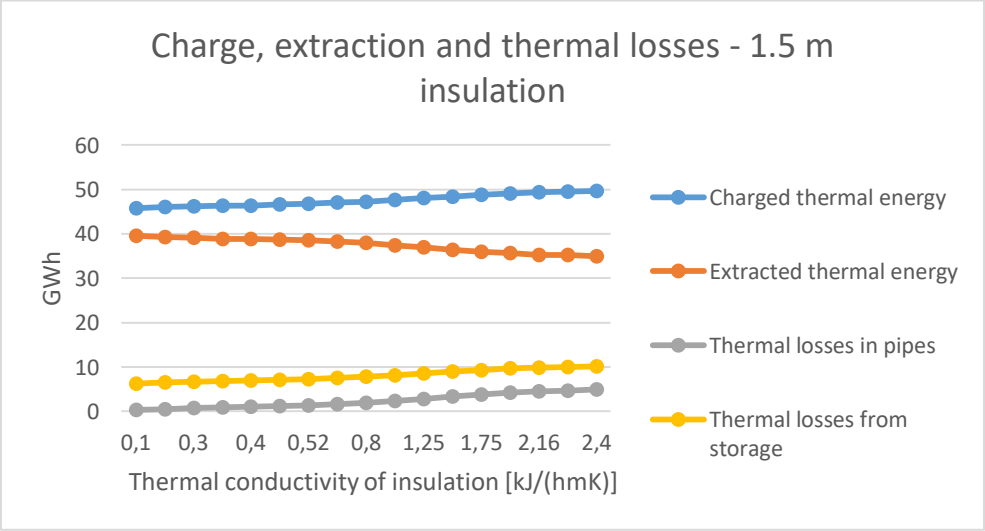

Figure 6.26 – Thermal performance of the storage for variant thermal conductivity for the insulation thickness of 1.5m.

Theoretical basis of results for variant thermal conductivity and insulation thickness

A lower value on the thermal conductivity property of the insulation layer of the storage yields a better insulating performance, since less thermal energy can be transported through the material. The insulating performance will also increase with increased thickness hence the comparison of the result between thermal conductivity and thickness regarding thermal energy accomplishment.

Analysis of results for the relation between thermal performance thermal conductivity and insulation thickness

When analysing the thermal performance results in *Figure 6.23* - *Figure 6.26* the following statements can be made regarding the dependency on the insulation thickness and thermal conductivity of the insulation.

- *Figure 6.22* shows that from a thermal efficiency perspective a low thermal conductivity of the insulation is preferable. This figure further show that an increased insulation thickness is preferable from a thermal efficiency perspective.
- *Figure 6.23* - *Figure 6.26* shows how the thermal performance is dependent on thermal conductivity of insulation, as well as insulation thickness. What can be concluded is that all graphs show similar tendencies for all curves.
- From a charging perspective an increase in insulation thickness reduces the possibility of charging. A lower thermal conductivity of the insulation layer also reduces the possibility of charging, and is hence negative from a charging perspective.
- With increased insulation thickness, and decreased thermal conductivity of the insulation, the possibility of extraction increases.
- The thermal losses from the storage, and horizontal pipe system, increase with increased thermal conductivity of the insulation, as well as with decreased insulation thickness.
- The results presented stresses the importance of moisture protection of the insulation as moisture and temperature (concluded from the project in *Stuttgart*, *section 2.4.3*) risk increasing the thermal conductivity. The results of such an event would risk causing a worse thermal performance, in accordance with the results presented in *Figure 6.23* - *Figure 6.26*.

When evaluating the material alternatives for a project, the thermal performance results presented in *Figure 6.22* - *Figure 6.26* can be used by assigning each material a thermal conductivity value. When these values are assigned one can use the graphs for comparing the thermal performance between different material alternatives with regards to thermal conductivity, and material thickness.

In the reference project the material alternatives were presented in *chapter 4*, along with their thermal properties. From these thermal property values the thermal performance can be evaluated from the graphs in *Figure 6.23* - *Figure 6.26*, as exemplified in *Figure 6.27*.

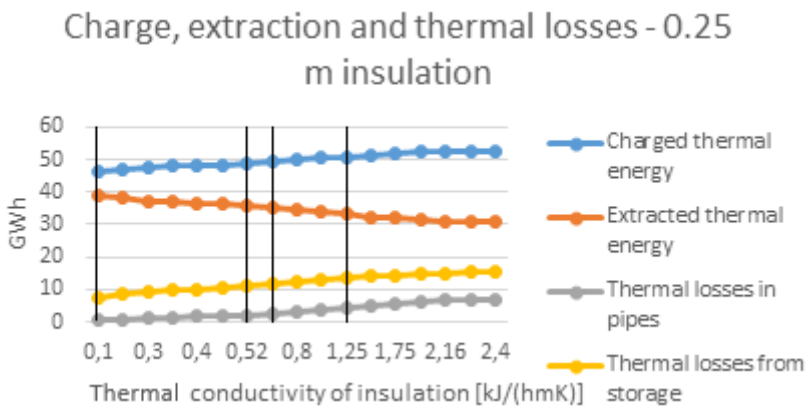

Figure 6.27 – Example of thermal performance for material alternatives in the reference project at Filborna. From left to right the black lines represent polystyrene, foam glass, expanded clay, slag gravel.

The thermal evaluation performed for the reference project show that the material with the lowest thermal conductivity (extruded polystyrene) also is the most preferable from a thermal extraction, and thermal losses perspective, which is logical. But as the material alternatives differ in material costs, this aspect has to be implemented into the material evaluation in order to properly compare the material alternatives. This economic evaluation is performed in *section 6.3*.

6.2.4 Analysis of insulation parameters with a header depth of 5 m

When analysing the insulation thickness along with the thermal conductivity of the insulating layer with regards to a header depth of 5 metres, results as presented in *Figure 6.28* - *Figure 6.32* are derived.

What differs in this analysis compared with the one presented in *section 6.2.2* is the water level in the boreholes. Here the header depth is 5 m (below the top of the boreholes) making the heat exchangers thermally inactive for the upper five metres, hence these top 5 metres will contribute to the insulation of the storage. This analysis has been performed due to the identified positive effects that the header depth showed in the results presented in *section 6.1.4*, and that it is of interest in the reference project.

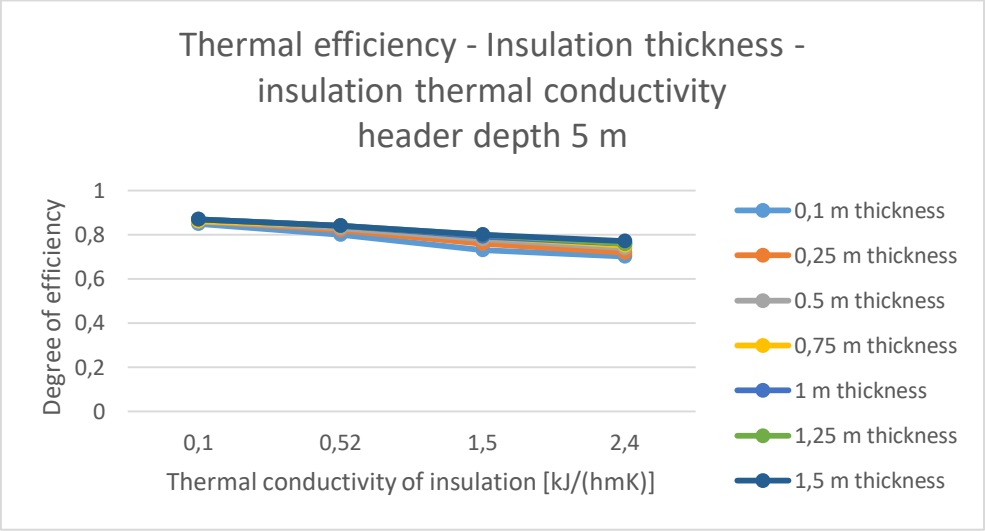

Figure 6.28 – Thermal efficiency (Charge/Extraction) dependent on the insulation thickness and its thermal conductivity.

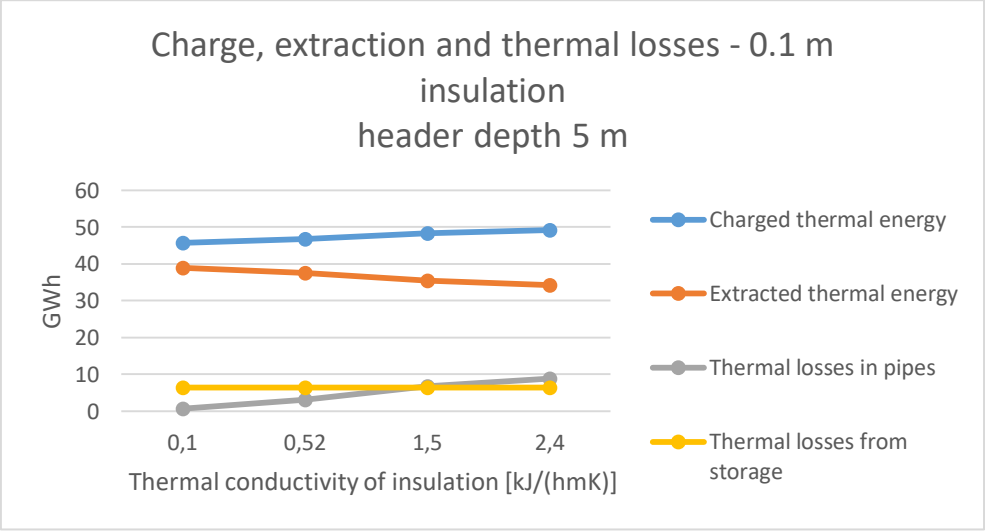

Figure 6.29 – Thermal performance of the storage for variant thermal conductivity for the insulation thickness of 0.1 m.

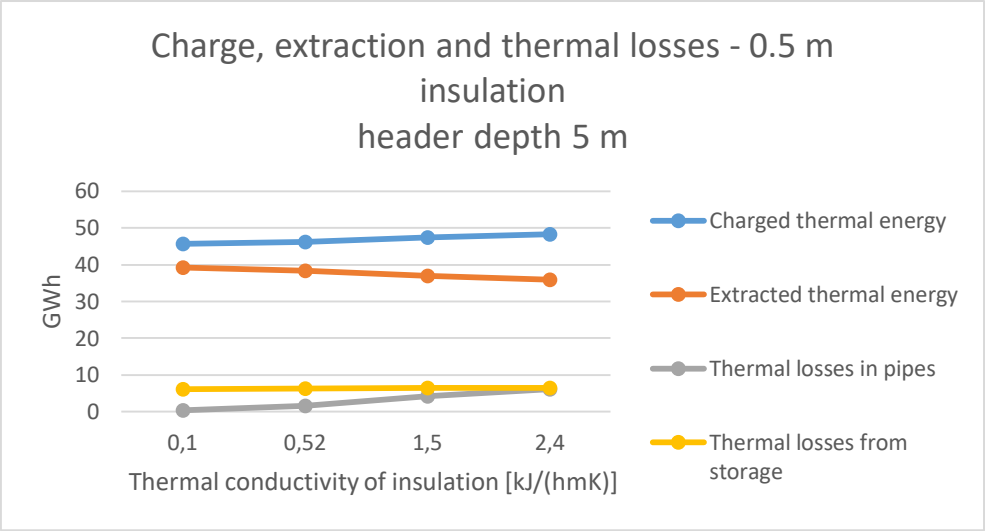

Figure 6.30 – Thermal performance of the storage for variant thermal conductivity for the insulation thickness of 0.5 m.

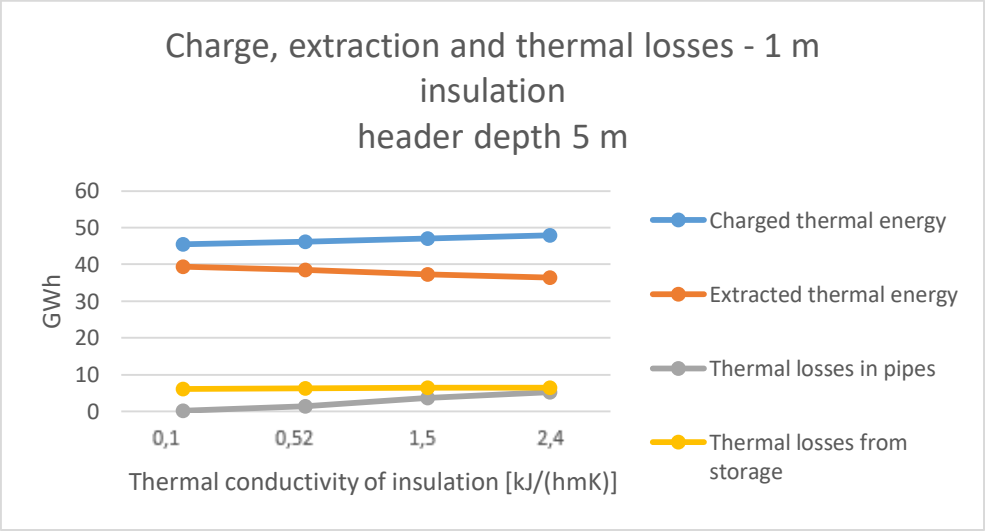

Figure 6.31 – Thermal performance of the storage for variant thermal conductivity for the insulation thickness of 1 m.

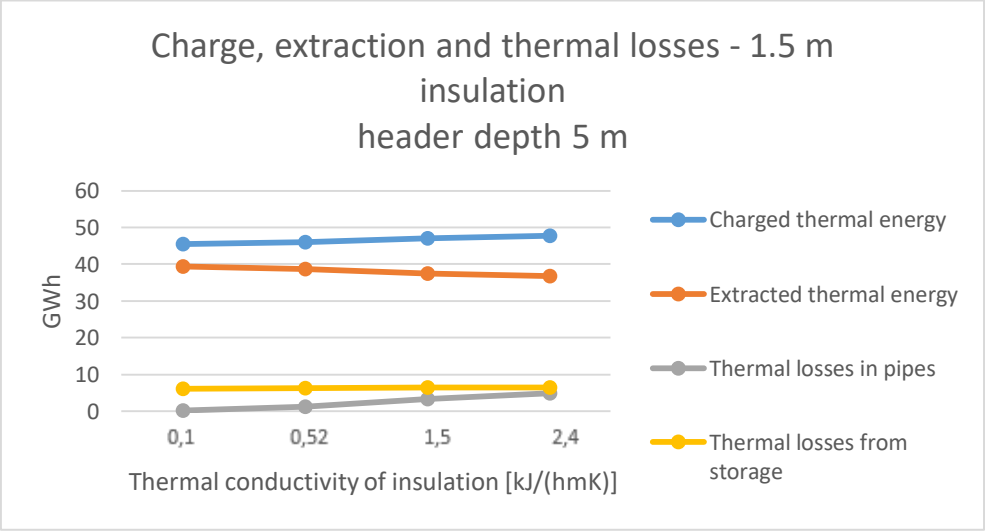

Figure 6.32 – Thermal performance of the storage for variant thermal conductivity for the insulation thickness of 1.5 m.

Theoretical basis of the results

The same theoretical basis to the results applies for this design as for the design where the header depth in the boreholes is zero (at the top of the boreholes) presented in *section 6.2.2*. A lower thermal conductivity of the insulating material will yield a better thermal performance of the storage. The performance of a storage will also increase with increased thickness of the insulating material, hence the comparison of the results between thermal conductivity and thickness regarding thermal energy performance. The upper 5 metres of the gypsum layer will contribute to the top insulation of the storage, decreasing the thermal losses from the storage resulting in greater thermal performance.

Analysis of results for the relation between thermal conductivity and insulation thickness

When analysing the thermal performance results in *Figure 6.28* - *Figure 6.32* the following statements can be made regarding the dependency on the insulation thickness and thermal conductivity of the insulation with regards to a header depth of 5 metres.

- *Figure 6.28* shows that from a thermal efficiency point of view, a lower thermal conductivity is preferable. It was also concluded that an increase in insulation thickness will yield better thermal efficiency.
- *Figure 6.29* - *Figure 6.32* shows how the thermal performance is dependent on thermal conductivity of insulation and its thickness. It can be concluded that all graphs illustrated the same tendencies for all results presented in the curves.
- From a charging perspective, an increased insulation thickness reduces the possibility of charging. A low thermal conductivity also reduces the charging capability, which is from a charging perspective negative.
- As the insulation thickness increases, and the thermal conductivity decreases, the possibility of extracting thermal energy increases.
- The thermal losses from the horizontal pipe system increases with increased thermal conductivity of the insulation material, as well as with decreased insulation thickness.
- The thermal losses from the storage can be identified in *Figure 6.29* - *Figure 6.32* as almost constant independent of thermal conductivity and thickness of the insulating layer.
- The results presented implies the effect of lowering the header depth as this increases the thermal performance and efficiency of the storage as presented in *Figure 6.28* - *Figure 6.32*. It also reduces the need of insulating the storage volume as the upper 5 metres contributes to the insulation. The insulation is though needed for the horizontal pipe system as to reduce the thermal losses from the horizontal pipe system.

The results show an additional increase in ability of storing thermal energy as greater thermal energy can be extracted. This as the thermal losses decrease due to the header depth of five metres, allowing for an increase of thermal energy being stored due to a higher mean temperature of the *BTES*. This temperature increase is illustrated in *Figure 6.33*.

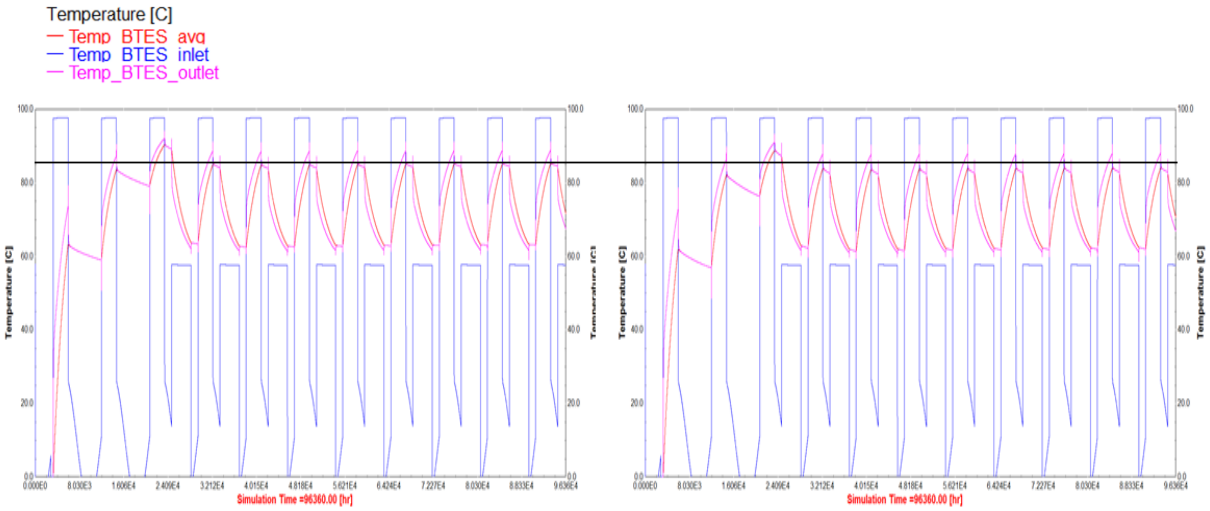

Figure 6.33 – Temperature variation in the BTES, left: Header depth 5 m, right: Header depth 0 m.

The results presented in *Figure 6.28* - *Figure 6.32* clearly show the impact of thermal performance with relation to lowering the header depth to 5 metres. It can be concluded from the results that a header depth of five metres will result in that the losses from the storage become almost independent of additional insulation. The thermal losses from the *BTES* are constant at 6 – 6.4 GWh over the total span of varying the insulation thermal conductivity and its thickness. The losses from the horizontal pipe system follows the same trend as the results presented in *section 6.2.2*. From the results it can be concluded that the change in charged and extracted thermal energy corresponds to the variation in losses for the horizontal pipe system with regards to alternating insulation design.

When considering for the design aspect of the insulation it is concluded that insulation is solemnly needed for the horizontal pipe. Same arguments apply as the ones presented regarding the design analysis in *section 6.2.2*, thicker layer with lower thermal conductivity is preferable. If the material alternatives in the reference project, presented in *chapter 4* are utilized, the thermal performance is exemplified in *Figure 6.34* with regards to a thickness of 0.25 m.

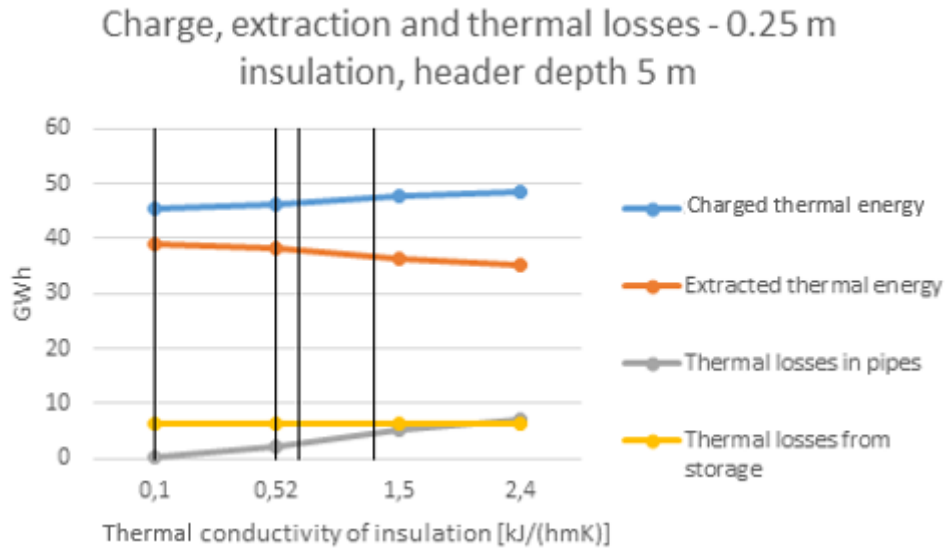

Figure 6.34 - Example of thermal performance for material alternatives in the reference project at Filborna. From left to right the black lines represent polystyrene, foam glass, expanded clay, slag gravel.

For insulation of the horizontal pipe system from a thermal performance perspective, the most favourable material of insulation is extruded polystyrene from a thermal extraction, and thermal

losses viewpoint. To verify this as the most preferable choice one must compare the costs regarding material, and construction. Which are related to the storage, and extraction, potential of each design alternative, making up the basis for finding economic value in the storage system. This economic analysis is performed in *section 6.3*.

6.3 *Implementation of the economic analysis*

The methodology of the economic analysis was presented in *section 5.3.3* which concluded in the results presented in *Figure 6.35*. The economic evaluation is based on the results derived from the thermal performance evaluation presented in *section 6.2.2*. These are based on the reference project, from which a general perspective is to be evaluated.

6.3.2 Economic analysis of system A

By implementing the methodology for economic analysis presented in *section 5.3.3* results as presented in *Figure 6.35*, for the reference project. *Figure 6.35* shows the value of the extracted thermal energy for different insulation thickness, as well as thermal conductivity. This value corresponds to the value of the extracted energy during one extraction cycle, not accounting for any costs.

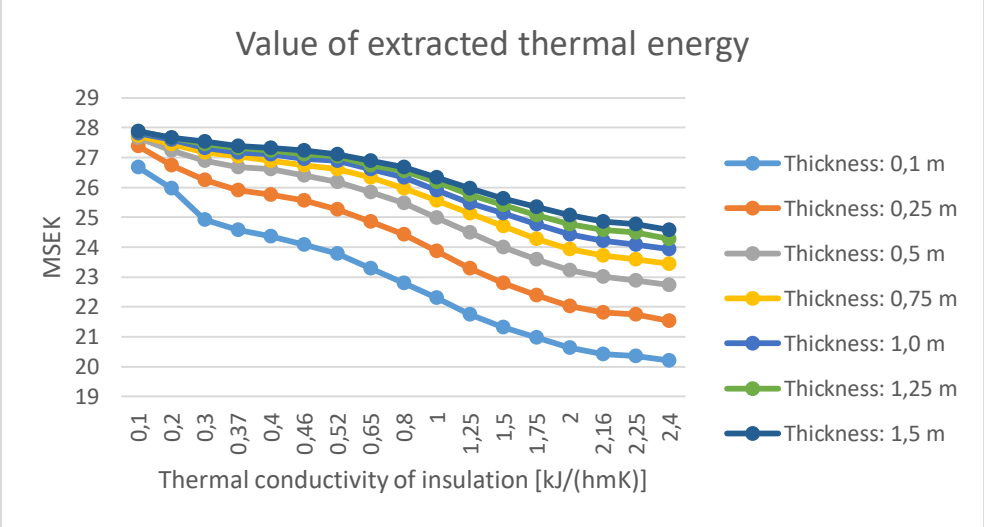

Figure 6.35 – Total value of extracted thermal energy for the reference project at Filborna.

When only considering the value of extracted energy it is clearly identifiable that an increased insulation thickness, along with a lower thermal conductivity of the insulation, brings a higher total extracted value. This ought to be in line with the general perspective as a better insulation capacity reduces losses and benefits the extraction possibilities. If one wants to compare material alternatives the material costs are to be implemented, this is performed in the following section.

Material approach to economic analysis

When the material perspective is implemented in accordance with *section 5.3.3* an equation system on the form y=kx+m is set up for each material alternative. Where k denotes the yearly value, x the year, and m the material investment cost. This with regards to thermal conductivity of material, as well as insulation thickness.

In the reference project the implementation of material costs is performed as shown in the following. The yearly value of extracted energy was presented in *Figure 6.35* and the material costs were presented in *chapter 4*. The yearly extracted value during full operation is presented in *Table 6.1*.

Table 6.1 – Yearly extracted value from storage

Thickness (m)	Slag gravel 1.26 kJ/(h m K) (MSEK/year)	Foam glass 0.52 kJ/(h m K) (MSEK/year)	Expanded clay 0.65 kJ/(h m K) (MSEK/year)	Extruded polystyrene 0.1 kJ/(h m K) (MSEK/year)
0.1	21.75	23.8	23.3	26.68
0.25	23.3	25.27	24.85	27.39
0.5	24.5	26.19	25.84	27.67
0.75	25.13	26.61	26.33	27.74
1.0	25.48	26.89	26.61	27.81
1.25	25.77	27.03	26.75	27.88
1.5	25.98	27.1	26.89	27.88

From the outline of the reference project the material costs can now be calculated for each insulation thickness, dependent on material alternative. This originates from that the insulation is cylindrically placed on top of the storage volume, not exceeding its outer boundary, since according to the results from *section 6.2.1* exceeding the boundary of the storage unit with insulation material will not add to the thermal performance.

$$Material\ cost = \pi \cdot r^2 \cdot (Layer\ thickness) \cdot (Material\ cost\ per\ unit\ volume)$$

Which in the reference is calculated according to material costs according to *chapter 4*, yielding the results as presented in *Table 6*.2, originating from the example equation below.

$$Material\ cost = \pi \cdot 90^2 \cdot d \cdot (Material\ cost\ per\ unit\ volume)$$

Table 6.2 - Material investment costs for material alternatives in the reference project.

Thickness (m)	Slag gravel (MSEK)	Foam glass (MSEK)	Expanded clay (MSEK)	Extruded polystyrene (MSEK)
0.1	0	1.45	1.4	1.78
0.25	0	3.63	3.5	4.45
0.5	0	7.27	7	8.91
0.75	0	10.9	10.5	13.36
1.0	0	14.53	14	17.81
1.25	0	18.16	17.49	22.27
1.5	0	21.8	20.99	26.72

As the general case stated an equation system of the form y=kx+m can now be applied, which compares the material alternatives in time with regards to yearly value and material investment cost. As in the reference case it would, from a pure material cost perspective, be most beneficial to use slag gravel, all material alternatives are compared with this as a mean of finding how long it takes for the material alternatives to have yielded the same value as for a corresponding thickness of slag gravel. This comparison is performed with the following formula, for which the results are presented in *Table 6*.3.

$$Number\ of\ years = \frac{Material\ cost}{Value\ of\ slag\ gravel - Value\ of\ alternative\ material}$$

Table 6.3 - Years until same value has been derived for an equivalent thickness of slag gravel

Thickness (m)	Foam glass (years)	Expanded clay (years)	Extruded polystyrene (years)
0.1	1	1	1
0.25	2	3	2
0.5	5	6	3
0.75	8	9	6
1.0	11	13	8
1.25	15	18	11
1.5	20	24	15

But as not all material thicknesses can be deemed logical, or motivational, a comparative analysis can be performed with the upmost limit for each material alternative.

- The slag gravel is assumed to have no cost and be in great supply. Hence a material thickness of 1.5 metres can be deemed the upmost limit.
- For foam glass and expanded clay, a limit of 0.5 metres can be assumed the upmost limit. Similar to the greatest thicknesses used in reference projects such as *Emmaboda*, *Carilsheim*, and *Munich* (*section 2.4*).
- Polystyrene is assumed to maximally have a thickness of 0.25 metres, which is deemed reasonable in relation to the projects in *Okotoks*, *Marstal* and *Neckarsulm* (*section 2.4*).

The results for accumulated value over time are presented in *Figure 6.36*, and show that the slag gravel is competitive up to approximately 3 years. After which polystyrene becomes the most preferable alternative from an extracted energy value perspective. But when polystyrene is ruled out due to constructional aspects, the alternative of foam glass becomes most preferable.

The years for the material alternatives to have accumulated equal value as 1.5 metres of slag gravel is for foam glass 35 years, expanded clay never gets equal to slag gravel, and for polystyrene it is only 3 years. Hence polystyrene would be the most preferable alternative from both a thermal and economic perspective. But not from a construction perspective, as this alternative requires additional constructional work in order of deriving an even surface for placement of the insulation. However the aspect of construction is in this project unknown and cannot be accounted for in the analysis further than from a theoretical perspective.

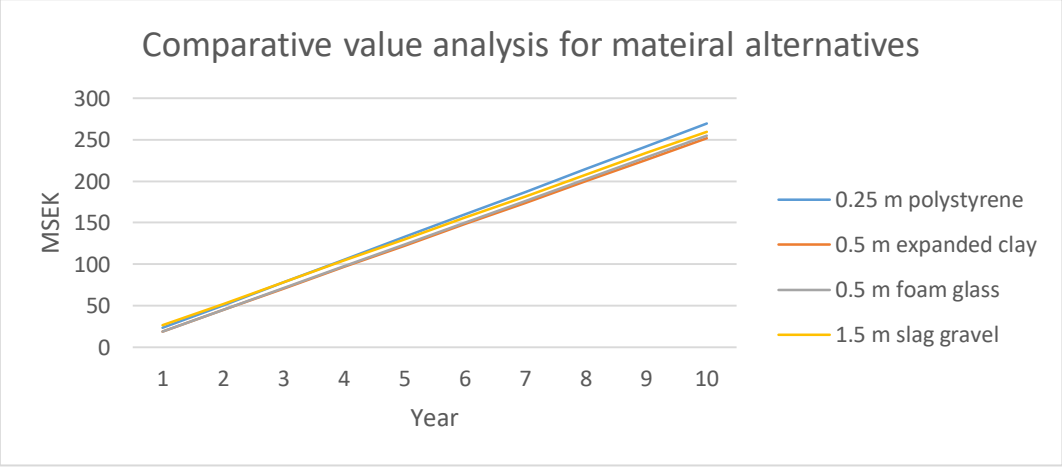

Figure 6.36- Comparative analysis of material alternatives with different thickness. As the curves overlap, graphic illustration becomes difficult as long periods of time are considered.

6.3.3 Secondary cost aspects in economic analysis

The secondary cost aspects include none implementable cost aspects, which are system specific and hence not applicable in a general perspective. Neither in the reference project, which is made up of a feasibility study, are these parameters set and implementable in the analysis. As a consequence of this only conceptually general aspects can be presented, as a basis of analysis.

The thermal storage systems come with the possibility of not only being used for seasonal storage, but also for cooling of thermal processes during excess heat. This reduces additional costs for other means of cooling.

Another aspect yielding additional costs is the maintenance aspects. This can be assumed homogenous for all material alternatives and would hence not be a differing factor in an analysis between material alternatives. The factor could alter between different system designs and should hence be kept in mind. This factor could also be set to include energy consumption of the system, which would reduce profit. But in a comparison between material alternatives this could be assumed homogenous between alternatives, and hence only reduce total value and not material specific value.

The thermal losses make up lost value from the storage, which depends on system design. This parameter can be analysed by seeing how much value is lost for each alternative. And see if this is deemed acceptable. For the reference project the value lost, relating to insulation thickness and thermal conductivity of insulation, is presented in *Figure 6.37*.

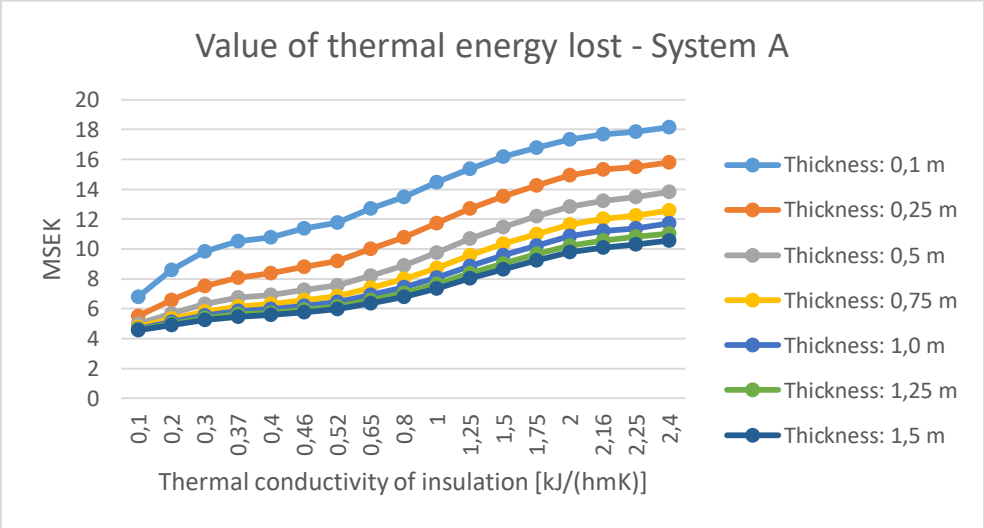

Figure 6.37 – Value of thermal energy lost.

6.4 Comparative study when implementing a heat pump

Consistent with the aim presented in *1.1* the system alteration of implementing a heat pump was to be analysed. The system setup was presented in *5.4* and shows the heat pump being implemented during extraction, this as to achieve further extraction from the storage. As the implementation of a heat pump allows for additional thermal extraction, this ought to be preferable from a thermal performance perspective. But the thermal benefits are redundant if not complemented with an economic analysis. This economic perspective implementation is to account for the operational costs, as well as investment and maintenance costs.

The economic analysis for the case of implementing a heat pump into the thermal storage system mainly aims towards investigating the value of the additional extracted thermal energy. As the heat pumps transfers energy from the carrier fluid leading into the storage to the carrier fluid exiting the storage, electrical energy is required (see *Figure 6.38*). The amount of electrical energy required per thermal energy equivalent is dependent on the coefficient of performance (COP) of the heat pump. The thermal value of the additional extracted energy hence has to be reduced by the value of the used electrical energy for the transfer. When implementing this approach into the reference project one derives a residual value of the additional thermal energy as shown in the equation below, where values of energy are derived from *5.3.2*.

$$Value\ of\ added\ energy\ from\ heat\ pump\ per\ GWh = 700\ kSEK - \frac{450}{COP}\ kSEK$$

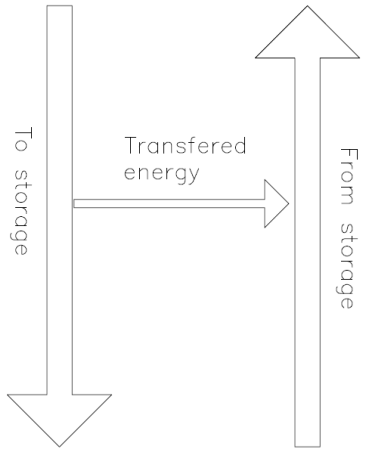

Figure 6.38 – Principle illustration of energy transfer performed by heat exchanger

A heat pump alternative is given by preconditions for the reference project. This alternative is a heat pump of type *61XWHZE*, which has a performance diagram as presented in *Figure 6.39*. This shows an approximate CPO-value of three, yielding that the value of the additional extracted energy is 550 kSEK/GWh.

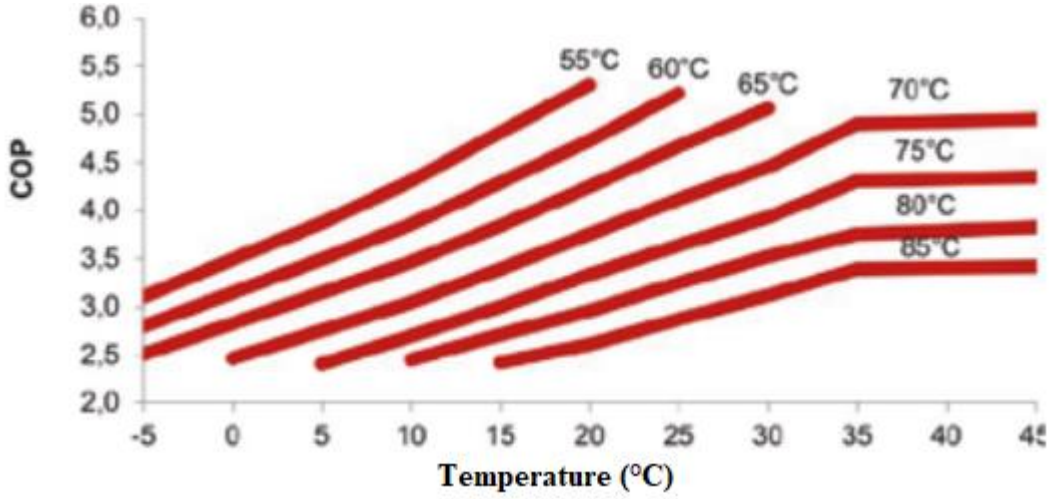

Figure 6.39 – COP-values for heat pump in reference project (Carrier N.D.).

From an analysis performed by *Hakan et al.* (2011), a principle investment cost could be derived based on the capacity in kW of the heat pump. The pump type mentioned for the reference project has a capacity of 2 MW (with six identical pumps), which yields an approximate investment cost of 30 MSEK. As the value of the extracted energy is set as 550 kSEK/GWh this would yield that the pump would have to extract 55 GWh in order to cover for the investment cost. This excludes cost-aspects from maintenance and other cost parameters, and requires further investigation as the response of the storage to this additional extraction is unknown.

6.5 *Environmental analysis*

The potential environmental effects that the thermal storage might yield were presented in *3.3* are analysed in the following with regards to the results derived.

Potential effects on the groundwater

As presented in *3.3.1* an increase in groundwater temperature risks affecting the microbiology of the groundwater. From the simulations performed in *TRNSYS* for the reference project it was clearly identifiable that a significant increase of average storage temperature takes place, as shown in *Figure 6.40*. This temperature increase would affect the local region, including the temperature of the local groundwater, hence an effect on the local microbiology could be prominent. The effects are though unknown, as presented in *3.3.1* where several external factors would have to be taken into consideration.

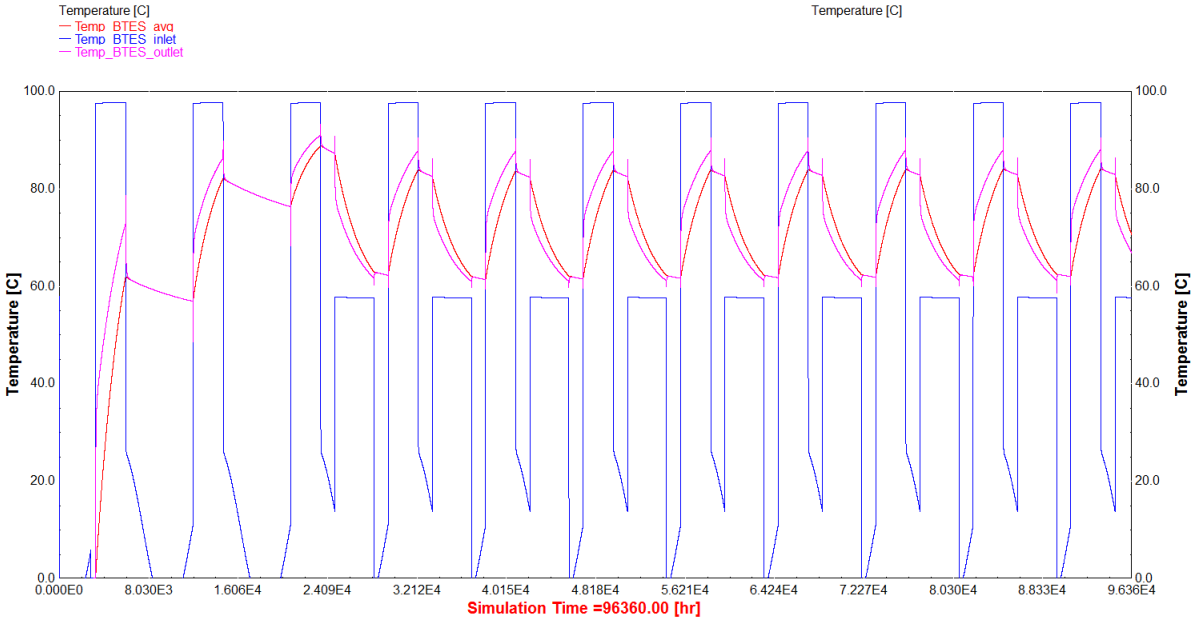

Figure 6.40 – Yearly variation of temperatures regarding the BTES. The red line shows the average temperature of the storage volume.

Potential environmental risks from using slag gravel

From the results presented in *appendix D* for chemical analysis of a slag gravel sample from *Filborna* some concerning content was identified. The samples showed the following concentrations of some potentially dangerous contents: manganese (1500 mg/kg), lead (770mg/kg), arsenic (21mg/kg), and mercury (0.046mg/kg).

Since the leaching water is controlled at *Filborna* the contents, nor the concentrations, were deemed to make up a risk substantial enough to restrict the use of slag gravel within the premise of the field site. This as it would not differ from the current deposition of the material. However, in a general case if the slag gravel was to be used as insulation layer in a similar project that does not control the leaching water it could get problematic. Having these substances leaching out in the environmental and groundwater could have negative environmental affects as well as costly sanitation operations for restoration the ground/groundwater and replacement of the current insulation material. This is most likely why there is no current general authorization for

using slag gravel in *Sweden* as a building or insulation material as mentioned in *4.2.1* except for disposal at a landfill.

Potential risks from implementation of a heat pump

System B introduces a second environmental risk, in the form of a heat pump. Potential environmental risks were discussed in *section 3.3.2*. These included the energy demand of the pump, and the refrigerant medium. The heat pump suggested in this reference case study was a *61XWH ZE* from *PUREtec*, which uses the refrigerant medium HFO R-1234ze. This has both low *GWP*, and *ODP*, values, which is preferable. But these impose a risk as they form trifluoroacetic acid (TFA) during degradation. (Makhnatch 2015). *TFA* affects the growth in plants in concentrations as low as 0.1 mg/Litre. Documentation has been made on humans that *TFA* is an irritant on skin and eyes and exposure can also result in increased liver weight (Boutonnet 1999).

6.6 System validity

System validity was checked simply via an energy balance over one charge, and one extraction, cycle. When the charged energy is subtracted with the extracted energy and thermal losses, this should yield a sum of zero if a steady state has been reached. This energy balance was performed as a mean of finding a convergence in space, and an example over yearly measured reference points in shown in *Figure 6.41*.

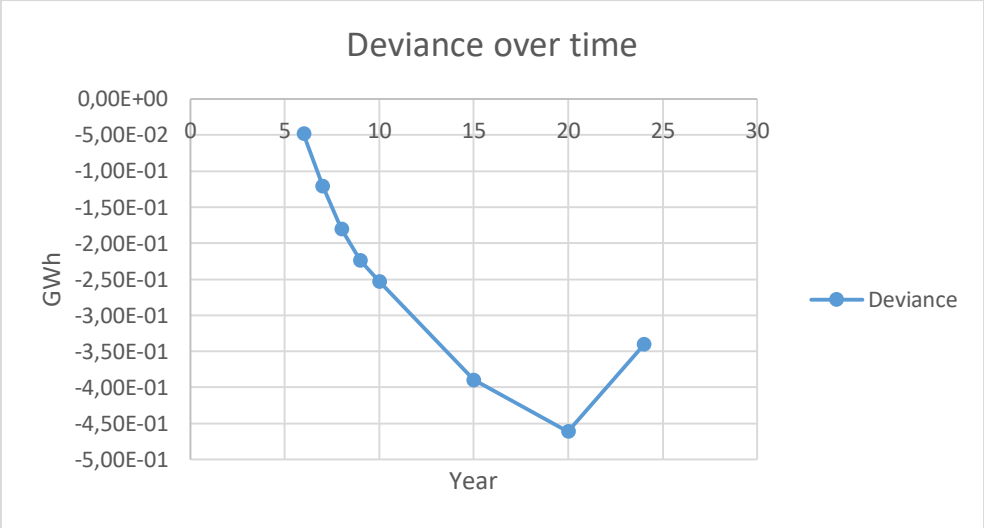

Figure 6.41 - Deviation from zero in the energy balance over a simulation time of 24 years.

7 Discussion

The results and analytical perspectives presented in *chapter 6*, are in the following analysed from both general perspectives, as well as in the specific case of the reference project at *Filborna*.

7.1 Modelling and system design perspectives

When modelling the storage volume in *TRNSYS* a *DST-model* was used for representing the properties of the volume, and its surroundings. The level of detail in the *DST-model* will hence be determining for the accuracy of the results derived. The *DST-model* does not allow for any stratification within the storage volume, of which the consequence is that generalized thermal properties had to be assigned to the storage unit. These generalized properties are to represent a homogenous storage mass, which yields that simplifications are needed. These simplifications yield that uncertainties are implemented into the model, effecting the final results.

In the reference project the thermal properties of the storage volume were derived from thermal response tests performed in one testing borehole. The results from this test were deemed representative for the whole volume, as it was performed within the storage volume. But basing the thermal properties of a storage volume of 3 million cubic metres on one thermal response test yields room for uncertainties due to a limited sample size. In order to derive more accurate thermal property values for the storage volume several thermal response tests, and geologic investigations, would have been needed as to minimize uncertainties.

The geologic model of the field site was as presented in *2.3.2* based on two test drillings, which were correlated in order of deriving geologic units. In line with the arguments for uncertainties of thermal properties for the storage volume, there are uncertainties regarding the geological conditions (thermal conductivity, heat capacity, etc.) as a limited range of tests have been performed in the planned field site. When assigning the geologic units thermal properties these were based on both the thermal response test performed, and tabulated values, in order to yield further validity. The gypsum was also complemented with a thermal conductivity test, which gave further validity to its assigned properties. But as for previous arguments, more tests would have been needed in order to reduce uncertainties, and minimize the risk of deviations unknown to the model designer.

Furthermore the test drillings performed for investigation of the geologic conditions did not account for groundwater flows, or the presence of highly conductive zones. Aspects that were brought forward as potential risks for additional thermal losses in *2.4*. Groundwater mapping would be critical for evaluating the potential effects of the groundwater. The concern was brought forward by *Hellström* (1989) as he stated that groundwater flows as low as 50 mm/day may yield significant effects on the thermal losses. From the description of the field site (*2.3.2*) it was shown that within the geology of the field site hydraulic conductivities as large as $3 \cdot 10^{-3}$ m/s can potentially be present. Corresponding to potential approximate flow velocities of 26 m/day, which exceeds the value of 50 mm/day by a factor of 518. Hence the factor of groundwater modelling would be of great interest to implement into *TRNSYS*, which alternatively can be performed with FeFlow, a program for just this. However some

convergence problem are likely to occur during integration in between these since they are different programs with different creators/companies.

Something which was brought up throughout the report is the relation between thermal properties and material conditions, such as temperature and moisture content. When these values were chosen, the choice itself was based on performed tests, as well as tabulated and declared values. But as the tests performed did not consider for moisture content of the tested material, in this case slag gravel and gypsum, which yields a source of error as the thermal properties can be assumed varying dependent on moisture content. The temperature and moisture dependency lead to the thermal analysis of the top insulation to consider for thermal conductivities ranging from 0.1-2.4, where 0.1 represents polystyrene, and 2.4 represents the thermal conductivity of water. As the water content in the insulating layer is unknown, by using the wide range of thermal conductivity yields that the analysis can be adapted to actual thermal properties of chosen material, when these parameters are set. Hence not having to rely on declared or tabulated values. In other words, as material properties have been determined, these can be translated into corresponding thermal performance in accordance with thermal performance graphs considering for the full range of thermal conductivities.

Future studies and evaluations must be made regarding moisture content in the insulating layer, and how to avoid or minimize it. From the project in *Brædstrup* (*2.4.4*) it was documented that there was a noticeable concern regarding the water content in the insulation material. The results from the analysis showed a water saturation of between 80-100 % in the insulation material. Which was constant over the third and fourth year of operation. From the results in *section 6.2.2* the effects of this has the potential decreasing the thermal performance of the storage as the thermal losses increase.

The *TRNSYS* modelling uses climate data derived from SMHI for 24 years (1995-2018), which are combined to form a model of hourly temperature variation over one year. This parameter is then implemented into the model to represent the annual temperature variation during each simulation year. But due to climate change that assumption might not be fully valid for long time simulations. Higher and lower weather extremes are to be expected which affects the simulation model in the way of affecting the temperature differences between the storage and its surface. For example lower temperatures during winter would yield greater potential for top losses, as the temperature difference, which is the driving force of heat transfer in accordance with Fourier's law (*Eq. 7*), increases. An inclusion of parameters taking the climate change into consideration would hence be of interest as to increase the validity of the model in relation to the weather aspects.

Noticeable from using the *TRNSYS* software is the possibility of dividing the calculation model into a more or less refined mesh. A more refined mesh comes with additional calculation time, hence a middle ground was found where deviations between results compared to a finer mesh were not deemed too deviant from each other.

As seen in *Figure 5.4* the first three years of operation were used as preheating of the storage as to raise the average temperature, and the surrounding ground. Preheating is performed to reduce the losses when the storage is in operation as the temperature differences between the

storage and the surrounding ground are not as big. The effect of altering the amount of preheating years, even excluding these, is a factor which could be investigated further.

One factor heavily affecting the results is that the thermal performance was deemed representative at the 10th year of operation. The results are not majorly variant between the closest number of years yielding it to be representative for the simulations performed. But in order to perform an extensive analysis the thermal end economical evaluation should account for the reduced thermal performance during the first years of operation.

As the borehole depth increases, the effect of the thermal gradient increases. This is a parameter not included in the analysis and is in the reference *DST-model* set to zero, which from *Figure 2.6* was deemed representative. But as depth increases evaluations should be made of the parameter if it is to yield potential for significant effects on the results.

As to improve upon the model a greater knowledge of the full-scale system design would have been needed as to, in a better manner, represent the dependencies within the system. Including inclusion of the thermal process from the cogeneration plant to heat exchanger and pump types. That could yield a better full-scale picture of the system at the same time as more data and dependencies are included, reducing uncertainties.

The model used for the reference storage volume did not account for that the horizontal pipe system was placed on top of the actual storage volume. The synergy effects of the system being placed on top of the storage volume could hence not be evaluated but as insulation thicknesses were kept equivalent for the storage and horizontal pipe system it was deemed that the model was representative.

As geologic conditions, as well as geologic layers, are modelled as homogenous throughout their volume, anisotropic conditions are excluded from being majorly considered within the model. This is most prominent for the storage volume itself which is modelled as one homogeneous material. As to derive adequate results the boundary conditions stated need to be in line with the real conditions of the geology, hence yielding uncertainties in simplifications and assumptions of the model.

7.2 Storage design parameters

It can from the results presented in the sensitivity study (*6.1*) be recognised that the influence on thermal performance varies greatly dependent on parameter. The parameters of storage volume, borehole depth, number of boreholes, heat exchanger efficiency, and header depth yielded significant impact on the thermal performance of the system. Whilst parameters such as number of boreholes in series and borehole radius had little to none effect of the thermal performance of the storage. These parameters are for the designer easy to adapt to the desired thermal performance, as well as the economic outline of a project. There are though parameters, such as gap thickness, which the designer cannot affect, as they are consequences of site conditions out of the designers control, in this case geology.

In the reference project (see *2.3.2*) fissure-zones could be identified from test drillings which may have to be taken into consideration in the final design, as well as in the modelling. Here

the designer has to decide if measures are needed in order to limit the effects of these, for example choose if injection methods are needed for reducing the gap.

The parameter of "length of the horizontal pipe system" stressed the desire to design a system with as short length of the horizontal pipe system as possible to reduce the total thermal losses. This in order to derive a system yielding better thermal performance and efficiency. Minimization of pipe length has potential to be economically profitable as less material is needed, which also is positive from an environmental perspective.

The parameters of borehole depth and storage volume both increase the need for geologic, and hydrogeological, knowledge as these imply that a greater volume is included. Increase in need of knowledge is in line with the risks imposed by groundwater flows, and highly conductive zones. More investigations are needed in comparison to smaller volume alternatives, as to avoid large deviations between simulations and reality.

One aspect left out of the parameter analysis in the sensitivity study (*6.1*) was the economic aspects of these parameter alterations. What for most parameters is seen as positive from a thermal performance perspective, tends to lead to increased costs. An example is the number of boreholes. An increased amount of boreholes would yield greater costs, and be time consuming. When designing a BTES all these parameters need to be evaluated for their thermally positive effects, in relation to the additional strain these would have on economic parameters.

7.3 Insulation design perspective

When analysing the results for insulation design (see *6.2*) it can be identified that the storage top insulation did not need to extend outside the surface area of the storage, according to *TRNSYS* simulations. This limits material use and is hence positive from economic and environmental perspectives.

The desired properties of the insulating layer is in accordance with *6.2.3* that it is to possess a great thickness as well as having a low thermal conductivity. Thus in order to benefit the thermal performance of the storage. But with increased layer thickness comes greater material costs, and the best insulating materials tend to be the most expensive. So once again a balance between thermal performance and economy is stressed.

Another perspective of insulation design, not brought forward in the analysis, is the use/combination of multiple material layers. As could be identified the alternative of extruded polystyrene yielded the best thermal performance synergies, whilst being the most expensive alternative. Slag gravel was showed to yield the opposite. But as slag gravel could be assumed to be in great supply a combination of the two would possibly be a good alternative for insulation. Implementing that the extruded polystyrene can have a reduced thickness, which is economically beneficial, and the rest complemented with an extensive thickness of slag gravel. How well this alternative would perform is unknown and would call for further analysis.

As mentioned the insulating material is in need of moisture protection in order to maintain its insulating properties. But according to the project in *Neckarsulm* (see *2.4.3*) a dry out effect is prominent for the insulation of a BTES, as the temperature of the storage is relatively high. How these aspects of thermal conductivity increase with moisture and temperature, along with the dry out effect, is unknown and would call for further analysis of the thermal performance

with regards to the possible effect. The project in *Brædstrup* (*2.4.4*) used a semi permeable layer, and the consequences were that moisture saturation of 80-100% were measured. The consideration of that the impermeable layers risk trapping moisture hence needs to be taken into consideration when designing the moisture protection of the insulating layer.

Another factor showing significant potential for adding to the thermal performance of the storage is a lowering of the header depth (*6.1.6*). Lowering the header depth would be a possible alternative for the need of an external insulating layer.

7.3.2 Material analysis

In order to derive a general perspective of material analysis one should not look to the specific results, but instead the methodology of the analysis for insulation thermal conductivity. If one models the designed storage with regards to variant values and thicknesses of the insulation similar results to the ones presented in 6.2.3 are derived. From these the material alternatives can be implemented as corresponding to specific values of thermal conductivity, which translates into thermal performance. Hence the methodology is generally applicable but not the results, since these relate to the reference case.

The material deemed most beneficial from an economic and environmental perspective is the slag gravel, due to the local source and limited area of possible use. One aspect brought forward is the uncertainty in material composition since the slag gravel is made from waste, and the composition of the waste is hard to control. Something which relates to risk of contamination of the groundwater via leaching, if not controlled. But as the storage is to be placed at a waste dump the leaching water is already controlled throughout the area, eliminating the risk of contamination. But in a general case if this aspect is not considered and slag gravel is to be used as a building or insulation material it risks bringing negative environmental effects, since as shown in *appendix D* it can include substances such as mercury, lead, arsenic, manganese, among other things.

When comparing the material alternative of polystyrene as insulation material to the rest of the alternatives, it is noticeable that choosing polystyrene would yield additional constructional costs, as an even surface is needed for placement. But as the material possesses superior insulating properties also here a balance between additional costs and increased thermal performance is needed. The reason why extruded polystyrene (XPS) was chosen as the polystyrene alternative, and not expanded polystyrene (EPS), was due to the increased permeability and lacking of load carrying capacity for *EPS*. In the construction phase it can be assumed that material is placed on top of the insulation upon which construction machines will drive. If it is found that the loads aren't as big *EPS* would be the preferable alternative since it has a lower cost compared to *XPS*. But in order to be on the safe side regarding load carrying capacity *XPS* was used as the investigatory alternative.

One factor in need of evaluation is the effects that temperature and moisture risk having on polystyrene. The temperature and moisture behaviour of the material is unknown and may cause significant changes in material properties. Which may result in it being a less favourable material alternative when considering all aspects brought up in this Master Thesis.

7.4 Economic analysis

From a general perspective the economic value is mainly found in the extracted thermal energy from the storage. The overall value is dependent on what the thermal energy is to be used for, and hence of what value it is to the user. In order of deriving profitability in a thermal energy storage system, the value of the stored energy must cover for all cost aspects that are consequences of the system, these range from investment coverage over time to maintenance costs. The outset is that the energy stored must increase in value to the user from storage phase, to extraction phase. This increase in value is the one that is to cover for all identifiable cost aspects. Examples of these are in the reference project construction related costs, energy demand of system, investment cost, maintenance costs, etc.

One cost positive aspect of thermal energy storage is its potential for to be used for cooling of thermal processes as well as a source of thermal energy for the same. By utilizing these storages for their cooling properties as well as storage properties the need for other means of cooling are reduced.

In the reference project the value was designated as equivalent to the one for district heating, which showed great potential for cost coverage. This as the energy could be sold commercially and hence bring in external economic value. If the energy was to be used by the plant itself it would only make up for a cost reduction of the current economic situation, something for which the potential of finding value is unknown, as it is heavily project specific.

The durability of the system is a factor which relates strongly to the maintenance cost aspect. A long-term durability is something necessary for gaining economic profitability for the investment, as maintenance otherwise may overcome economic gain. One aspect heavily relating to durability is water. Water present in insulating layers tend to reduce insulating capacities and over time cause degradation of the material, which is negative from a durability perspective.

7.4.2 Comparative analysis with existing projects

As brought forward in the projects in *Marstal* and *Dronninglund* an approximate investment cost of 0.4 €/kWh, corresponding to 4 SEK/kWh, could be identified. Extracting approximately 40 GWh would correspond to an investment cost of 160 MSEK. The investment cost is in the *Filborna* case unknown but this value could be kept in mind if one wants to analyse how the extracted value covers for the investment cost, based on a limited range of experience.

7.4.3 Sources of error in the economic analysis

The economic analysis mainly entailed the cost aspect of material costs for comparative studies. This analysis was based in the applicability of an equation system on the form of y=kx+m, where k corresponded to the extracted value per year. As a reference the 10^{th} year of operation was chosen as representative for the steady state. But as variations in energy extraction were clearly identifiable during the first years of operation, when steady state was not reached, yield a longer period of time before material alternatives would have turned a profit. This is mainly implementable when comparing with the slag gravel alternative as the time it would take to have derived an accumulated equivalent value as slag gravel would be shifted forwards in time. Hence an analysis for time until profitability, with regards to the uneven thermal extraction during the first years of operation would be of interest.

Such perspective could further be complemented with the unknown variations in stored thermal energy. Yearly variations due to external factors, such a climate, could drastically alter the amount of thermal energy stored and have great effect for how economically beneficial the thermal storage alternative becomes.

But the most important economic aspect left out of the analysis is the systems possibility for covering its investment cost. If coverage cannot be found, within the desired time period, one should consider altering the system or finding other solutions.

7.5 Environmental analysis

From an environmental perspective it is of importance to discuss the transport distance which will be needed for each material alternative. All material alternatives, except the locally produced slag gravel, requires transportation to the field site. The logical environmental effect is increased CO_2 emissions due to this fact. The reference alternatives of foam glass and expanded clay may require very long transports, up to 400 km one way, whilst the polystyrene can be found more locally. When choosing insulating material one should hence initially see to the local market as to minimize environmental effects.

When discussing the environmental effect regarding the choice of insulation material, one must consider the effects that the production of the material has. Such an approach can be done with regard to CO_2 emissions.

- The locally produced slag gravel is a bi-product from the incineration process of the cogeneration plant, and hence has no great CO_2-emissions.
- When looking into the production for expanded clay it is identifiable that this is a process requiring temperatures of approximately 1200 degrees Celsius. In order to reach these temperatures a great deal of energy is required and the process can hence be assumed to be very high in CO_2-emissions.
- The product of foam glass showed a CO_2-emission of approximately 7.8 kg per cubic metre produced, which corresponds to driving 80 km with a newer car using diesel as fuel. A positive effect of foam glass is though that the glass used could not be used for other purposes, which is positive.
- Polystyrene has a CO_2-emission of approximately 2.6 kg CO_2/kg (*4.2.4*), which is lower than what can be assumed for foam glass and slag gravel due to their high temperature demand.

From an environmental point of view, using slag gravel is undoubtedly the most preferable alternative of the ones covered in the reference project. It is a bi-product produced at the cogeneration plant and is currently only deposited at the landfill. Hence it is locally produced, there is also no need for transportation which concludes that one could say its environmental effect is zero. And the material can be assumed to be in great supply giving the possibility of having very thick layers.

In conclusion, it is questionable to which extent a thermal injection/extraction to a groundwater source can affect the groundwater. Further studies over longer time periods will have to be conducted in order to conclude which affect a thermal injection/extraction can have.

7.6 Comparative study for alternative system

When analysing the alternative of implementing a heat pump into the storage system it was found that the additional energy that it would extract was to be reduced in value as to compensate for the electrical demand of the heat pump. In order to find economic profitability of this implementation of a heat pump, the COP-value of the pump is desired to be as high as possible, as to limit the reduction of value of the additional extracted energy. A fact must be kept in the mind of the designer as the additional value from the heat pump is to cover for the investment of the pump itself as to be a profitable alternative.

7.7 Validity of analysis

A validity study was presented in *6.6* showing the deviations over simulation time, motivating the use of the 10^{th} year for deriving results. But apart from these deviations there are other practical aspects to consider for system validity.

One key aspect is the relation between practical design compared to planned/modelled design. This includes none ideal/ not planned, deviations from design.

- If the boreholes are not drilled perfectly vertical, it would affect both the storage volume, as well as the interaction with the surrounding boreholes. A shallower storage would be derived which is more dependent on boundary conditions on top of the storage. Hence risk causing greater thermal losses. By not being perfectly vertical the spacing between boreholes will vary dependent on depth. Altering the thermal processes taking place in the storage, effects which are not accounted for in current models.
- Presence of conductive zones, and groundwater flows, would induce additional thermal losses if not accounted for in the design.
- When the parameter of "storage volume" is analysed the 10^{th} year of operation may not be sufficient from a steady-state perspective, as this state might not have been reached for greater volumes.

The results, upon which the analysis was based, were solemnly derived from *TRNSYS*, which hence only would yield validity in relation to other *TRNSYS* designs. But as the results derived were in line with existing theoretical background the general perspective was extractable from these results.

Another factor not taken into consideration is the effects of rain on the thermal performance. The effect of increased/decreased rainfall will not solely affect the insulation layer of the storage. It will affect the groundwater level as well and change the preconditions of the storage, altering its performance.

8 Conclusions

The sensitivity study showed a great sensitivity of the thermal system with regards to multiple design and insulation parameters. Uncertainties within these parameters when designing the thermal storage system risk causing significant deviance between expected and practical thermal performance of the storage. General conclusions on the analysed parameters are listed below.

- Varying the storage volume (major influence)
- Varying borehole depth (major influence)
- Varying borehole radius (minor influence)
- Influence of gap between heat exchanger and borehole wall (major influence)
- Influence of header depth (major influence)
- Varying the number of boreholes (major influence)
- Varying the number of boreholes in series (no influence)
- Varying the length of the horizontal pipe system (small influence)
- Varying the efficiency of the heat exchanger (major influence)

This is a fact which is important when modelling a thermal storage using *TRNSYS* as the simulations are found to be heavily dependent on several parameters. Good geologic, and hydrogeological, knowledge is key for deriving a good model.

The analysis of insulation design showed that an increased thickness and lower thermal conductivity of the insulation is preferable from a thermal performance perspective. This in order to reduce top losses from the storage. In the reference project it was concluded that from an insulation perspective polystyrene was the preferable material as this had the lowest thermal conductivity, giving the possibility of maintaining a thinner layer and reducing material use. But when regarding the insulation dependent of thickness the slag gravel alternative was deemed preferable due to its small material cost, which for the other alternatives had a significant impact as layer thickness increased.

One main conclusion drawn from the project is the width of all uncertainties that might affect the models. These uncertainties range from the uncertainties in thermal properties due to moisture or temperature, to groundwater and presence of conductive zones in the geology. It can be concluded that extensive investigations are needed in order to properly model the storage system in order of deriving reasonable results. Geologic and hydrogeological conditions are needed as well as system component details and setup.

From the perspective of thermal conductivity of materials it can be concluded that in order to maintain thermal properties of materials used for insulation these are needed to be protected from moisture in order not to lose/reduce their insulating properties.

It can further be concluded that when designing a thermal storage one must keep in mind the return time for the investment, as well as the overall return from the system in order to find a satisfactory solution. This aspect may be heavily influential when choosing design parameters as those presented in the sensitivity study.

In order to perform an economic analysis of the thermal storage system one must have good knowledge of all cost, and value, parameters that this is to entail.

9 Future studies

The combination of groundwater modelling and TRNSYS within this field is something that would be of significant interest for this, and future, projects. This could be performed using software such as FeFlow.

Thermal conductivity properties of the slag gravel at different moisture contents are much of interest in order to validity its' insulating properties and field of usage.

The implementation of a heat pump into the thermal storage system is one aspect which should be evaluated further as this shows great potential for possible economic gains.

10 References

Abrahamsson, E. & Milesson, J. (2013). *Geoenergilager Xylem – Visualisering och lönsamhet*. Thesis in Energy and Environmental. Växsjö: Linnaeus University. http://www.diva-portal.org/smash/get/diva2:632285/FULLTEXT01.pdf [accessed 2019-04-23]

Arm, M., Flyhammar, P., Grönholm, R., Kristensson, M. & Lind, B. B. (2016). *Användning och modifiering av metallseparerat slaggrus*. (Energiforsk rapportserie 2016:331). Stockholm: Energiforsk. https://energiforskmedia.blob.core.windows.net/media/22069/anvandning-och-modifiering-av-metallseparerat-slaggrus-energiforskrapport-2016-331.pdf [accessed 2019-04-09]

Biancucci, M. (2015). *Modelling of a large borehole heat exchangers installation in Sweden*. Master Thesis, Department of Energy technology. Stockholm: Royal Institute of Technology. diva2:902940 [accessed 2019-04-09]

Bjurström, H., Hjalmarsson, A. & Sedendahl, K. (1999). *Handbok för restprodukter från förbränning*. Stockholm: Fjärrvärmeföreningen.

Bonte, M., Stuyfzand, P. J., Hulsmann, A. & Beelen, P. V. (2011). *Underground Thermal Energy Storage: Environmental Risks and Policy Development in the Netherlands and European Union*. Ecology and Society, 16(1) [accessed 2019-03-28]

Boudaghpour, S. & Hashemi, S. (2008). *A study on Light Expanded Clay Aggregate (LECA) in a Geotechnical View and its Application on Greenhouse and Greenroof Cultivation*. International journal of geology, Issue 4, Volume 2. [accessed 2019-05-08]

Boustead (2005). *Polystyrene (Expandable)(EPS)*. Brussels: PlasticsEurope. http://www.inference.org.uk/sustainable/LCA/elcd/external_docs/eps_31116f05-fabd-11da-974d-0800200c9a66.pdf [accessed 2019-04-09]

Boutonnet, C. J. (1999). *Environmental risk assessment of trifluoroacetic acid*. Human and Ecological Risk Assessment, 5(1), pp. 59-124. doi: 10.1080/10807039991289644 [accessed 2019-05-13]

Carrier (N.D.). *Smart Värmedrift*. http://www.carrierab.se/media/98695/ns1839a_10026_brochure_61xwhze_carrier.pd [2019-05-27]

Carslaw, H.S. & Jaeger, J.C. (1959). *Conduction of heat in solids*. Oxford University Press, Amen House, London E.C.4.

Catolico, N., Ge, S. & McCartney, J. S. (2015). *Numerical Modeling of a Soil-Borehole Thermal Energy Storage System*. 15(1), doi: 10.2136/vzj2015.05.0078

Claesson, J., Eftring, B., Eskilson, P. & Hellström, G. (1985). *Markvärme en handbok om termiska analyser: en handbok om termiska analyser: Del II Värmelager*. Stockholm: Liber.

Clarke, B. & Hamdhan, I. (2010). *Determination of Thermal Conductivity of Coarse and Fine Sand Soils.* Proceedings World Geothermal Congress 2010. Bali, Indonesia 25-29 April 2010. [accessed 2019-03-03]

Cuypers, R., De Jong, A., Vliet, L., Hoegaerts, C. & Roelands, M. (2016). *Thermochemical Heat Storage – from Reaction Storage Density to System Storage Density*. Energy Procedia, 91, pp. 128-137. doi: 10.1016/j.egypro.2016.06.187 [accessed 2019-02-27]

Eckert, E. G. R. & Robert, D. M. (1972). *Analysis of Heat and Mass Transfer*. New York: Hemisphere Publishing Corporation.

EDP International AB (2017). *Environmental Product Declaration* [Brochure]. https://gryphon4.environdec.com/system/data/files/6/13405/epd1088_Hasopor_Hasopor%20foam%20glass%2010-60%20mm_2017.pdf [accessed 2019-04-12]

Emmaboda Energi & Miljö AB (2018). *2016 DoA Fjärrvärme.* https://www.ei.se/sv/start-fjarrvarmekollen/foretag/emmaboda-energi-miljo-ab/?Rapport=2017-101224.pdf [2019-02-13]

Engineers Edge (2019). *Water – Density Viscosity Specific Weight.* https://www.engineersedge.com/physics/water__density_viscosity_specific_weight_13146.htm [2019-04-03]

Eriksson, L. & Hägglund, J. (2007). *Handbok. Skumglas i mark- och vägbyggnad*. Lindköping: Swedish Geotechnical Institute.
SGI-INF--08/18--SE

Finja (2019). *Grund, Cellplast.* https://www.finja.se/produkter/grund-cellplast [2019-05-27]

Forsén, M. (2005). *Heat pumps: Technology and environmental impact*. Sweden: Swedish Heat pump Association.
http://ec.europa.eu/environment/ecolabel/about_ecolabel/reports/hp_tech_env_impact_aug2005.pdf [accessed 2019-05-07]

Garnier, F., Lesueur, H., Motelica-Heino, M. & Ignatiadis, I. (2011). *Aquifer biothermoremediation using heat pumps: sound theoretical basis and results on thermal, geochemical and biological impacts on aquifers*. Orleans, France: University of Orleans. https://hal-brgm.archives-ouvertes.fr/hal-00593563/document [accessed 2019-04-01]

Hahne, E., Seiwald, H. & Reuss, M (1999). *Underground seasonal heat storage for a solar heating system in Neckarsulm, Germany.* Bulletin d'Hydrogéologie, (17). Centre d'Hydrogéologie, University of Neuchâtel.

Hakan, D., Özden, A. & Özgür, A. (2011). *Economical analysis of a chemical heat pump system for waste heat recovery.* World Renewable Energy Congress. Linköping, Sweden 8-12 May 2011.

Heidemann, W., Müller-Steinhagen, H. & Ochs F. (N.D.). *Effective thermal conductivity of the insulation of high temperature underground thermal stores during operation*. Stuttgart: Institute of Thermodynamics and Thermal Engineering.

https://pdfs.semanticscholar.org/f4f9/7224585d8d79f70e525b005564ccb8fe0ac1.pdf [accessed 2019-03-10]

Heier, J. (2013). *Energy Efficiency through Thermal Energy Storage-Possibilities for the Swedish Building Stock*. Licentiate Thesis, Department of Energy Technology. Stockholm: KTH School of Industrial Engineering and Management. http://urn.kb.se/resolve?urn=urn:nbn:se:kth:diva-118734 [accessed 2019-05-18]

Hellström, G. (1989). *DUCT GROUND HEAT STORAGE MODEL. Manual for Computer Code.* Lund: Lund of University.

Hellström, G. (1991). *GROUND HEAT STORAGE. Thermal Analyses of Duct Storage Systems. I. Theory.* Lund: University of Lund.

International Energy Agency (2018 A). *Global Energy & co2 Status Report 2018*. https://www.iea.org/geco/ [2019-04-24]

International Energy Agency (2018 B). *Renewables*. https://www.iea.org/topics/renewables/ [2019-04-24]

International Energy Agency (N.D.). *Technology roadmaps*. https://www.iea.org/topics/renewables/technologyroadmaps/ [2019-01-29]

Johansen, O. (1977). *Thermal conductivity of soils*. Hanover: Corps of Engineers, U.S. Army.

Jonsson, P. (2013). *Lecablock, en alternativ lösning till ytterväggar i ett passivhus*. Thesis, Department of Building Technology. Umeå: University of Umeå. diva2:668752 [accessed 2019-04-12]

LECA (2015). *Byggvarudeklaration 2015* [Brochure]. https://www.leca.se/sites/default/files/dokument/bvd/A-559075-0195-0-2.pdf [accessed 2019-02-19]

LECA (N.D.). *Egenskapsredovisning lättklinker* [Brochure]. https://www.leca.se/sites/default/files/dokument/broschyrer/leca-lattklinker-egenskapsredovisning.pdf [accessed 2019-02-19]

Makhnatch, P. (2015). *Något om HFO köldmedier*. https://www.kth.se/itm/inst/energiteknik/forskning/ett/projekt/koldmedier-med-lag-gwp/low-gwp-news/nagot-om-hfo-koldmedier-1.602602 [2019-05-13]

Malmberg, M. (2017). *Transient modelling of a high temperature borehole thermal energy storage coupled with a combined heat and power plant*. Master Thesis, Department of Industrial Engineering and Management. Stockholm: KTH Royal Institute of Technology. diva2:1197590 [accessed 2019-05-17]

Mangold, D. & Schmidt, T. (N.D.). *New steps in seasonal thermal energy storage in Germany*. Stuttgart, Germany. Solites - Steinbeis Research Institute for Solar and Sustainable Thermal Energy Systems.

http://intraweb.stockton.edu/eyos/energy_studies/content/docs/FINAL_PAPERS/14A-2.pdf [accessed 2019-04-11]

Mangold, D., Riegger, M. & Schmidt, T. (2007). *Solare Nahwärme und Langzeit-wärmespeicher*. Stuttgart: Steinbeis Forschungsinstitut für solare und zukunftsfähige thermische Energiesysteme. http://www.solites.de/download/literatur/AB-SUN%20VI%20FKZ%200329607L.pdf [accessed 2019-04-11]

Masse Modin, R. & Sundberg, J. (2012). *EPS i grund – Värmeledningsförmåga och krypning*. Thesis, Department of Building Materials. Helsingborg, Sweden: Lund University. http://lup.lub.lu.se/luur/download?func=downloadFile&recordOId=2760007&fileOId=8961451 [accessed 2019-05-16]

Naturvårdsverket (2016). *Isolermaterial kan vara farligt avfall*. Stockholm: Naturvårdsverket. https://www.naturvardsverket.se/Documents/publikationer6400/978-91-620-8740-1.pdf?pid=16464 [accessed 2019-04-14]

Nordell, B. (2000). *Large-scale Thermal energy storage*. Luleå: Luleå University of Technology. http://large.stanford.edu/courses/2013/ph240/lim1/docs/nordell.pdf [accessed 2019-03-27]

Nordell, B., Scorpo, A. L., Andersson, O., Rudell, L. & Carlsson, B. (2016). *Long-term long Term Evaluation of Operation and Design of the Emmaboda BTES – Operation and Experiences 2010-2015*. Luleå: Luleå University of Technology. ISBN 978-91-7583-530-3 [accessed 2019-01-30]

Nordell, B. (1987). *The borehole heat storage in rock at the Luleå University of Technology*. Stockholm: Swedish Council for Building Research. ISBN 91-540-4713-7 [accessed 2019-04-09]

OECD (2012). *Energy*. OECD Green Growth Studies. doi: 10.1787/9789264115118-en [accessed 2019-05-20]

Olesen, B. W. & Krasimiroy, G. P. (2011). *Building Thermal Energy Storage – Concepts and Applications*. Denmark: ICIEE, Department of Civil Engineering, Technical University of Denmark. http://orbit.dtu.dk/files/6383088/BUILDING%20THERMAL.pdf [accessed 2019-04-24]

Olofsson, J. (2014). *Materialåtervinning av förpackningar och tidningar*. Master Thesis, Department of Technology and Society. Lund: University of Lund. id: 4769642

Owens Corning (N.D.). *FOAMULAR Extruded Polystyrene (XPS) Insulation SI and I-P Units for Selected Properties* [Brochure]. http://www.foamular.com/assets/0/144/172/174/1fb2fb08-5923-46de-b387-f4bdc3f68d50.pdf [accessed 2019-02-27]

PlanEnergi (2013). *Boreholes in Brædstrup*. Denmark: PlanEnergi. http://planenergi.dk/wp-content/uploads/2018/05/15-10496-Slutrapport-Boreholes-in-Br%C3%A6dstrup.pdf [accessed 2019-02-13]

Rogers, T. (2015). *Everything you need to know about polystyrene (PS)*. https://www.creativemechanisms.com/blog/polystyrene-ps-plastic [2019-05-29]

Sandia National Laboratories. (2006). *Advantages of Using Molten Salt*. https://www.webcitation.org/60AE7heEZ?url=http://www.sandia.gov/Renewable_Energy/solarthermal/NSTTF/salt.htm [2019-02-13]

Sarbu, I. & Sebarchievici, C. (2018). *A Comprehensive Review of Thermal Energy Storage*. Sustainability, 10(1). doi: 10.3390/su10010191 [accessed 2019-05-27]

Sibbitt, B. McClenahan D., Djebbar, R., Thornton, J., Wong, B., Carriere, J. & Kokko, J. (2012). *The Performance of a High Solar Fraction Seasonal Storage Distric Heating System – Five Years of Operation*. Energy Procedia, 30, pp. 856-865. doi: 10.1016/j.egypro.2012.11.097 [accessed 2019-02-27]

Sibbitt, B., Onno, T., McClenahan, D., Tornton, J., Brunger, A., Kokko, J. & Wong, B. (N.D.). *THE DRAKE LANDING SOLAR COMMUNITY PROJECT – EARLY RESULTS*. Canada: Drake Landing Solar Community. https://www.dlsc.ca/reports/bjul15/EPD_March_April_2007.pdf [accessed 2019-02-21]

Sipola, J. (2011). *Tjälinträngning I fyllningsdammars tätkärna I anslutning till betongkonstruktioner*. Master Thesis, Department of Civil Engineering and Natural Resources. diva2:1019059 [accessed 2019-04-1248]

SMHI (2019). *Ladda ner metreologiska observationer*. https://www.smhi.se/klimatdata/meteorologi/ladda-ner-meteorologiska-observationer/#param=airtemperatureInstant,stations=all,stationid=62040 [2019-05-27]

State of Green (2018). *Large-scale solar water heating and seasonal storage pit in Gram*. https://stateofgreen.com/en/partners/ramboll/solutions/large-scale-solar-heating-and-seasonnal-heat-storage-pit-in-gram/ [2018-03-11]

State of Green (N.D.) *World's largest thermal heat storage pit in Vojens*. https://stateofgreen.com/en/partners/ramboll/solutions/world-largest-thermal-pit-storage-in-vojens/ [2019-02-13]

Statens Geotekniska Institut (2019). *Jords Tekniska egenskaper*. https://www.swedgeo.se/sv/kunskapscentrum/om-geoteknik-och-miljogeoteknik/geoteknik-och-markmiljo/jordmateriallara/jords-tekniska-egenskaper/ [2019-05-27]

Sundberg, J. (1991). *Termiska egenskaper i jord och berg*. Linköping: Swedish Geotechnical Institute. http://www.swedgeo.se/globalassets/publikationer/info/pdf/sgi-i12.pdf [accessed 2019-04-11]

SWECO (2012). *Geologisk och hydrogeologisk modell för Filbornaområdet, helsingborg* [corporate material]. Helsingborg: SWECO. [accessed 2019-05-21]

Sørensen, P. A. & Schmidt, T. (2018). *Design and Construction of Large Scale Heat Storages for District Heating in Denmark*. 14th International Conference on Energy Storage. Adane Turkey 25-28 April 2018. http://planenergi.dk/wp-content/uploads/2018/05/Soerensen-and-

Schmidt_Design-and-Construction-of-Large-Scale-Heat-Storages-12.03.2018-004.pdf [accessed 2019-02-13]

The Engineering Toolbox (2019). *Specific Heat of Solids.* https://www.engineeringtoolbox.com/specific-heat-solids-d_154.html [2019-04-03]

Thermopedia (2011). *FOURIER'S LAW*. http://www.thermopedia.com/content/781/ [2019-05-22]

Trafikverket (1998). *Bestämning av kornstorleksfördelning genom siktanalys.* VV Publ. 1998:68. https://trafikverket.ineko.se/Files/sv-SE/10863/RelatedFiles/1998_68_bestamning_av_kornstorleksfordelning_genom_siktningsanalys_619_1998.pdf [accessed 2019-03-08]

York, K. P., Jahangir, S., Solomon, T. & Stafford, L. (1998). *Effects of a Large Scale Geothermal Heat Pump Installation on Aquifer Microbiota.* Pomona, Richard Stockton Collage. http://citeseerx.ist.psu.edu/viewdoc/download;jsessionid=B671D9CD2872ACAC6B5FDF3C52262B86?doi=10.1.1.510.1293&rep=rep1&type=pdf [accessed 2019-03-28]

Öresundskraft (2018). *Elnätspris 2019*. https://oresundskraft.se/privat/produkter-tjaenster/elnaet/elnaetspriser/laegenhet-2019/ [2019-04-08]

Öresundskraft (2019 A). *Distributionsnät.* https://oresundskraft.se/om-oeresundskraft/produktion-och-distribution/distributionsnaet/aengelholm/ [07-02-2019]

Öresundskraft (2019 B). *Fjärrvärme normalprislista konsument*. https://oresundskraft.se/media/1582831/prislista_2019_fjv_konsument_helsingborg.pdf [2019-04-08]

Öresundskraft Kraft & Värme (2018). *Loggningsrapport* [corporate material]. Helsingborg: Öresundskraft Kraft & Värme.

Appendices

Appendix A – Material properties

The material properties needed for the modelling in *TRNSYS* are presented in the following. These entail thermal properties (thermal conductivity and specific heat) for the modelled materials as well as additional material data for the carrier fluid, which is presented under the section of the carrier fluid. Materials and volumes for which thermal property data is provided are listed below, these include both segments within and outside the thermal storage volume.

i) Thermal storage volume (needed for the storage volume in the *DST-model*)
ii) Gypsum (outside the storage volume in the *DST-model*)
iii) Till (outside the storage volume in the *DST-model*)
iv) Sedimentary bedrock (outside the storage volume in the *DST-model*)

Thermal storage volume

The thermal conductivity of the storage volume was derived from thermal response tests performed in a testing well at the field site. These tests gave the thermal conductivity of the storage volume as a whole, which includes the sedimentary bedrock, the overlying till and gypsum layer, as well as the topsoil.

$$\lambda_{St.V} = 3.5 \left[\frac{W}{m \cdot K}\right] = \frac{3.5 \cdot 3600}{1000} = 12.6 \left[\frac{kJ}{h \cdot m \cdot K}\right]$$

The specific heat capacity of the storage volume is taken as the same value as for the sedimentary bedrock, as most of the energy is to be stored within the bedrock itself. The specific heat capacity value is based on the mineral content of the sedimentary rock, which mainly consists of sand stones, silt stones and shales. For these rock types specific heat values are tabulated by *The Engineering Toolbox* (2019) and an evaluation of a specific heat value can be made, assuming a density of 2650 kg/m^3 for the average of the storage volume.

$$C_{St.V} = 920 \left[\frac{J}{kg \cdot K}\right] \approx 2400 \left[\frac{kJ}{m^3 \cdot K}\right]$$

Gypsum

The thermal conductivity of the gypsum was derived from thermal conductivity tests performed by *Elastocon*. The results of these tests show a load and depth dependent variance of the thermal conductivity of the gypsum. This variance shows a thermal conductivity varying between 0.13-0.31 [W/(m K)] yielding the thermal conductivity span in [kJ/(h m K)]. The full results from the thermal conductivity tests performed are presented in *Appendix K*. A finer stratification is possible using the thermal conductivity tests presented in *appendix K*.

$$\lambda_{gy} = 0.13 - 0.31 \left[\frac{W}{m \cdot K}\right] = 0.13 \cdot 3.6 - 0.31 \cdot 3.6 \approx 0.47 - 1.1 \left[\frac{kW}{h \cdot m \cdot K}\right]$$

The specific heat capacity of the gypsum was not given by the tests performed for thermal conductivity, but instead collected from tabulated values from *The Engineering Toolbox* (2019) showing a specific heat capacity as presented below. Assuming a density of 2500 kg/m^3 as the gypsum is assumed not fully packed.

$$C_{gy} = 1090 \left[\frac{J}{kg \cdot K}\right] \approx 2700 \left[\frac{kJ}{m^3 \cdot K}\right]$$

Till

The thermal conductivity of the till, located between the gypsum and the bedrock, is evaluated from its content and from the thermal response tests performed. Tabulated values showing a thermal conductivity around 2.5-3.5 [W/(m K)] for sandy and clayish soils (Clarke & Hamdhan 2010) and a thermal response test showing a thermal conductivity of the storage volume as 3-3.5 [W/(m K)], the thermal conductivity was set as 3.0 [W/(m K)] as the greater values from the thermal response test were assumed linked with the higher thermal conductivity of the underlying bedrock.

$$\lambda_{till} = 3.0 \left[\frac{W}{m \cdot K}\right] = 3.0 \cdot 3.6 = 10.8 \left[\frac{kJ}{h \cdot m \cdot K}\right]$$

The specific heat capacity is derived from *Sipola* (2011) assuming a bulk density of 2300 kg/m^3 for till. This resulted in an approximate specific heat capacity which is presented below.

$$C_{till} = 1100 \left[\frac{J}{kg \cdot K}\right] \approx 2400 \left[\frac{kJ}{m^3 \cdot K}\right]$$

Being kept in mind when assigning the thermal properties was the assumption that the till layer was fully saturated as the groundwater level is located within this layer.

Sedimentary bedrock

There has over the years been a clear separation between metallic and non-metallic materials when discussing thermal conductivity of solids. For metallic materials, thermal heat can be transferred by phonons, free (or valence) electrons and lattice waves. For non-metallic materials, thermal heat can only be transported through the material by phonons. For phonons, thermal energy is transported through vibrations of the crystal structure, this is called lattice waves (Eckert & Robert 1972).

Since sedimentary rock is formed through diagenesis, which is a term used for describing how deposited sediments are consolidated into compact rock through high pressure. The mineral composition of the rock is location dependent and will vary a lot since the rock will consist of sediments and deposits from water flows, wind, etc. that carries particles. It is most common for non-metallic deposits in the southern parts of *Sweden* since the bedrock mostly consists of old bedrock from the Precambrian time period. Stretching between 4600-540 million years ago and the rock mainly consists of granite, hence the sedimentary rock mostly consists non-metallic deposits in the south of *Sweden* (Eckert & Robert 1972).

The thermal conductivity of the sedimentary bedrock is evaluated from tabulated values for the mineral content of the bedrock. The rock types known in the sedimentary rock are sandstones, silt stones and shales, materials for which thermal conductivities are tabulated by *The Engineering Toolbox* (2019). The tabulated values are analyses parallel with the thermal response tests showing a thermal conductivity of 3-3.5 [W/(m K)]. Under the assumption that the bedrock has the greater thermal conductivity of the present geologic materials the value of this is set to the highest in the range showed by the thermal response test.

$$\lambda_{BR} = 3.5 \left[\frac{W}{m \cdot K}\right] = 3.5 \cdot 3.6 = 12.6 \left[\frac{kJ}{h \cdot m \cdot K}\right]$$

This value is coherent with the approximate values presented by *Sundberg* (1991) for sedimentary rock in *Figure A.1*.

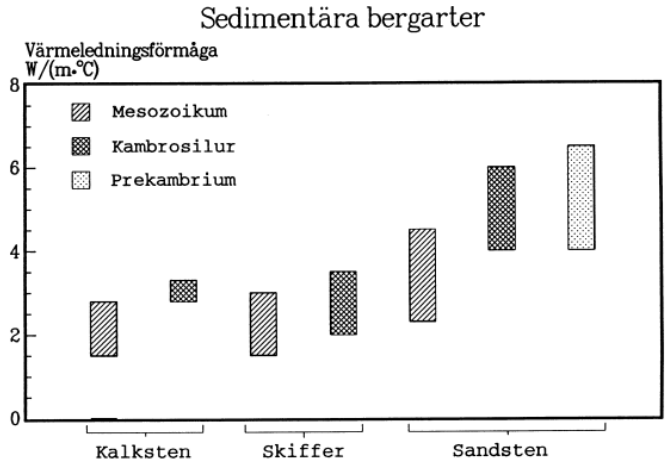

Figure A.1 – Kalksten: limestone. Skiffer: Shales. Sandsten: Sandstone (Sundberg 1991)

The specific heat capacity is given for the mineral content by *The Engineering Toolbox* (2019) and assumed as a type of mean for these giving the following value. Assuming a density of 2650 kg/m^3 of the sedimentary rock.

$$C_{BR} = 920 \left[\frac{J}{kg \cdot K}\right] \approx 2400 \left[\frac{kJ}{m^3 \cdot K}\right]$$

Carrier fluid - Water

The carrier fluid/transport medium of the thermal system is water, for which the material properties of density, viscosity, thermal conductivity and specific heat are needed in the *TRNSYS* modelling. The density of the water is taken as 1000 [kg/m^3], and the viscosity as 0.404 [mPa s] for water at 70 degrees as given by *Engineers Edge* (2019). The thermal conductivity of the water is given by 2.38 [kJ/(h m K)] and the specific heat by 4.2 [kJ/(kg K)] as the values presented below.

$$\lambda_{Water} = 0.67 \left[\frac{W}{m \cdot K}\right] = 0.67 \cdot 3.6 = 2.38 \left[\frac{kJ}{h \cdot m \cdot K}\right]$$

$$C_{Water} = 4200 \left[\frac{J}{kg \cdot K}\right] = 4200 \left[\frac{kJ}{m^3 \cdot K}\right]$$

Summary of thermal properties

Table A.1 – Thermal properties of geologic units.

Material	**Thermal conductivity [kJ/(h m K)]**	**Specific heat capacity [J/(kg K)]**
Storage volume	12.6	2300
Gypsum	1.1	1090
Till	10.8	1700
Sedimentary bedrock	12.6	920
Carrier fluid (water)	2.38	4200

Appendix B – Material properties for insulating slag gravel

The thermal conductivity for the slag gravel was tested by *Elastocon* (2019-01-09 and 2019-03-11 gypsum 2019-03-22 slag gravel), via the method given by *Elastocon*. The thermal conductivity of the slag gravel was tested via a C-Therm TCi Thermal Conductivity Analyser with a Transient Line Source (*TLS*) sensor. The material was placed in a glass container in the middle of which the *TLS* sensor was placed. Each material was tested for five specimens for the different load cases. Reference materials were used for calibrations before testing. The results from testing are presented below.

Table B.1 – Thermal conductivity results of slag gravel produced from Elastocon.

Test specimen – "2"			
Test number	Thermal conductivity $[W/m \cdot K]$	Starting time [min]	End time [min]
1	0.401	4.4243	6.141
2	0.411	4.212	5.757
3	0.400	4.126	5.768
4	0.411	4.144	6.009
5	0.407	4.145	5.725
Mean value	**0.406**		

Table C.2 – Thermal conductivity results of slag gravel produced from Elastocon.

Test specimen – "3"			
Test number	Thermal conductivity $[W/m \cdot K]$	Starting time [min]	End time [min]
1	0.204	4.096	5.926
2	0.204	3.664	5.966
3	0.203	3.601	5.717
4	0.200	3.402	5.163
5	0.200	3.240	6.399
Mean value	**0.202**		

Table D.3 – Thermal conductivity results of slag gravel produced from Elastocon.

Test specimen 3 – "0-3"			
Test number	Thermal conductivity $[W/m \cdot K]$	Starting time [min]	End time [min]
1	0.246	4.394	6.803
2	0.276	3.606	6.803
3	0.286	3.293	6.802
4	0.260	3.485	6.618
5	0.257	3.953	6.181
Mean value	**0.260**		

Table E.4 – Thermal conductivity results of slag gravel produced from Elastocon.

Test specimen 4 – "3-6"			
Test number	Thermal conductivity $[W/m \cdot K]$	Starting time [min]	End time [min]
1	0.289	5.004	6.347
2	0.307	4.521	6.18
3	0.285	4.394	6.346
4	0.323	4.741	6.347
5	0.286	4.648	6.347
Mean value	**0.289**		

Table F.5 – Thermal conductivity results of slag gravel produced from Elastocon.

Test specimen 5 – "6-24"			
Test number	Thermal conductivity $[W/m \cdot K]$	Starting time [min]	End time [min]
1	0.318	4.991	6.397
2	0.348	4.647	6.292
3	0.375	5.048	6.293
4	0.350	4.824	6.293
5	0.308	4.721	6.292
Mean value	**0.348**		

Appendix C – Sieving tests of slag gravel

Aim and background

The main task of this Master Thesis was to evaluate insulation aspect of the planned *HT-BTES* with regards to thermal efficiency. A part of this study entailed material choices for the insulating layer, for which slag gravel, a bi-product from the incineration process, was one alternative. In order to evaluate the thermal and hydrological properties of this material to some extent, sieving tests of the materials were performed in order to derive the granular distribution. The distribution can be related to properties such as water content, capillary rise, and thermal characteristics.

Method

The sieving tests were performed in accordance with the method outline given by *Trafikverket* (1998). The methodology used for deriving the fractional distributions was the utilization of a sieving machine which uses square nets with different square sizes for deriving how much the material which passes each net. The granular size slits in the sieving apparatus varied from 22.4 mm to 0.063 mm. The sieves were placed with the smallest on the bottom and the largest on top. The sample was firstly weighed before testing and thereafter poured into the sieves. The sieves were then vibrated for 10 minutes with 20 second intervals and an amplitude of 0.5. When the vibrating part of the sieving process was done each sieve was weighed, after which the remainder of the sample was removed and the empty sieve weighed again and the mass of the remainder of sample on each sieve was calculated as the differential between the sieve before and after the removal of the remainder of sample.

Figure C.1 – Sieving machine.

Table G.1 – Maximum weight of material dependent on sieve width.

Sieve width (mm)	Maximum amount of material stayed on one sieve (g)
22.4	1050
16	900
11.2	800
8	700
5.6	600
4	500
2	400
1	300
0.5	200
0.25	175
0.125	150
0.063	100

The sum of the different fractions weight (including the material which passes the last sieve) may not deviate more than 0.5 % from the initial weight. The adjustments may be performed in accordance with the following *C.2* for minor deviations.

Table H.2 – Correction dependent on deviation.

Total weight in % of initial weight	Correction
99.8 %	The two largest percentages are increased with 0.1 %
99.9 %	The largest percentage is increased with 0.1 %
100.1 %	The largest percentage is lowered by 0.1 %
100.2 %	The two largest percentages are reduced with 0.1 %

In total five samples of slag gravel were tested. Two of the samples were unsorted, these were collected on the 1st of February 2019. Three of them were sorted with different fraction ranges, and where collected on the 15th of February 2019.

- Sample 1: Pure slag gravel. Collected from one of the piles of slag gravel at the site, a pile which had not undergone sieving and was directly from the incinerator ovens.
- Sample 2: Slag gravel mixed with asphalt granulates which currently is used for the roads on the site.
- Sample 3: Pure slag gravel, collected from a pile which consisted of fractional distribution 0-3 mm.
- Sample 4: Pure slag gravel, collected from a pile which consisted of fractional distribution 3-6 mm.
- Sample 5: Pure slag gravel, collected from a pile which consisted of fractional distribution 6-22.4 mm.

Results

Table I.3 – Sieving results correlating to Sample 1-5 of slag gravel.

Sample 1 – Pure slag gravel	
Sample properties	Total weight: 2106,6 g Collected: 1st of February 2019 Sieving test: 5th of February 2019
Sieving test	
Sieve	Remaining mass (g)
22.4 mm	156.7
16 mm	166.1
11.2 mm	291.3
8 mm	322.7
5.6 mm	273.7
4 mm	218.6
2 mm	303.5
1 mm	239.5
0.5 mm	121.1
0.25 mm	1.7
0.125 mm	0.3
0.063 mm	0
Total amount	2095.2 g
Difference from original weight	-11.4 g

Sample 2 – Slag gravel + Asphalt granulates	
Sample properties	Total weight: 2893 g Collected: 1st of February 2019 Sieving test: 5th of February 2019
Sieving test	
Sieve	Remaining mass (g)
22.4 mm	81.1
16 mm	153.8
11.2 mm	325.1
8 mm	407.9
5.6 mm	365.6
4 mm	316.7
2 mm	423.8
1 mm	339.1
0.5 mm	235.8
0.25 mm	158.2
0.125 mm	70
0.063 mm	20.3
Total amount	2897.4 g
Difference from original weight	+4.4 g
Sample 3 – Slag gravel (6-24)	
Sample properties	Total dry weight: 1844 g Collected: 15th of February 2019 Sieving test: 22nd of February 2019
Sieving test	
Sieve	Remaining mass (g)
22.4 mm	0
16 mm	69.8
11.2 mm	597.9

8 mm	918
5.6 mm	187.8
4 mm	21
2 mm	4.7
1 mm	2.1
0.5 mm	3.6
0.25 mm	5.6
0.125 mm	6
0.063 mm	8.1
Rest	2.3
Total amount	1826.9
Difference from original weight	-17.1
Sample 4 – Slag gravel (3-6)	
Sample properties	Total dry weight: 2117,9 g Collected: 15th of February 2019 Sieving test: 22nd of February 2019
Sieving test	
Sieve	Remaining mass (g)
22.4 mm	0
16 mm	3
11.2 mm	2
8 mm	111.9
5.6 mm	434.8
4 mm	657.1
2 mm	756.9
1 mm	52.4
0.5 mm	17.7
0.25 mm	18
0.125 mm	21.4

0.063 mm	10.6
Rest	1
Total amount	2086.8
Difference from original weight	-31.1
Sample 5 – Slag gravel (0-3)	
Sample properties	Total dry weight: 1426 g Collected: 15th of February 2019 Sieving test: 22nd of February 2019
Sieving test	
Sieve	Remaining mass (g)
22.4 mm	0
16 mm	1.5
11.2 mm	1.9
8 mm	2.1
5.6 mm	2.3
4 mm	4.4
2 mm	253.7
1 mm	411.8
0.5 mm	312.1
0.25 mm	259.9
0.125 mm	118.9
0.063 mm	45.6
Rest	6.7
Total amount	1420.9
Difference from original weight	-5.1

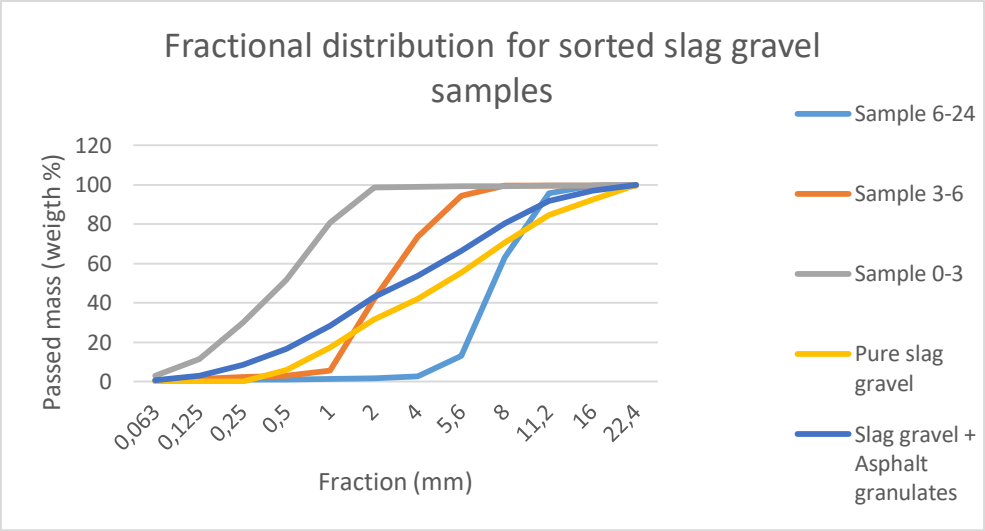

Figure C.2 – Sieving curves for slag gravel samples.

Evaluation

The sieving test showed a greater amount of finer material in the sample consisting of slag gravel mixed with asphalt. Hence the porosity of the sample of pure slag gravel can be assumed greater. A greater amount of air in a material is related to the porosity and as air has a very good insulating performance this is seen as positive if the pure slag gravel was to be used for insulting in comparison to the slag gravel mixed with asphalt.

During the sieving test of the two specimens it was noted that the pure slag gravel was noticeably more moist than the sample of slag gravel mixed with asphalt. This could be an explanation to the low content of finer fractions that was measured during the laboratory test.

The slag gravel mixed with asphalt is used as road material at the work site and is probably not available in sufficient amount either way and if slag gravel is used it is recommended to be pure slag gravel and not a mix.

The material samples 3-5 showed fractional distribution according to what the manufacturer of the samples proclaimed. This implies that the final distribution of the insulation material will with a high certainty have the fraction distribution that was ordered. Resulting in properties of which will correspond with the ones used during the simulation process.

The material weight on each sieve depended on the possibility of removing all material from the sieve after it had been weighed with the material in it. This was mostly possible except for some minor fractions stuck at 1-2 mm, but the effect of this is deemed negligible.

The sample of 3-6 corresponds to a granulate distribution of sandy gravel, while the sample of 6-24 corresponds to a granulate distribution for gravel. Materials which have corresponding low values of capillary rise, and are seen as permeable, giving draining properties. Hence the material layers consisting of these materials are not to capillary transport water if this becomes present at the bottom of the layer, neither are these to hold free drainable water.

Appendix D – Material analysis of slag gravel

A chemical analysis of slag gravel was made by *Eurofins Environmental Testing Sweden AB* (between 2018-03-15 and 2018-03-29) in order to observe the composition of slag gravel. This in verify the possibility areas of utilisation for the material, if it could be used commercially or solely at the current location where the leaching water is controlled.

Provnummer:	177-2018-03150861
Provbeskrivning:	
Matris:	Aska
Provet ankom:	2018-03-15
Utskriftsdatum:	2018-03-29
Provmärkning:	Filborna, slaggaska mars 2018

Analys	Resultat	Enhet	Mätо.	Metod/ref	
Provberedning krossning, malning	1.0			SS 187117:1997	a)
Fukthalt	17.6	%	10%	EN 14774-1,2,3:2009 mod/15414-1,2,3:2011 mod/SS187	a)
Klor Cl	0.49	% Ts	15%	SS 187185	b)*
Oförbränt	0.9	% Ts	10%	SS 187187:1995	a)
Svavel S	2.3	% Ts	5%	SS 187187:1995	a)
Svavel S lev.tillstånd	1.9	%	5%	SS 187187:1995	a)
Aluminium Al	48000	mg/kg Ts	25%	EN 13656 mod. / ICP-AES	a)
Aluminiumoxid Al2O3	90000	mg/kg Ts	25%	EN 13656 mod. / ICP-AES	a)
Fosfor P	3100	mg/kg Ts	20%	EN 13656 mod. / ICP-AES	a)
Fosforoxid P2O5	7000	mg/kg Ts	20%	EN 13656 mod. / ICP-AES	a)
Järn Fe	59000	mg/kg Ts	25%	EN 13656 mod. / ICP-AES	a)
Järnoxid Fe2O3	84000	mg/kg Ts	25%	EN 13656 mod. / ICP-AES	a)
Kadmium Cd	1.8	mg/kg Ts	30%	EN 13656 mod. / ICP-MS	a)
Kalcium Ca	160000	mg/kg Ts	30%	EN 13656 mod. / ICP-AES	a)
Kalciumoxid CaO	220000	mg/kg Ts	30%	EN 13656 mod. / ICP-AES	a)
Kalium K	10000	mg/kg Ts	25%	EN 13656 mod. / ICP-AES	a)
Kaliumoxid K2O	12000	mg/kg Ts	25%	EN 13656 mod. / ICP-AES	a)
Kisel Si	180000	mg/kg Ts	20%	EN 14385 / ICP-AES	a)*
Kiseloxid SiO2	380000	mg/kg Ts	30%	EN 14385	a)*
Magnesium Mg	16000	mg/kg Ts	25%	EN 13656 mod. / ICP-AES	a)
Magnesiumoxid MgO	26000	mg/kg Ts	25%	EN 13656 mod. / ICP-AES	a)
Mangan Mn	1500	mg/kg Ts	20%	EN 13656 mod. / ICP-AES	a)
Manganoxid MnO2	2300	mg/kg Ts	20%	EN 13656 mod. / ICP-AES	a)

Provnummer:	177-2018-03150861
Provbeskrivning:	
Matris:	Aska
Provet ankom:	2018-03-15
Utskriftsdatum:	2018-03-29
Provmärkning:	Fliborna, slaggaska mars 2018

Analys	Resultat	Enhet	Mätо.	Metod/ref	
Natrium Na	28000	mg/kg Ts	20%	EN 13656 mod. / ICP-AES	a)
Natriumoxid Na2O	38000	mg/kg Ts	20%	EN 13656 mod. / ICP-AES	a)
Titan Ti	10000	mg/kg Ts	20%	EN 13656 mod. / ICP-AES	a)
Titanoxid TiO2	17000	mg/kg Ts	20%	EN 13656 mod. / ICP-AES	a)
Arsenik As	21	mg/kg Ts	25%	EN 13656 mod. / ICP-MS	a)
Antimon Sb	140	mg/kg Ts	15%	EN 13656 mod. / ICP-MS	a)
Barium Ba	7900	mg/kg Ts	30%	EN 13656 mod. / ICP-AES	a)
Beryllium Be	< 2.6	mg/kg Ts	30%	EN 13656 mod. / ICP-MS	a)
Bly Pb	770	mg/kg Ts	20%	EN 13656 mod. / ICP-MS	a)
Kobolt Co	38	mg/kg Ts	30%	EN 13656 mod. / ICP-MS	a)
Koppar Cu	2800	mg/kg Ts	20%	EN 13656 mod. / ICP-AES	a)
Krom Cr	400	mg/kg Ts	25%	EN 13656 mod. / ICP-MS	a)
Molybden Mo	< 21	mg/kg Ts	25%	EN 13656 mod. / ICP-AES	a)
Nickel Ni	190	mg/kg Ts	35%	EN 13656 mod. / ICP-MS	a)
Tenn Sn	91	mg/kg Ts	20%	EN 13656 mod. / ICP-MS	a)
Vanadin V	58	mg/kg Ts	25%	EN 13656 mod. / ICP-MS	a)
Zink Zn	3400	mg/kg Ts	25%	EN 13656 mod. / ICP-AES	a)
Bor B	390	mg/kg Ts	25%	EN ISO 11885:2009 / SS 028150 utg 2	a)*
Kvicksilver Hg	< 0.046	mg/kg Ts	25%	SS028150mod/SS-EN ISO17852mod	a)*

Appendix E – Moisture absorption test of slag gravel

Aim and background

As a mean of proving present moisture absorption of the slag gravel material evaluated for the reference project at *Filborna* an absorption test was performed. This to prove that the slag gravel shows potential for moisture absorption, which has effects on the thermal properties of the material.

Method

Material samples for the slag gravel samples "3-6" and "6-24" (see *appendix B*) were dried at 150 degrees and weighed, after which these were submerged in water in separate containers. In total seven samples of each material type were investigated. Each day, for seven days, one sample of each type was drained and weighed. The difference in weight corresponds to the absorbed water amount, which via division with the dry weight yields the water content in weight-%.

Results

The moisture absorption for the first seven days are presented in *E.1*.

Table J.1 – Moisture absorption results of slag gravel.

Test specimen	Days submerged	Dry weight (g)	Moist weight (g)	Moisture content (weight-%)
3-6A	1	126	140	0.11
3-6B	2	116	136	0.17
3-6C	3	168	186	0.11
3-6D	4	124	140	0.13
3-6E	5	132	148	0.12
3-6F	6	116	132	0.14
3-6G	7	126	144	0.14
6-24A	1	156	170	0.09
6-24B	2	222	244	0.1
6-24C	3	140	156	0.11
6-24D	4	228	252	0.11
6-24E	5	166	198	0.19
6-24F	6	164	182	0.11
6-24G	7	180	200	0.11

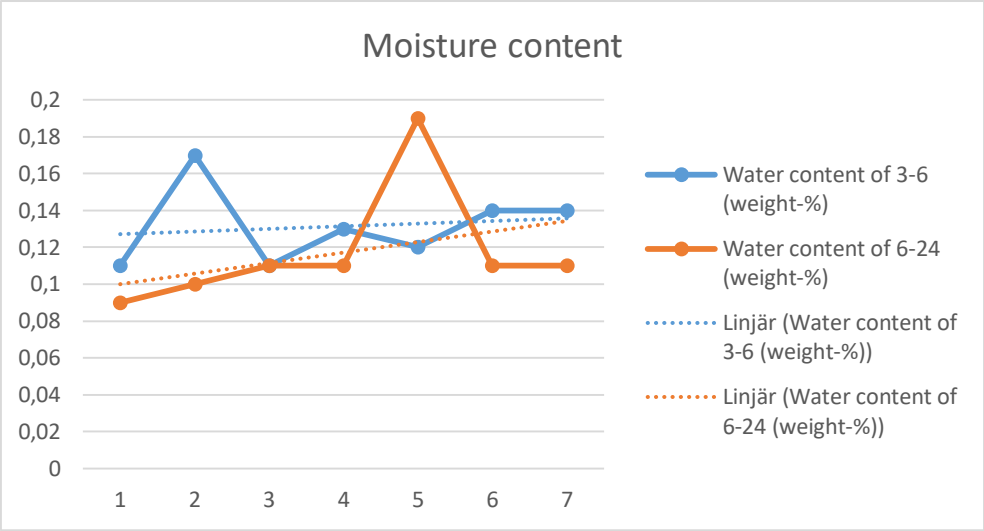

Figure E.1 – Moisture content of slag gravel dependent on time. X-axis in days, y-axis represents water content.

Evaluation

The results show a prominent moisture absorption, which gives reason for a thermal property dependency on moisture content. From the fact that thermal properties are water content dependent it is concluded that in order to further verify the properties of the slag gravel thermal conductivity measurements are needed for variant moisture contents.

Appendix F – Material properties for foam glass

The material properties for foam glass are derived from the product leaflets from the manufacturer of the foam glass product, which in this case is *HASOPOR*. The data from the product leaflets are presented in the *F.1*, showing thermal and hydrological properties.

Table K.1 – Material properties of foam glass derived from HASOPOR.

Material properties for foam glass		
	Foam glass A (HASOPOR light)	**Foam glass B (HASOPOR standard)**
Grain size	10-50 [mm]	10-50 [mm]
Dry density	180 [kg/m^3]	225 [kg/m^3]
Dimensioning density	2.7-3.5 [kN/m^3]	3.4-4.0 [kN/m^3]
Thermal conductivity, (λ_D) (dry material)	0.102 [W/mK]	0.110 [W/mK]
Corrected heat conductivity, (λ_w) (25% moisture weight)	0.129 [W/mK]	0.145 [W/mK]
Water absorption after 28 days in water	31 [weight-%]	30 [weight-%]
Water absorption after 68 weeks in water	40 [weight-%]	50 [weight-%]

Appendix G – Material properties for insulating expanded clay

Thermal and hydrological material properties for expanded clay are collected from one of the main manufacturers, *LECA*. These properties are presented in the *G.1*.

Table L.1 – Material properties of expanded clay derived from LECA.

Material properties for expanded clay	
Grain size	11-20 [mm]
Dry density	260 ±15 % [kg/m^3]
Dimensioning density	495 ±15 % [kg/m^3]
Compact density	2500 [kg/m^3]
Thermal conductivity, λ_D (dry material)	0.11 [W/mK]
Thermal conductivity, λ_W (50 % moisture ratio)	0.18 [W/mK]
Water absorption 300 days	<60 [weight-%]

Appendix H – Material properties for extruded polystyrene

The material properties for XPS Styrofoam are derived from the product leaflets provided from the manufacturer, in this case Ownes Corning foam insulation, LLC. The data of the product are presented in *H.1*, showing the thermal properties.

Table M.1 – Material properties of extruded polystyrene (XPS) derived from Owens Corning (N.D.)

Material properties for XPS Styrofoam					
	Foamular 150 insulation	**Foamular 250 insulation**	**Foamular 400 insulation**	**Foamular 600 insulation**	**Foamular 1000 insulation**
Thickness	100 [mm]	100 [mm]	100 [mm]	100 [mm]	100 [mm]
Density	20.8 [kg/m^3]	24.8 [kg/m^3]	28.9 [kg/m^3]	35.3 [kg/m^3]	48.1 [kg/m^3]
Thermal conductivity	0.029 [W/mK]	0.029 [W/mK]	0.029 [W/mK]	0.029 [W/mK]	0.029 [W/mK]
Thermal resistance	3.53 [m^{2}K/W]	3.53 [m^{2}K/W]	3.53 [m^{2}K/W]	3.53 [m^{2}K/W]	3.53 [m^{2}K/W]
Thickness	75 [mm]	75 [mm]	75 [mm]	75 [mm]	75 [mm]
Density	20.8 [kg/m^3]	24.8 [kg/m^3]	28.9 [kg/m^3]	35.3 [kg/m^3]	48.1 [kg/m^3]
Thermal conductivity	0.029 [W/mK]	0.029 [W/mK]	0.029 [W/mK]	0.029 [W/mK]	0.029 [W/mK]
Thermal resistance	2.65 [m^{2}K/W]	2.65 [m^{2}K/W]	2.65 [m^{2}K/W]	2.65 [m^{2}K/W]	2.65 [m^{2}K/W]
Thickness	50 [mm]	50 [mm]	50 [mm]	50 [mm]	50 [mm]
Density	20.8 [kg/m^3]	24.8 [kg/m^3]	28.9 [kg/m^3]	35.3 [kg/m^3]	48.1 [kg/m^3]
Thermal conductivity	0.029 [W/mK]	0.029 [W/mK]	0.029 [W/mK]	0.029 [W/mK]	0.029 [W/mK]
Thermal resistance	1.77 [m^{2}K/W]	1.77 [m^{2}K/W]	1.77 [m^{2}K/W]	1.77 [m^{2}K/W]	1.77 [m^{2}K/W]

Appendix I – Parameter model for horizontal pipes

Table N.1 – Parameters used for the horizontal pipe model in TRNSYS

Horizontal pipe properties		
Length of buried pipe	7000	m
Inner diameter of pipe	0,051	m
Outer diameter of pipe	0,062	m
Thermal conductivity of pipe material	0,56	kJ/(h m K)
Buried pipe depth	1,25	m
Thickness of insulation	0,5	m
Thermal conductivity of insulation	1,5	kJ/(h m K)
Density of fluid	1000	kg/m3
Thermal conductivity of fluid	2,38	kJ/(h m K)
Specific heat of fluid	4,2	kJ/(kg K)
Viscosity of fluid	0,0004	kg/(m h)
Initial fluid temperature	58	C
Thermal conductivity of soil	10,8	kJ/(kg m K)
Density of soil	2300	kg/m3
Specific heat of soil	1	kJ/(kg K)
Average surface temperature	10	C
Amplitude of surface temperature	25	C
Day of minimum surface temperature	23	
Number of fluid nodes	500	
Number of radial soil nodes	-1	
Number of axial soil nodes	10	
Number of circumferential soil loads	10	
Smallest load size	0,0254	m
Node size multiplier	1,2	
Far field distance	100	m

Appendix J – DST-model for storage

Table O.1 – Parameters for DST-model used in TRNSYS.

Store properties			
Parameter	**Value**	**Unit**	**Comment**
Storage volume	3 000 000	m^3	
Borehole depth	120	m	
Header depth	0	m	0 metres is used as the reference.
Number of boreholes	1500		
Number of boreholes in series	3		
Number of radial regions	20		
Number of vertical regions	20		
Thermal conductivity of storage	12.6	$\frac{kJ}{h \cdot m \cdot K}$	
Storage heat capacity	2400	$\frac{kJ}{m^3 \cdot K}$	
Maximum storage temperature	100	°C	
Initial surface temperature of storage volume	0	°C	
Initial thermal gradient of storage volume	0	°C /m	
Number of ground layers	3		
Thermal conductivity of layer – 1	1.1	$\frac{kJ}{h \cdot m \cdot K}$	
Heat capacity of layer – 1	2700	$\frac{kJ}{m^3 \cdot K}$	
Thickness of layer – 1	15	m	
Thermal conductivity of layer – 2	10.8	$\frac{kJ}{h \cdot m \cdot K}$	
Heat capacity of layer – 2	2400	$\frac{kJ}{m^3 \cdot K}$	
Thickness of layer – 2	3	m	

Thermal conductivity of layer – 3	12.6	$\frac{kJ}{h \cdot m \cdot K}$	
Heat capacity of layer – 3	2400	$\frac{kJ}{m^3 \cdot K}$	
Thickness of layer – 3	1000	m	Infinite depth
Duct properties			
Tube-in-tube indicator	– 11		The 11 indicates the type of collector, and the minus indicates that it is heat
Outer pipe, Outer radius	50.8	mm	
Outer radius of inner tube	31	mm	
Inner radius of inner tube	25.5	mm	
Inner radius of outer tube	45	mm	
Thermal conductivity of pipe	181	$\frac{kJ}{h \cdot m \cdot K}$	Steel
Thermal conductivity of gap	10	$\frac{kJ}{h \cdot m \cdot K}$	
Gap thickness	0	m	
Reference borehole flowrate	2000	kg/h	
Thermal conductivity of fill	2.38	$\frac{kJ}{h \cdot m \cdot K}$	
Reference temperature	10	°C	
Pipe-to-pipe heat transfer	0		
Specific heat of fluid	4.2	$\frac{kJ}{kg \cdot K}$	
Fluid density	1000	kg/m^3	
Insulating layer			
Insulation indicator	2		Only top insulation, no fold
Insulation height fraction	0.04		
Insulation thickness	0.5	m	
Thermal conductivity of insulation	1.5	$\frac{kJ}{h \cdot m \cdot K}$	
Simulation properties			

Number of simulation years	50		
Number of preheating years	0		These are done using an in-data file preheating the first three years of operation, hence having no extraction of energy during this time.
Maximum preheat temperature	10	°C	
Minimum preheat temperature	5	°C	
Preheat face delay	90	Days	
Average air temperature - Preheat years	10	°C	
Amplitude of air temperature – Preheat years	25	Δ°C	
Air temperature phase delay – preheat years	247	Days	

Appendix K – Material properties for gypsum

The tests of thermal conductivity of gypsum were conducted via a C-Therm TCi Thermal Conductivity Analyzer with an MTPS sensor. Approximately 1,8 ml of gypsum powder was placed in the "TCi Small Volume Kit", connected to the MTPS sensor. The measurements of thermal conductivity were conducted by placing no load, a 2 kg load and a 4 kg load on the test specimen. For each material five specimens were measured for thermal conductivity for each load case. All measurements were conducted at room temperature (23 °C).

Table P.1 – Thermal conductivity results of gypsum produced from Elastocon.

Test specimen – "UB1 2-3m"		
Test number	Thermal conductivity under no load $[W/m \cdot K]$	Thermal conductivity under 2 kg load $[W/m \cdot K]$
1	0.120	0.130
2	0.120	0.130
3	0.120	0.130
4	0.120	0.130
5	0.120	0.130
6	0.120	0.130
7	0.120	0.130
8	0.120	0.130
9	0.120	0.130
10	0.120	0.130
Mean value	**0.120**	**0.130**
Comment	Yellowish in colour, suspecting influence from top soil	

Table Q.2 – Thermal conductivity results of gypsum produced from Elastocon.

Test specimen 1 – "UB1 4-5m"			
Test number	Thermal conductivity under no load $[W/m \cdot K]$	Gypsum powder under load 2 kg	Gypsum powder under load 4 kg
1	0.200	0.210	0.220
2	0.200	0.210	0.220
3	0.200	0.210	0.220
4	0.200	0.210	0.220
5	0.200	0.210	0.220
Mean value	**0.200**	**0.210**	**0.220**

Table R.3 – Thermal conductivity results of gypsum produced from Elastocon.

Test specimen – "UB1 8-9m"		
Test number	Thermal conductivity under no load $[W/m \cdot K]$	Thermal conductivity under 2 kg load $[W/m \cdot K]$
1	0.280	0.300
2	0.280	0.300
3	0.280	0.300
4	0.280	0.300
5	0.280	0.310
6	0.280	0.310
7	0.280	0.310
8	0.280	0.310
9	0.280	0.310
10	0.280	0.310
Mean value	**0.280**	**0.310**
Comment	Greyish in colour, suspecting clay content.	

Table S.4 – Thermal conductivity results of gypsum produced from Elastocon.

Test specimen 2 – "UB1 9-10m"			
Test number	Thermal conductivity $[W/m \cdot K]$	Gypsum powder under load 2 kg	Gypsum powder under load 4 kg
1	0.190	0.200	0.210
2	0.190	0.200	0.210
3	0.190	0.200	0.210
4	0.190	0.200	0.210
5	0.190	0.200	0.210
Mean value	**0.190**	**0.200**	**0.210**

Table T.5 – Thermal conductivity results of gypsum produced from Elastocon.

Test specimen 3 – "UB1 12-13m"			
Test number	Thermal conductivity $[W/m \cdot K]$	Gypsum powder under load 2 kg	Gypsum powder under load 4 kg
1	0.200	0.210	0.210
2	0.200	0.210	0.210
3	0.190	0.210	0.210
4	0.200	0.210	0.210
5	0.200	0.210	0.210
Mean value	**0.198**	**0.210**	**0.210**